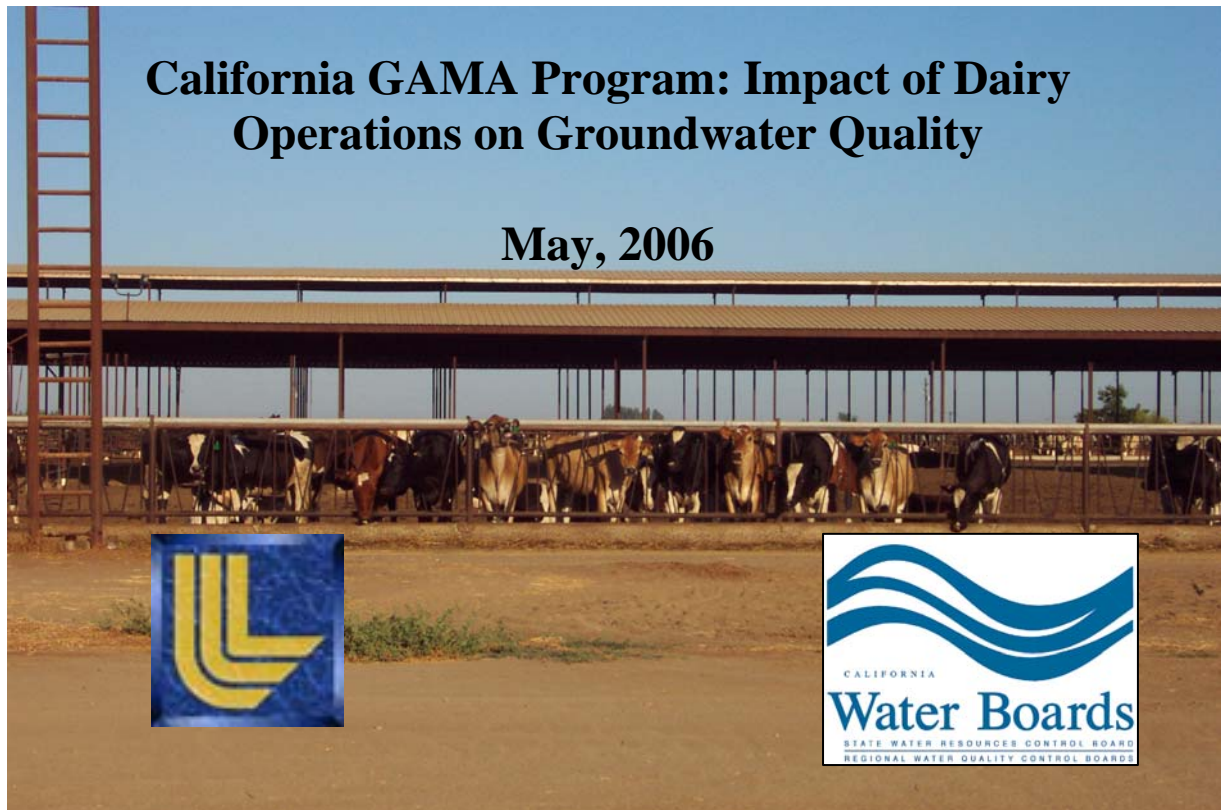


LAWRENCE LIVERMORE NATIONAL LABORATORY

Prepared in cooperation with the
CALIFORNIA STATE WATER RESOURCES CONTROL BOARD



This work was performed under the auspices of the U.S. Department of Energy by the University of California, Lawrence Livermore National Laboratory under contract No. W-7405-ENG-48.

DRAFT

DRAFT - DO NOT DISTRIBUTE OR CIRCULATE

California GAMA Program: Impact of Dairy Operations on Groundwater Quality

Bradley K. Esser,

Lawrence Livermore National Laboratory, L-231, P.O. Box 808, Livermore, CA 94550

OUTLINE

Study Sites: Hydrogeologic Setting

Northern sites

Southern sites

Study Sites: Sampling and Instrumentation

KCD1

KCD2 and KCD3

MCD and SCD

Methods

CPT/DP methods

Drilling methods

Sample collection and field parameters

Chemical composition

Stable isotope mass spectrometry

Membrane inlet mass spectrometry (excess N₂)

Noble gas mass spectrometry (³H/³He dating)

PCR methods

Data

Sediment data

Bacterial population data

Results and Discussion

Saturated-zone denitrification at KCD1 and MCD (Appendix A)

The impact of dairy manure lagoons on groundwater quality (Appendix B)

A new tracer for manure lagoon seepage

Saturated-zone denitrification at northern San Joaquin Valley dairy sites

Source, fate and transport of nitrate at KCD1

The search for a donor

Groundwater model

Agricultural system

Conclusions

References

Tables

Table 1. KCD2, KCD3, and SCD chemical data

Table 2. KCD1 sediment data

Table 3. KCD1 PCR data

Appendix A (Saturated zone denitrification: potential for natural attenuation of nitrate contamination in shallow groundwater under dairy operations)

Appendix B (Assessing the Impact of Animal Waste Lagoon Seepage on the Geochemistry of an Underlying Shallow Aquifer)

DRAFT - DO NOT DISTRIBUTE OR CIRCULATE

STUDY SITES: HYDROGEOLOGIC SETTING

During the investigation, samples were collected and analyzed from a total of five dairies in the San Joaquin-Tulare Basins of California: three in Kings County, one in Stanislaus County, and one in Merced County (Figure 1). Groundwater samples were collected from production wells on each of the dairies. On three of the dairies, samples were also collected from monitoring wells: one of sites in Kings County was instrumented by LLNL, and the two sites in Stanislaus and Merced Counties were instrumented by UC-Davis. Samples were collected from manure lagoons at four of the sites.

Two concentrations of dairy exist in the State of California, both in the southern two-thirds of the Central Valley, which is a low relief structural basin from 60 to 100 km wide and 700 km long. The northern concentration is in Merced and Stanislaus Counties, and the southern concentration is in Kings and Tulare Counties. Both concentrations of dairy industry occur in the San Joaquin Valley groundwater basin, as designated by the California Department of Water Resources (2003). The San Joaquin Valley groundwater basin comprises two of the Central Valley's three large structural sub-basins: the San Joaquin Basin and the Tulare Basin. In this document, we will use San Joaquin Valley and San Joaquin-Tulare Basins interchangeably.

Northern sites: The two northern sites (SCD and MCD) are part of an extensive shallow groundwater monitoring network on five representative dairies set up by Thomas Harter of UC-Davis and the UC Cooperative Extension. The following description of the study area and the dairies is adapted from Harter et al. (2002).

The northern sites study area is in the central-eastern portion of the northern San Joaquin Valley, an area of low alluvial plains and fans bordered by the San Joaquin River to the west, tertiary upland terraces to the east, the Stanislaus River to the north, and the Merced River to the south. The region has a long history of nitrate and salt problems in groundwater (LOWRY, 1987; PAGE and BALDING, 1973).

The main regional aquifer is in the upper 100-200 m of basin deposits, which consist of Quaternary alluvial and fluvial deposits with some interbedded hardpan and lacustrine deposits. Groundwater generally flows from the ENE to the WSW following the slope of the landscape. The average regional hydraulic gradient ranges from approximately 0.05% to 0.15%. The water table at the selected facilities is between 2 and 5 m below ground surface. Measured K values range from 0.1 to 2×10^{-3} m/s, as consistent with the predominant texture of the shallow sediments.

The dominant surface soil texture is sandy loam to sand underlain by silty lenses, some of which are cemented with lime. Water holding capacity is low and water tables are locally high (and maintained by community drainage systems and shallow groundwater pumping). Border flood irrigation of forage crops has historically been the dominant cropping system among dairies in the study area. Low-salinity (0.1–0.2 $\mu\text{S}/\text{cm}$) surface water from the Sierra Nevada is the main source of irrigation water.

DRAFT - DO NOT DISTRIBUTE OR CIRCULATE

A number of hydrogeologic criteria make the area suitable as a field laboratory for investigating recharge water quality from dairies: 1) Groundwater in the area is highly vulnerable because of the sandy soils with high infiltration rates and shallow water tables. 2) The shallow groundwater table and small long-term fluctuations in water level (1-2 m) allow sampling from vertically narrow groundwater zones with well-defined recharge source areas. 3) These same two factors also allow installation of a relatively inexpensive fixed-depth monitoring well network that is also inexpensive to sample.

The five dairy facilities in the UC-Davis network are progressive with respect to herd health, product quality, and overall operations. Improvements in manure and pond management have continually occurred since the inception of the project. The dairies are located in a geographic and hydrogeologic environment that is representative of many other dairies on the lowlands of the northern San Joaquin Valley. The manure management practices employed at these dairies over the past 35 years, particularly with respect to corral design, runoff capture, and lagoon management, have been recognized by industry, regulators, and university extension personnel as typical or even progressive relative to other California dairies (see references in HARTER et al., 2002). Over the past 30–40 years, the herd size on these dairies has continually grown from less than 100 at their inception to over 1000 animal units in the 1990s.

In 1993, UC-Davis installed 6 to 12 monitoring wells on each dairy for a total of 44 wells. Monitoring wells are strategically placed upgradient and downgradient from fields receiving manure water, near wastewater lagoons (ponds), and in corrals, feedlots, and storage areas (henceforth referred to as “corrals”). Wells are constructed with PVC pipe (3 or 5 cm diameter) and installed to depths of 7–10 m. The wells are screened from a depth of 2–3 m below ground surface to a depth of 10 m. Water samples collected from monitoring wells are representative of only the shallowest “first-encounter” groundwater.

Southern sites: To augment the UC-Davis dairy monitoring network, LLNL chose to establish sites in the southern San Joaquin Valley groundwater basin. LLNL developed a list of five potential cooperators, sampled three sites, and chose to instrument one site. The cooperators were chosen with the expertise and assistance of the University of California Cooperative Extension (Thomas Harter, Carol Collar and Carol Frate). Sampling sites were chosen from the list of cooperator dairies using regional water quality data, including NAWQA data from the USGS and water quality dairy data from the Central Regional Water Quality Control Board (Fresno office). The site chosen for more extensive instrumentation was chosen with the following criteria: 1) a cooperative operator, 2) a shallow depth to groundwater to allow cost-effective installation of multi-level wells and synoptic soil-groundwater surveys, 3) a dairying operation typical for the region, and 4) regional evidence for nitrate contamination and denitrification.

The three dairies sampled are within the Tulare Lake Groundwater Subbasin of the San Joaquin Valley Groundwater Basin (CALIFORNIA DWR, 2003) (Figure 1). The sites are located south of the Kings River and north-northeast of the Tulare Lake basin, the natural internal drainage for this hydrologically closed system. Groundwater hydraulic gradients are regionally from the Kings River toward Tulare Lake, but are generally low and are

DRAFT - DO NOT DISTRIBUTE OR CIRCULATE

locally influenced by recharge from unlined irrigation canals and by agricultural and municipal groundwater extraction. Surface soils at these sites are predominantly Nord series (USDA NATIONAL RESOURCE CONSERVATION SERVICE, 2006), and are developed on distal Kings River alluvial fan deposits (WEISSMANN et al., 2003; WEISSMANN et al., 1999; WEISSMANN and FOGG, 1999; WEISSMANN et al., 2002a), which in general are less sandy and have more fine-grained interbeds than the sediments in the northern UC-Davis monitoring network. Groundwater levels in the area are in general deeper (50-200' below ground surface) and more variable (50' over 2-5 years) than in the north. A deeper depth to groundwater and heavier textured soils indicate that southern groundwaters should be less vulnerable to contamination than northern groundwaters. The regional groundwater is highly impacted by agricultural activities and contains elevated concentrations of nitrate and pesticides (BUROW et al., 1998b; BURROW et al., 1998).

Two of the three dairies sampled (KCD2 and KCD3) have deep water tables typical of the region. The one dairy that LLNL instrumented is located in an area to the west of Hanford characterized by a shallow perched aquifer, with depth to groundwater on the order of 15 feet. DWR water level data for wells in the area indicate that this perched aquifer developed in the mid-1960's in response to local groundwater overdrafting (CARLE et al., 2005), and is separated by an unsaturated zone from the deeper regional aquifer (that is sampled by wells on KCD2 and KCD3 to the east and south of Hanford).

The three dairy sites sampled by LLNL in Kings County each have close to the average of 1000 dairy cows, fed in free stalls with flush lanes. The manure management practices employed at these dairies, with respect to corral design, runoff capture, and lagoon management, are typical or progressive relative to other California dairies (see references in HARTER et al., 2002). The most intensively studied dairy, KCD1, operates three clay-lined wastewater lagoons that receive wastewater after solids separation. Wastewater is used for irrigation of 500 acres of forage crops (corn and alfalfa) on the dairy and on neighboring farms; dry manure is exported to neighboring farms. This dairy is also immediately adjacent to another dairy operation, and many of the conclusions regarding nitrate impact apply to dairy practices shared by both operations.

DRAFT - DO NOT DISTRIBUTE OR CIRCULATE

STUDY SITES: SAMPLING AND INSTRUMENTATION

KCD1 (Figure 1, Appendix A-Figure 1, Appendix B-Figure 1): The primary site in Kings County was sampled on multiple occasions, from existing production wells, from LLNL-installed monitor wells, from manure lagoons and irrigation canals, and with direct push soil and water sampling methods. A total of 31 days were devoted to collecting 139 water samples at the site, including 29 direct push samples, 17 surface water samples from 3 manure lagoons and a nearby irrigation canal, 16 groundwater samples from 9 production wells, and 60 groundwater samples from 17 monitor wells. A large number of subsurface soil samples were also collected, both as continuous drill core and as depth-discrete grab samples. Production and monitor wells were sampled on semi-regular intervals between August 2003 and August 2005.

KCD1 was instrumented with five sets of multi-level monitoring wells and one “up-gradient” well near an irrigation canal (Figure ??). The multi-level well “clusters” consisted of wells installed in separate boreholes approximately 5’ apart. A first set of three nested 2” wells in one cluster was installed in September 2003. In August 2004, three new well clusters were installed, each with four 2” wells. Also at that time, an upgradient 2” well was installed, and a small cluster of three 1.25” wells were installed. Two aquifers underlie the KCD1 dairy site, a shallow perched aquifer and a more regionally extensive deep aquifer. The deep aquifer is instrumented with one 2” well screened at 178-180’ below ground surface (bgs) that was installed in September 2003. The remaining monitor wells are all in the shallow perched aquifer and are screened between 18’ and 65’ bgs.

In August 2004, shortly before the second set of well clusters were installed, a CPT/DP survey (see methods section) was conducted across the site (Figure ??). Depth discrete water and soils samples were collected at this time, after which the holes were grouted and abandoned. With the exception of the upgradient monitor well near the canal, CPT/DP sites included locations near all of the multi-level monitor well clusters.

The production wells are screened in both the shallow and deep aquifer, and have 20-30’ long screens. Domestic supply wells, one of which was sampled, are screened in the deep aquifer, and typically have 20’ long screens. Agricultural supply wells, eight of which were sampled, typically have 30’ long screens, with the top of the screen at 30’ bgs. Information on screen length and depth is from conversations with the water well company which installed the more recent wells and has extensive experience in the region (Figure ??).

KCD2 and KCD3 (Figure 1): The second and third Kings County dairy sites were sampled during initial screening of Kings County sites in August 2003. At each site, groundwater pumped from a domestic supply well was analyzed for inorganic cations and anions (including nitrate, nitrite and ammonia), dissolved gases by membrane-inlet mass spectrometry, and tritium/helium-3 mean groundwater age by noble gas mass spectrometry. Groundwater in the area is 120-150 feet below ground surface, and the Corcoran Clay is generally 400-450’ below ground surface and 90-100’ thick. At each

DRAFT - DO NOT DISTRIBUTE OR CIRCULATE

site, groundwater was sampled from wells screened between 200 and 300 feet below ground surface.

The second dairy was sampled again in April 2005. On this occasion, groundwater from the same domestic supply well sampled in 2003 was re-sampled, and manure lagoon and field water from six sampling locations was sampled. The groundwater was analyzed as before; while the lagoon water samples were analyzed for inorganic cations and anions (including nitrate, nitrite and ammonia), and dissolved gases by membrane-inlet mass spectrometry.

MCD and SCD (Figure 1, Appendix A-Figure 1: The Merced County and Stanislaus County Dairies (MCD and SCD) were sampled on three occasions: August 2003, April 2005 and June 2005. Almost 40 samples were taken broken down as follows: 30 MCD samples and 9 SCD samples; 28 groundwater samples from 22 wells, 1 lagoon water sample, and 1 tile drain sample. Groundwater samples were analyzed for field parameters (temperature, conductivity, dissolved oxygen and ORP); inorganic cations and anions (including nitrate, nitrite and ammonia), dissolved gases by membrane-inlet mass spectrometry, tritium/helium-3 mean groundwater age by noble gas mass spectrometry, stable isotopic composition of nitrate and water, and organic co-contaminants. Tritium/helium-3 samples were not taken from the surface water sampling sites. These sites and data from these sites are described in Harter et al. (2002)

DRAFT - DO NOT DISTRIBUTE OR CIRCULATE

METHODS

CPT/DP Methods: Standard cone penetrometer/direct push methods were used to characterize the shallow hydrostratigraphy at the site. The survey was accomplished using a 20-25 ton CPT rig and accompanying support rig. The dead weight of the CPT rig was used to push the cone penetrometer to depths up to 90 feet using a hydraulic ram located at the center of the truck. Soil parameters such as cone bearing, sleeve friction, friction ratio and pore water pressure were measured as the cone penetrometer was advanced. These measurements were sent through the cone rods to the CPT rig's on-board data acquisition system. All data was processed in real time in the field, and CPT plots of tip resistance, sleeve friction; friction ratio and pore pressure were provided in the field along with a table of interpreted soil parameters. For development of geostatistical models of subsurface hydraulic properties, soil behavior types determined by CPT (ROBERTSON et al., 1983) were calibrated and validated against a 200-foot continuous core log recovered from the first site (Figure ??)

After CPT logging, a second hole was developed for collecting depth-discrete groundwater and soil samples using direct push methods. For water, a Hydropunch groundwater sample was taken at specified depth intervals. The Hydropunch operates by pushing 1.75-inch diameter hollow rods with a steel tip. A filter screen is attached to the tip. At the desired sampling depth, the rods are retracted, exposing the filter screen and allowing for groundwater infiltration. A small diameter bailer is then used to collect groundwater samples through the hollow rod. Typically, 4 or more 40 ml VOA vials were collected. For soil, a piston-type soil sampler was used to collect undisturbed soil samples (12" long x 1" diameter) that were stored on ice or dry ice immediately upon retrieval. After completion of logging and sampling, CPT/DP sampling holes were grouted under pressure with bentonite using the support rig.

Drilling methods: Monitor wells were emplaced using standard methods. The first and deepest 200-foot bore-hole was drilled with a mud-rotary rig; subsequent wells were drilled using hollow-stem auger. In the deep 200-foot hole, continuous log core was recovered and logged by a State-certified geologist (Figure ??) and down-hole geophysical data were obtained, including caliper, gamma ray, electro-magnetic induction, and spontaneous potential and resistivity logs. Wells were cased with either 2" or 1.25" PVC pipe with short (generally 2') slotted screens and sand packs, and completed with a sanitary seal. Early wells (installed in 2003) were completed with stovepipe installation, which were subsequently converted to ground-level flush-mount installations in 2004 to accommodate farm activities. All wells installed in 2004 were completed with a flush-mount installation. The 2"-diameter wells were developed using standard bail, surge and pump methods.

Sample collection and field parameters: Groundwater samples were collected after purging the well by either pumping or bailing, after determining water level against a marked datum. Groundwater from production wells was sampled, whenever possible, from upstream of any storage or pressure tank. A variety of methods were used to draw samples from monitor wells, depending on their diameter. Two-inch diameter monitor

DRAFT - DO NOT DISTRIBUTE OR CIRCULATE

wells were sampled with a Grundfoss MP-1 submersible pump and Teflon-lined sample line. Smaller 1.25"-diameter monitor wells were sampled with small-diameter Teflon bailers or with a bladder pump and Teflon sample line.

When practical, field measurements of temperature (°C), conductivity ($\mu\text{S}/\text{cm}$), pH, dissolved oxygen (mg/L) and oxidation reduction potential (mV using Ag/AgCl with 3.33 mol/L KCl as the reference electrode) were carried out using a Horiba U-22 ® water quality analyzer. Sampling protocols were specific for different sets of analytes (see sampling sheet in Appendix C), and differed with regard to filtration, sample volume and container, the presence of headspace, and the use of gloves.

Chemical composition analysis: Samples for anions and cations were filtered in the field to 0.45 μm , and stored cold and dark until analysis. Anion (NO_3^- , SO_4^{2-} , Cl^- , F^- , Br^- , PO_4^{3-} , NO_2^-) and cation (Ca^{2+} , Mg^{2+} , Na^+ , K^+ , Li^+ , NH_4^+) concentrations were determined by ion chromatography using a Dionex DX-600. Total inorganic and organic carbon (TIC/TOC) was determined on unfiltered samples poisoned with mercuric chloride using a carbon analyzer (OI Analytical TOC Analyzer 1010). Dissolved inorganic carbon (DIC) concentrations were estimated in the water samples by employing the PHREEQC geochemical model (PARKHURST and APPELO, 2002) to achieve charge balance in the samples by adjusting and speciating DIC at the measured pH values. Dissolved organic carbon was also measured in a subset of samples as CO_2 gas pressure after acidification with orthophosphoric acid.

Sediment sulfur and carbon content was determined by elemental analysis by Actlabs (Ancaster, Ontario, Canada). Total C and S were determined on an ELTRA CS 2000 carbon sulfur analyzer. A weighed sample is mixed with iron chips and a tungsten accelerator and is then combusted in an oxygen atmosphere at 1370°C. The moisture and dust are removed and the CO_2 gas and SO_2 gas are measured by a solid-state infrared detector. Sulphate S was determined by elemental analysis of the residue from roasting at 850° C. Reduced S was determined by difference. Carbonate C was determined by digestion of the sample in 2 N perchloric acid followed by coulometric titration. Graphitic C was determined by elemental analysis of the residue from roasting at 600° C. Organic C was determined by difference.

Stable isotope mass spectrometry: Samples for nitrate N and O isotopic compositions are filtered in the field to 0.45 μm , and stored cold and dark until analysis. Anion and cation concentrations are determined by ion chromatography using a Dionex DX-600. The nitrogen and oxygen isotopic compositions ($\delta^{15}\text{N}$ and $\delta^{18}\text{O}$) of nitrate in 26 groundwater samples from KCD1 and MCD were measured at Lawrence Berkeley National Laboratory's Center for Isotope Geochemistry using a version of the denitrifying bacteria procedure (CASCIOTTI et al., 2002) as described in Singleton et al. (SINGLETON et al., 2005). In addition, the nitrate from 34 samples were extracted by ion exchange procedure of (SILVA et al., 2000) and analyzed for $\delta^{15}\text{N}$ at the University of Waterloo. Analytical uncertainty is 0.3 ‰ for $\delta^{15}\text{N}$ of nitrate and 0.5‰ for $\delta^{18}\text{O}$ of nitrate.

DRAFT - DO NOT DISTRIBUTE OR CIRCULATE

Isotopic compositions of hydrogen and oxygen in water ($\delta^2\text{H}$ and $\delta^{18}\text{O}$) were determined at LLNL using a VG Prism II $\text{\textcircled{R}}$ isotope ratio mass spectrometer, and are reported in per mil values relative to the Vienna Standard Mean Ocean Water (VSMOW). Isotopic composition of oxygen in water using the CO_2 equilibration method (EPSTEIN and MAYEDA, 1953), and have an analytical uncertainty of 0.1‰. Hydrogen isotope compositions were determined using the Zn reduction method (COLEMAN et al., 1982)

Membrane inlet mass spectrometry (excess N_2): Previous studies have used gas chromatography and/or mass spectrometry to measure dissolved N_2 gas (BOHLKE and DENVER, 1995; MCMAHON and BOHLKE, 1996; VOGEL et al., 1981; WILSON et al., 1990; WILSON et al., 1994). Both methods require extraction of a gas sample, which adds time and can limit precision. Membrane inlet mass spectrometry (MIMS) allows precise and fast determination of the concentrations of nitrogen, oxygen and argon dissolved in groundwater samples without a separate extraction step. This method has been used to document denitrification in estuarine and ocean settings (AN et al., 2001; KANA et al., 1994), as well as for detection of volatile organic compounds in water (KETOLA et al., 2002). The MIMS technique has also proven useful for determining excess N_2 from denitrification in groundwater systems (BELLER et al., 2004).

Samples for N_2 , O_2 , Ar, CO_2 and CH_4 concentration were analyzed by MIMS. A water sample at atmospheric pressure is drawn into the MIMS through a thin silicone rubber tube inside a vacuum manifold. Dissolved gases readily permeate through the tubing into the analysis manifold, and are analyzed using a quadrupole mass spectrometer. Water vapor that permeates through the membrane is frozen in a dry ice cold trap before reaching the quadrupole. The gas abundances are calibrated using water equilibrated with air under known conditions of temperature, altitude and humidity (typically 18 °C, 183 m, and 100% relative humidity). A small isobaric interference from CO_2 at mass 28 (N_2) is corrected based on calibration with CO_2 -rich waters with known dissolved N_2 , but is negligible for most samples. Typical sample size is 5 mL, and each analysis takes approximately 3 minutes. Dissolved oxygen, methane, carbon dioxide and argon content are measured at the same time as nitrogen. Samples are collected for MIMS analysis in 40 mL amber glass VOA vials, with no headspace, and kept cold during transport. Samples are analyzed within 24 hours to minimize the risk of gas loss or biological fractionation of gas in the sample container. The MIMS is field portable, and can be used on site when fieldwork requires extended time away from the laboratory, or when samples cannot be readily transported to the laboratory.

Noble gas mass spectrometry ($^3\text{H}/^3\text{He}$ dating): Dissolved noble gas samples are collected in copper tubes, which are filled without bubbles and sealed with a cold weld in the field. Dissolved noble gas concentrations were measured at LLNL after gas extraction on a vacuum manifold and cryogenic separation of the noble gases. Concentrations of He, Ne, Ar and Xe were measured on a quadrupole mass spectrometer. Calculations of excess air and recharge temperature from Ne and Xe measurements are described in detail in Ekwurzel (2004), using an approach similar to that of Aeschbach-Hertig et al. (2000). The ratio of ^3He to ^4He was measured on a VG5400 mass spectrometer.

DRAFT - DO NOT DISTRIBUTE OR CIRCULATE

Tritium samples are collected in 1 L glass bottles. Tritium was determined by measuring ^3He accumulation after vacuum degassing each sample and allowing three to four weeks accumulation time. After correcting for sources of ^3He not related to ^3H decay (AESCHBACH-HERTIG et al., 1999; EKWURZEL et al., 1994), the measurement of both tritium and its daughter product ^3He allows calculation of the initial tritium present at the time of recharge, and apparent ages can be determined from the following relationship based on the production of tritiogenic helium ($^3\text{He}_{\text{trit}}$):

$$\text{Groundwater Apparent Age (years)} = -17.8 \times \ln(1 + ^3\text{He}_{\text{trit}}/^3\text{H})$$

The reported groundwater age is the mean age of the mixed sample, and furthermore, is only the age of the portion of the water that contains measurable tritium. Average analytical error for the age determinations is ± 1 year, and samples with ^3H that is too low for accurate age determination (<1 pCi/L) are reported as >50 years. Loss of ^3He from groundwater is not likely in this setting given the relatively short residence times, lack of water table fluctuations, and high infiltration rates from irrigation. Groundwater age dating has been applied in several studies of basin-wide flow and transport (EKWURZEL et al., 1994; POREDA et al., 1988; SCHLOSSER et al., 1988; SOLOMON et al., 1992). Mean ^3H - ^3He apparent ages are determined for water produced from 20 KCD monitor wells at depths of 6 m to 54 m, and from 14 sites at MCD. The apparent ages give a measure of the time elapsed since water entered the saturated zone, but only of tritium-containing portion of the groundwater sample. Apparent ages therefore give the mean residence time of the fraction of recently recharged water in a sample, and are especially useful for comparing relative ages of water from different locations at each site. The absolute mean age of groundwater may be obscured by mixing along flow paths due to heterogeneity in the sediments (WEISSMANN et al., 2002b).

Quantitative real-time Polymerase Chain Reaction (rt-qPCR): We have developed a simple bioassay to quantify populations of denitrifying bacteria in moderate amounts of aquifer material (on the order for a few grams of sediment or filtrate). The method detects the presence of bacterial genes that encode nitrite reductase, a central enzyme involved in denitrification. The assay is not species-specific, but rather a functional test for the presence of bacterial populations capable of nitrite reduction. Nitrite reduction is considered to be the “committed” step in denitrification, and bacteria capable of nitrite reduction are generally also capable of nitric and nitrous oxide reduction to nitrogen gas (TIEDJE, 1988). Currently, the assay provides valuable information on the distribution of denitrifying bacteria populations in aquifers. Ultimately, data on denitrifier populations (i.e., biomass) can be used in combination with specific (i.e., biomass-normalized) denitrification rate constants to determine subsurface denitrification rates.

Real-time, quantitative Polymerase Chain Reaction (rt-qPCR) analysis (Gibson et al., 1996; Heid et al., 1996; Holland et al., 1991), specifically the 5'-nuclease or TaqMan[®] assay, was chosen for this assay because it offers many advantages over traditional methods used to detect specific bacterial populations in environmental samples, such as DNA: DNA hybridization (Beller et al. 2002). Although most real-time PCR applications to date have involved the detection and quantification of pathogenic bacteria in food or

DRAFT - DO NOT DISTRIBUTE OR CIRCULATE

animal tissue, the technique has recently been used to quantify specific bacteria in environmental samples (Hristova et al., 2001; Suzuki et al., 2000; Takai and Horikoshi, 2000).

Real-time qPCR is a rapid, sensitive, and highly specific method. The rt-qPCR assay developed targets two variants of the nitrite reductase gene: *nirS* (Fe-containing nitrite reductase) and *nirK* (Cu-containing nitrite reductase). Homologous gene sequences were used to develop a primer/probe set that encompasses functional *nir* genes of known denitrifying soil bacteria (including heterotrophic and autotrophic species) and that does not result in false positive detection of genes that are not associated with denitrification. The rt-qPCR primers and probes were designed based on multiple alignments of 14 *nirS* and 20 *nirK* gene sequences available in GenBank. During development of the assay, the first nitrite reductase gene (*nirS*) reported in an autotrophic denitrifying bacterium (*T. denitrificans*) was sequenced and amplified, and demonstrated to have high homology to *nirS* in a phylogenetically diverse set of heterotrophic denitrifying bacteria.

Real-time PCR was also be used to quantify total eubacterial population, based on detection of the sequence encoding the eubacterial 16S rRNA subunit, which is specific for bacteria.

Wastewater co-contaminants: A number of co-contaminants expected to occur on a dairy farm from the dairy operation proper or from associated field crop production were determined using GC-MS or LC-MS. Co-contaminants targeted included herbicides, pesticides, VOCs, fecal sterols, caffeine and nonylphenol. The analysis of these compounds and a discussion of their distribution at the dairy sites is in Moran et al. (2006).

DRAFT - DO NOT DISTRIBUTE OR CIRCULATE

DATA

Chemical, isotopic, dissolved gas, and groundwater age data for the KCD1 and MCD sites are discussed in Appendix A and Appendix B, and are tabulated in Table 1 of Appendix A and Table 1 of Appendix B. Chemical composition, stable isotope, and groundwater age data for KCD2, KCD3 and SCD2 are tabulated in Table 1 of the main report. In addition, membrane inlet mass spectrometry data for KCD2 is presented graphically in Figure ???. Neither Appendix A nor Appendix B contains sediment C and S data or bacterial population data, which are discussed below.

Sediment data: In zones sampled for groundwater at the KCD1 site, sediment texture as determined from well logging, CPT and laser diffraction particle size analysis ranges from sand to clayey silt (with trace to >95% fines). Sedimentary carbonate C is extremely low (generally < 0.003 wt %); organic C is low but generally detectable (0.05-0.10 wt %), although occasional beds have 0.1-1.3% organic C; sulfate S ranges from nondetectable (<0.017) to 0.08 wt%; and reduced S is only detectable in a few wells (<0.01 to 0.15 wt %). For organic C and total S, no strong vertical gradients exist, and no significant difference exists between sediment in the oxic groundwater column, sediment in the anoxic water column, and sediment at the interface. Sediment data are summarized in Table 2, and represented graphically in Figure ??? and Figure ???.

Bacterial population data: In this study we use the abundance of the *nir* gene, as determined by rt-qPCR, to map the vertical distribution of denitrifying bacterial populations in the saturated zone. We use the abundance of the eubacterial 16S rRNA gene, as determined by rt-PCR, to map the vertical distribution of total eubacteria in the subsurface. The analyses were performed on soil returned from four locations at the KCD1 dairy during the course of the DP sampling survey in August 2003. Soil samples were placed on ice upon recovery, and subsequently stored frozen until analysis. Total *nir* data are reported as gene copies per 5 g of sediment, and comprise both *nirS* and *nirK* assay results. Total eubacteria data are reported as cells per 5 g sediment. The data are tabulated in Table 3 and in Figure ???.

Relative abundances of *nirS*, *nirK* and eubacteria are consistent with previous studies in non-groundwater systems: *nirS* and *nirK* gene copies typically constitute ~5% and ~0.1% of total bacteria, respectively. Total *nir* abundance varies by almost four orders of magnitude and is not well-correlated with total eubacteria ($R^2 \sim 0.19$ for 5 locations with multiple depths). Peak populations occur either at or below the redoxcline where strong vertical gradients exist in ORP, nitrate and excess nitrogen. Where *nir* abundance is high, total *nir* gene copies tend to constitute a larger fraction of total bacteria (up to 18%).

The presence of high and localized *nir* populations near the interface between oxic high-nitrate groundwater and suboxic low-nitrate groundwater indicates active denitrification is occurring near that interface.

DRAFT - DO NOT DISTRIBUTE OR CIRCULATE

RESULTS AND DISCUSSION

Saturated-zone denitrification at KCD1 and MCD

Appendix A is a manuscript prepared for submittal to a peer-review journal. The manuscript addresses evidence for saturated-zone denitrification in groundwaters impacted by dairy operations. The manuscript abstract follows.

Results from field studies at two central California dairies (KCD1 and MCD) demonstrate the prevalence of saturated-zone denitrification in shallow groundwater with $^3\text{H}/^3\text{He}$ apparent ages of 30 years or younger. Confined animal feeding operations are suspected to be major contributors of nitrate to groundwater but saturated zone denitrification could effectively mitigate their impact to groundwater quality. Denitrification is identified and quantified using stable isotope compositions of nitrate coupled with measurements of excess N_2 and residual NO_3^- . Nitrate in dairy groundwater from this study has $\delta^{15}\text{N}$ values (4.3–61 ‰), and $\delta^{18}\text{O}$ values (-4.5–24.5 ‰) that plot with a $\delta^{18}\text{O}/\delta^{15}\text{N}$ slope of 0.5, consistent with denitrification. Dissolved gas compositions, determined by noble gas mass spectrometry and membrane inlet mass spectrometry, are combined to document denitrification and to determine recharge temperature and excess air content. Dissolved N_2 is found at concentrations well above those expected for equilibrium with air or incorporation of excess air, consistent with reduction of nitrate to N_2 . Fractionation factors for oxygen and nitrogen isotopes appear to be smaller ($\epsilon_{\text{N}} \approx -10\text{‰}$; $\epsilon_{\text{O}} \approx -5\text{‰}$) at a location where denitrification is found in a laterally extensive anoxic zone 5 m below the water table, compared with a site where denitrification occurs near the water table and is strongly influenced by localized lagoon seepage ($\epsilon_{\text{N}} \approx -50\text{‰}$; $\epsilon_{\text{O}} \approx -25\text{‰}$).

Spatial distribution of saturated-zone denitrification at the KCD1 site

At the KCD1 site, multiple lines of evidence indicate saturated-zone denitrification. These include the presence of excess nitrogen from denitrification at depth, the correlation between nitrate- $\delta^{15}\text{N}$ and $-\delta^{18}\text{O}$ (which has a slope characteristic of denitrification), and the presence of denitrifying bacteria (which occur at above background levels only where excess nitrogen is present). The lateral extent of denitrification at the site and the excess nitrogen and isotopic evidence for denitrification at the site are discussed in Appendix B. Bacterial distributions give valuable evidence for the localization of denitrification.

Denitrifying bacteria populations at the KCD1 site have a high dynamic range, with peak populations occurring at the oxic-anoxic interface in the perched aquifer where strong gradients in oxidation-reduction potential, nitrate and excess nitrogen exist. Denitrifying bacteria populations are not well correlated with total bacteria ($R^2 \sim 0.19$ for 5 locations with multiple depths). The relative population abundances of Nir gene copies, however, are consistent with previous studies in non-groundwater systems: *nirS* and *nirK* gene copies typically constitute $\sim 5\%$ and $\sim 0.1\%$ of total bacteria.

DRAFT - DO NOT DISTRIBUTE OR CIRCULATE

The depth of oxic-anoxic interface is remarkably constant at 37-41 feet bgs. This transition is not strongly correlated with lithology or sediment composition (organic-C or total-S content), although it generally occurs in sand. At the irrigated field monitoring sites, the redox interface corresponds to the interface between shallower “young” groundwater (having young apparent ^3H - ^3He ages and low mixing ratios of pre-1955 water) and deeper “old” groundwater (with higher fractions of pre-modern water). The depth of the zone corresponds to the top of several agricultural production pump screens in the area, suggesting that pumping may be a factor.

Saturated-zone denitrification at northern San Joaquin Valley dairy sites

Both of the northern dairy sites (MCD and SCD) are a part of the northern San Joaquin Valley monitoring network described in Harter et al. (2002). Chemical data from these sites have been used to calibrate and validate regional models for nitrogen loading to the shallow groundwater system (VAN DER SCHANS, 2001). The wells sampled are all shallow piezometers that draw first-encounter water, with the exception of one deeper domestic supply well (W-98, Table 1 of Appendix A). A significant finding of the current study is that evidence for saturated-zone denitrification at MCD and SCD only exists in first-encounter wells that are predicted by other criteria (groundwater gradient, the presence of ammonia, total dissolved solids, etc) to be impacted by recharge from lagoons or corrals, i.e. from the dairy operation proper. Wells so impacted include W02, W03, W16, W17, V01, and V21 on the MCD site (Table 1 of Appendix A), and Y03 and Y10 on the SCD site (Table 1). No evidence for denitrification exists in first-encounter wells that are impacted only by wastewater irrigation of either field crops (MCD) or of orchards (SCD). This finding is significant in two respects:

- The UC-Davis nitrate loading model for the region is in agreement with available spatial and time-series groundwater nitrate concentration data. The model does not explicitly consider denitrification of nitrogen fluxes from lagoons and corrals. The absence of evidence for denitrification in first encounter groundwater impacted by wastewater irrigation validates the model assumption that denitrification is not occurring and strengthens confidence in the model as a predictive tool.
- The deep domestic well W-98 is predicted by the UC-Davis model to have approximately 50 mg/L nitrate (T. Harter, personal communication). Groundwater from this well actually has very low nitrate (0.4 mg/L), but does have 45 mg/L nitrate-equivalent of excess N_2 indicating that the mass fluxes and transport in the model are accurate. The mean $^3\text{He}/^3\text{H}$ groundwater age also matches well with model travel time predictions. The good agreement between predicted nitrate and excess nitrogen in W-98 is consistent with a groundwater impacted by wastewater irrigation in which denitrification is occurring at some depth below the water table, as is the case at KCD1 in Kings County.
- The association of denitrification with groundwater impacted by manure lagoon seepage is consistent with the findings from the KCD1 study (see Appendix B)

DRAFT - DO NOT DISTRIBUTE OR CIRCULATE

To the extent that saturated-zone denitrification is significant and is associated with nitrogen loading from wastewater irrigation from dairy operations (as has been shown on one site, and indicated on another), the process needs to be considered when assessing total impact of dairy operations on the groundwater resource. The most effective way to characterize saturated-zone denitrification is the installation of multi-level monitor wells in conjunction with the determination of nitrate stable isotope composition and excess nitrogen content.

The impact of dairy manure lagoons on groundwater quality

Appendix B is a manuscript prepared for submittal to a peer-review journal. The manuscript addresses the impact of dairy manure lagoon seepage on groundwater quality, and discusses a new tracer for manure lagoon seepage. The manuscript abstract follows.

Dairy facilities and similar confined animal operation settings pose a significant nitrate contamination threat to groundwater via oxidation of animal wastes and subsequent transport through the subsurface. While nitrate contamination resulting from application of animal manure as fertilizer to fields is well recognized, the impact of manure lagoon leakage on groundwater quality is less well characterized. For this study, a dairy facility located in the southern San Joaquin Valley of California (KCD1) has been instrumented with monitoring wells as part of a two-year multidisciplinary study to evaluate nitrate loading and denitrification associated with facility operations. Among the multiple types of data collected from the site, groundwater and surface water samples have been analyzed for major cations, anions, pH, oxidation-reduction potential, dissolved organic carbon, and selected dissolved gases (CO_2 , CH_4 , N_2 , Ar, Ne). Modeling of geochemical processes occurring within the dairy site manure lagoons suggests substantial off-gassing of CO_2 and CH_4 in response to mineralization of organic matter. Evidence for gas ebullition is evident in low Ar and Ne concentrations in lagoon waters and in groundwaters downgradient of the lagoon, presumably as a result of gas “stripping”. Shallow groundwaters with Ar and Ne contents less than saturation with respect to atmosphere are extremely rare, making the fractionated dissolved gas signature an effective tracer for lagoon water in underlying shallow groundwater. Preliminary evidence suggests that lagoon water rapidly re-equilibrates with the atmosphere during furrow irrigation, allowing this tracer to also distinguish between seepage and irrigation as the source of lagoon water in underlying groundwater. Together with ion exchange and mineral equilibration reactions, identification of lagoon seepage helps to constrain key attributes of the local groundwater chemistry, including input and cycling of nitrogen, across the site.

A new tracer for manure lagoon seepage

The manuscript in Appendix B uses only data collected from the KCD1 site. To further test the hypothesis that gas stripping in biologically active manure lagoons, we sampled manure lagoon water from several locations at KCD2 site. At this site, manure-laden water flows from free stall flush lanes to a settling lagoon (Lagoon 1) through an intake

DRAFT - DO NOT DISTRIBUTE OR CIRCULATE

near the bottom of the lagoon to a larger holding lagoon (Lagoon 2) to a distribution standpipe to furrows in nearby fields. Samples were collected from the surface of Lagoon 1 near the outtake from the flush lanes, from the outlet of Lagoon 1 into Lagoon 2, from the surface of Lagoon 2 near the intake to the field distribution system, from a distribution standpipe, and from a field furrow about halfway down the length of the furrow. At the time of sample collection in April 2005, water in the distribution standpipe and in the field furrows was entirely from the manure lagoon, and was not mixed with well water or canal water. The results are shown in Figure ???.

As discussed in Appendix B, biological activity in the lagoon consumes oxygen and strips atmospheric gases from the lagoon water through ebullition of carbon dioxide and methane. This effect of this activity is evident in the absence of detectable oxygen in any of the lagoon samples, and in lagoon water argon partial pressures that are close to or far below saturation argon partial pressures. For non-reactive gases such as argon, the “gas-stripping” effect is most evident in the sample drawn from the outlet of Lagoon 1 into Lagoon 2, which presumably represents water from near the bottom of Lagoon 1. This sample has extremely low argon, and may be representative of lagoon seepage through the bottom or sides of the lagoon. Atmospheric re-equilibration does not take place until the water is delivered to the field – the water sample drawn from the distribution standpipe has no detectable oxygen, while surface water from half-down a furrow is at about 40% saturation. We suspect that percolation through the soil zone and through an oxic vadose zone, which is characterized by incorporation of excess air, will result in complete re-equilibration or over-equilibration with soil gases.

Dissolved gas samples from a number of manure lagoons on five dairy sites (KCD1, KCD2, MCD, and SCD) are characterized in general by deficiency in reactive and non-reactive atmospheric gases, and in detail by a wide range in non-reactive gas pressures from near equilibrium to far below equilibrium. The only other mechanism known to produce such signals is methane production either in marine sediments or in the deep subsurface in association with natural gas formation (see references in Appendix B). Currently the presence of an air “deficit” (i.e. atmospheric noble gases below saturation values) in shallow groundwater samples associated with dairy operations can be considered as indicative of the presence of a manure lagoon seepage component. To determine the mixing ratio of lagoon seepage with other water sources, however, will require a more quantitative understanding on the dissolved gas content in manure lagoons and manure lagoon seepage.

Source, fate and transport of dairy nitrate

On the KCD1 site, a number of observations indicate that the dairy operation and associated wastewater irrigation are the source of high nitrate in first encounter groundwaters at the site:

- The isotopic composition of nitrate-N and –O is consistent with a manure or septic nitrogen source (see Appendix A).

DRAFT - DO NOT DISTRIBUTE OR CIRCULATE

- The young age of the first encounter waters, which we have accurately simulated using an irrigation recharge model (see groundwater transport discussion below) are inconsistent with transport from offsite.
- Nitrate co-contaminants can be traced to a specific application event on the site (see MORAN, 2006). In a subset of wells on the site, norflurazon and its degradation product, desmethylnorflurazon, were detected. Norflurazon was applied to a corn field in excess of the intended amount approximately two years prior to sampling. The well closest to the field contains norflurazon; a more distal well contains the degradation product, desmethylnorflurazon.

The unconfined aquifer at KCD1 is strongly stratified with respect to electron donor concentration (oxygen and nitrate), redox state (ORP), and excess nitrogen. The transition zone is sharp: nitrate levels can drop from significantly above maximum contaminant levels to nondetectable over a depth range of five feet. Our data indicate that the water immediately below the transition zone also has a significant wastewater component.

- Low nitrate groundwaters have nitrate isotopic compositions that are consistent with denitrification of manure or septic source nitrate.
- Some low-nitrate waters have below-saturation dissolved gas pressures that indicate a component of manure lagoon seepage (see Appendix B and discussion of A New Tracer for Manure Lagoon seepage above.)
- Groundwater transport modeling (see discussion below) that assumes recharge dominated by wastewater irrigation accurately simulates the mean age and pre-modern mixing ratios for low-nitrate groundwaters below the transition zone.

The strong spatial association of high denitrifier bacterial populations with the transition zone is consistent with active denitrification occurring in this zone and being at least one source of denitrified groundwater seen below the zone. We cannot currently convert *nir* gene copy populations into denitrification rates, and so cannot estimate what fraction of denitrification occurs in the transition zone and what fraction occurs upgradient (proximal to a manure lagoon seepage plume, for example). What is clear, however, is that active denitrification is currently occurring on the dairy site in localized subsurface zones.

The relationship of the dairy operation (including wastewater irrigation and manure lagoon seepage) to the establishment of redox stratification and saturated-zone denitrification is more complex. Any model of the evolution of redox stratification and denitrification must first provide an electron donor and then produce a sharp transition zone (~5 feet in vertical extent) at a remarkably uniform depth across the site (~35-40 feet bgs). A number of hypotheses can be put forward:

- Lateral transport of manure lagoon seepage

DRAFT - DO NOT DISTRIBUTE OR CIRCULATE

- Reducing sediment conditions
- Vertical transport of wastewater irrigation
- Agricultural pumping and nitrogen loading from dairy operations

The first hypothesis is discussed in McNab et al. (Appendix B), and assumes that oxidation of organic carbon derived from manure creates the reducing conditions and provides the electron donor necessary for denitrification. While manure lagoon seepage is associated with excess nitrogen and does appear to drive denitrification locally, reactive transport modeling of lagoon seepage shows that the modeled zone of denitrification does not extend far from the lagoon, and that the modeled zone of low redox potential (where $pE < 0$) is localized. These model results are driven by the relative magnitudes of lagoon seepage and wastewater irrigation percolation rates, and are consistent with dissolved gas evidence indicating that lagoon seepage is not a major component in most site groundwaters. We conclude that manure lagoon seepage is not the cause of the laterally extensive reduced zone observed at the KCD1 site.

Reducing conditions in the natural system

A number of lines of evidence exist that indicate that reducing groundwater conditions are common in the region surrounding the KCD1 site. At a number of NAWQA sites in the region that are not believed to be impacted by dairy wastewater, nitrate in deeper waters is nondetectable and iron and manganese concentrations are high, an association consistent with suboxic or anoxic conditions (BUROW et al., 1998a; BUROW et al., 1998b). The most convincing evidence comes from the deep well at the KCD1 site (KCD1-1D, Table 1 in Appendix A). Groundwater in the lower aquifer sampled by this well is tritium dead with a mean groundwater age in excess of 50 years. Radiogenic ^4He content indicates an age on the order of 100 years or more. Neither nitrate nor excess nitrogen is present, indicating that source waters were low in inorganic nitrogen species. This groundwater has extremely low chloride and has isotopically lighter water than water sampled in the perched aquifer. Finally, this groundwater is reduced as indicated by both field ORP and DO measurements, and measurements of volatile sulfide compounds in the water. These observations are consistent with recharge by source waters un-impacted by agriculture and the occurrence of naturally reducing conditions along the flow path. The electron donor driving the evolution of the natural reducing system is unclear. The water is low in TOC (0.8 mg/L). Sediment organic C and reduced S contents are generally low (< 0.1 wt %), but are sufficient to produce reducing conditions, particularly since sediments with organic carbon contents of over 1 wt% have been characterized. Reducing conditions may have also been created during recharge (in the hyporheic zone during riverbank infiltration).

The existence of regionally reducing conditions is also evident in the redox state of sedimentary iron in site sediments. Above approximately 60' bgs, sediment core is stained with orange, red and brown ferric iron oxides; below 60', this stain is not present. The existence of a denitrification zone approximately 20-25' above the iron reduction zone is consistent with the energetics of these reactions.

DRAFT - DO NOT DISTRIBUTE OR CIRCULATE

Simple one-dimensional transport models that simulate the evolution of irrigation water as it vertically percolates through a sediment column and reacts with sediment along the percolation path can reproduce the sharpness and uniform depth of the observed redox boundary if 1) a layer of laterally extensive reducing sediment exists at the redox boundary or 2) if the boundary marks the transition between oxidizing and reducing sediment. Neither of these conditions is observed at the site. The redox boundary is not correlated with sediment texture, nor do any gradients exist in sedimentary organic C or reduced S that correlate with the depth of the redox boundary.

The impact of wastewater irrigation on groundwater quality

We have employed a reactive modeling approach using PHREEQC that addresses multispecies solute transport, soil-water reactions (mineral phase equilibria and ion exchange), and reaction kinetics for redox reactions involving nitrogen species as means for identifying the potential roles of different electron donors in the denitrification process at the site. The model parameters are shown below:

Parameters

- 10-m column
 - 10 volume elements (mobile pore water)
 - 10 volume elements (immobile pore water)
- Initial composition:
 - 25% Quartz
 - 15% Na-montmorillonite (ion exchanger)
 - 15% K-mica (“C” model; no K-mica = “X” model)
 - 1% Goethite (HFO surface)
 - 0.02 mol/kg organic carbon

Step 1: Set up initial conditions

- Flush column with 300 pore volumes:
 - 1 mM NaCl
 - mM KCl
- After flushing
 - Equilibrium with CO₂(g) and O₂(g), calcite, dolomite,
 - Undersaturated with gypsum

Step 2: Simulate irrigation

- Flush column with 2 pore volumes with a mixture of agricultural well water and lagoon water (~0.02 M NH₄⁺; ~0.01 M K⁺) – agricultural well water.
- Allow equilibration with calcite, ion exchanger, and HFO surface.

The reactive transport simulations results generally matches most major cation and anion distributions with depth. Moreover, the quantities of organic carbon required to produce a redox front (via diffusion-limited transport through low-permeability lenses) are consistent with measurements from soil samples (which are low). These results do not depend on any lagoon influence. Reactive transport modeling of vertical flow under the

DRAFT - DO NOT DISTRIBUTE OR CIRCULATE

irrigated field demonstrates that general geochemistry in wells distal from the manure lagoons can be explained *without* postulating a lagoon influence.

Stochastic groundwater modeling

A shallow perched aquifer exists in the distal region of the Kings River fan in San Joaquin Valley, California, as a result of overdraft in the deeper portion of the groundwater basin. The Kings River, unlined canals, and irrigation provide recharge to sustain the perched aquifer. The bottom of the perched aquifer is located about 25 m below ground surface (bgs). Agricultural wells at KCD1 with screened intervals approximately between 9 and 18 m bgs extract groundwater and mix it with dairy lagoon water for crop irrigation. The water table is typically 3 to 6 m bgs. Excess nitrogen data indicate that denitrification is occurring below the water table in a thin zone between 11 and 13 m bgs. Questions remain as to how the physical effects of vigorous groundwater pumping, irrigation, and canal recharge in the perched aquifer influence nitrate transport and denitrification processes.

We use the numerical flow and transport model NUFT to simultaneously simulate three-dimensional variably-saturated groundwater flow processes including canal recharge, agricultural pumping, and irrigation (CARLE et al., 2005). Nitrate in surface irrigation is simulated as a tracer. Heterogeneity of sandy, silty, and clayey zones in the system is characterized stochastically by applying transition probability geostatistics to data from 12 cone-penetrometer logs that vertically transect the perched aquifer. Heterogeneity is found to play a large role in creating the perched aquifer and in causing vertical compartmentalization of flow patterns. Most nitrate that reaches the water table is captured by agricultural pumping. However, the simulations indicate nitrate would reach greater depths if denitrification were not occurring.

Groundwater Hydrology. In the distal reaches of the Kings River within the Tulare Lake Basin, groundwater is extracted from both a perched zone (less than ~ 25 m deep) and a deep zone. Before the 1950's, water levels were nearly equal in both zones (DWR data). Overdraft in the deep zone has caused water level declines of over 100 feet (30 m). Perched zone water level elevations near Lemoore, California, persist well above the deep zone, as evident from DWR water level elevation maps for 2001-2002. The Kings River, unlined ditches and canals, and irrigation appear to provide recharge to sustain the perched aquifer. Crop irrigation uses canal diversions and both shallow and deep groundwater

Groundwater level elevations in different wells screened in the perched aquifer are remarkably similar over time and correlate to canal diversions. This suggests canal leakage and irrigation from canal diversions provides substantial recharge to the perched aquifer. Leakage from the canal is estimated at 10% by the irrigation district.

Dairy Site. Several dairies are located within the area of the perched aquifer. KCD1 is located about one mile east of the canal. The dairy grows much of its own feed – corn and alfalfa. The crops are irrigated primarily with water pumped from the shallow

DRAFT - DO NOT DISTRIBUTE OR CIRCULATE

aquifer. Crops are fertilized largely by mixing in effluent from the dairy operation that is collected in a lagoon. The lagoon water and other fertilizers provide sources of nitrate (NO₃) that appear to impact upper portions of the perched aquifer, but not lower portions of the perched aquifer or the deep aquifer. Other nearby farms also irrigate with canal diversions or groundwater pumped from the deep aquifer. Thus, overdraft from the deep aquifer helps, in part, to sustain the perched aquifer.

Modeling Approach. The modeling approach is designed to include consideration of the major factors and processes affecting groundwater flow, nitrate transport, and groundwater age dating:

- *Heterogeneity:* Use hydrofacies-based geostatistics.
- *Variably Saturated Flow:* Couple vadose zone and saturated zone using LLNL's NUFT code.
- *Boundary Head Conditions:* Use DWR water levels (w. temporal change) in perched and deep zone.
- *Perched and Deep Zone:* Use modeling to determine leakage that maintains perched condition.
- *Canal Leakage and Irrigation:* Distinguish different sources with different tracer simulations.
- *Tritium/Helium-3 Age Dating:* Add decay to tracer simulations, simulate apparent age estimate.
- *Groundwater Mixing:* Keep track of proportions of groundwater from different sources.

Geostatistics. Based on our interpretation of lithologic and CPT logs, we define three hydrofacies: "sand", "silt", and "clayey" categories. We quantify vertical and horizontal spatial variability (above) with a transition probability matrix using the CPT data categorized as hydrofacies. The solid lines represent 1-D Markov chain models used to develop a 3-D Markov chain model for stochastic simulation of realizations of hydrofacies architecture (below).

Hydraulic properties. Hydraulic properties are estimated from a combination of pump test analysis, soil core measurements, and model calibration. A Van Genuchten model is used to predict unsaturated hydraulic conductivity and capillary pressure. A continuous 1-m thick aquitard layer at 46-47 m elevation sustains the perched aquifer conditions. This aquitard layer correlates to a distinctive clay layer identified in our initial characterization lithologic log.

HYDROFACIES	K (m/d)	POROSITY
Sand	30	0.40
Silt	0.24	0.43
Clayey	0.014	0.45
Sandy Loam Soil	3.0	0.41
Aquitard	1.4e-6	0.45
canal (sandy)	10.0	0.41

DRAFT - DO NOT DISTRIBUTE OR CIRCULATE

Flow simulation. We use LLNL's NUFT code to simulate variably saturated flow according to the Richards equation. The simulation runs from late 1949 through 2001. Initial conditions are equilibrated to local head measurements and rainfall recharge of 1 cm/year. For boundary conditions, x-direction and bottom boundaries are conditioned to observed piezometric heads. A saturation=1.0 condition is applied to the canal when canal diversions occur (between early April and early October). Six wells are pumped during irrigation season at a rate greater and proportionate to crop evapotranspiration (ET). Recharge from irrigation is distributed proportionately to crop (ET), with about 25 cm/yr within the dairy crop fields and 10 cm/yr in surrounding areas.

Piezometric head in the perched aquifer remains relatively steady, although in fall 1992 (during a drought) head is noticeably lower. However, head in the deep aquifer drops considerably since the 1950s, to the extent that the top of the deep zone begins to desaturate in the 1960s. In effect, the aquifer system near the dairy field site now functions like two unconfined aquifers stacked on top of each other

Transport simulation. We use LLNL's NUFT code to simulate tracer transport from different recharge sources. The three primary recharge sources near the dairy site are canal, dairy crop irrigation, and irrigation from surrounding areas. The transport simulation results indicate that nitrate entering the saturated zone from dairy crop irrigation would be contained (like pump & treat?). Nitrate containment occurs within the high permeability sand-dominated perched aquifer because the dairy irrigation wells screened in the perched aquifer effectively capture nearly all recharge from dairy crop irrigation. The dairy irrigation wells pump groundwater at rates far higher than the recharge from dairy crop irrigation. The dairy irrigation wells also extract groundwater originating from irrigation of surrounding areas, canal leakage, and older groundwater

Apparent Age Simulation. Excess tritium was released into the atmosphere from above-ground nuclear weapons testing between 1952 to 1963. Bomb source tritium/helium-3 ratios provide a promising tool for estimating groundwater age, as the half life of tritium decay to helium-3 is 12.3 years. However, groundwater age estimates for a particular location in the saturated zone are inevitably affected by mixing of groundwater by diffusion and dispersion, transients, and non-point sampling (e.g. a well screen). Additionally, the bomb source of atmospheric tritium is non ideal because it varies in concentration over time. One should accept that tritium/helium-3 ratio measurement provides an *apparent* age estimate that, nonetheless, is a useful tool for estimating an averaged age of *mixed* groundwater.

We use NUFT to address the uncertainties of interpreting of tritium/helium-3 ratios. NUFT can account for a half life in tracer transport. To simulate apparent age of groundwater, we tag all surface recharge sources for two tracer scenarios with and without a half life. We simulate apparent groundwater age for two scenarios: (1) for an "ideal source" that assumes constant tritium concentration over time and (2) for a "bomb source" where tritium concentration varies as measured. The simulated tritium/helium-3 ratios are backed out of the differences in simulated concentration.

DRAFT - DO NOT DISTRIBUTE OR CIRCULATE

The simulation of apparent age show excellent agreement for two wells at toward the south of the dairy site and at the canal (below). Simulated ages are less than measured tritium/helium-3 ages in shallow groundwater probably because the simulations began decay at the ground surface and not the water table. Young groundwater at the well east of the dairy site might be explained by lack of a shallow clayey zone. These simulations of apparent age indicate variation in concentration of bomb source tritium will lead to some underestimation of groundwater age, particularly for older modern groundwater.

Conclusions. Coupling flow and transport simulations with groundwater age data and geostatistical simulations of hydraulic properties provides invaluable insights. The hydrofacies architecture consists of laterally continuous sand with interbeds of silt and clayey zones. Maintaining head and saturation in perched zone requires a continuous ~1 m-thick clay layer at ~ 25 m bgs. Flow simulation desaturates upper portions of the deep zone below the confining layer, and is consistent with observation of “dry zone” below ~ 25 m bgs. The perched zone draws older water and recharge mostly from irrigation and less so from canal leakage. The dairy site pumps more groundwater from the perched aquifer than is recharged by crop irrigation, and thus physically contains lateral and vertical migration of nitrate contamination. Without denitrification, nitrate concentrations would be greater below ~11.3-12.5 m (37-41 ft) bgs. Tritium/helium-3 groundwater ages are generally consistent with this flow model conceptualization; however, the current model could use better resolution and further calibration.

Agricultural overprint on an autotrophic system

What is the electron donor for the denitrification observed at the oxic-anoxic interface? Sediment organic-C and total-S concentrations in the deep and perched aquifer are comparable and are sufficient (assuming most of the S to be present in reduced phases) to create reducing conditions and support denitrification. PCR data do indicate the presence of autotrophic bacteria capable of using reduced S as an electron donor at one shallow site (Site 3) upgradient of the main dairy operation, and geochemical modeling is consistent with pyrite oxidation. The vertical variability in sediment C and S, however, does not explain the sharpness or location of the oxic-anoxic interface. Total organic carbon in site groundwaters varies from < 1 to 20 mg/L. Other potential dissolved-phase electron donors such as thiosulfate were not characterized. Geochemical modeling is consistent with organic C oxidation, although simple models that assume shallow and deep waters have similar initial chemical compositions do not match observed compositions tightly. At a shallow site (Site 2) downgradient of the lagoons, waters at the redox interface show evidence for a manure lagoon seepage component not evident in salinity.

An agricultural overprint on a autotrophic system: The deep aquifer at the KCD1 site consists of old water un-impacted by agricultural inputs. The water is tritium-dead and has a radiogenic ⁴He age of approximately 100 years. This water is also anoxic. The electron donor responsible for reducing conditions is not known. Groundwater DOC is

DRAFT - DO NOT DISTRIBUTE OR CIRCULATE

low, as is sediment solid-phase total S and organic C. Reduced sediment phases, however, are sufficient to create reducing conditions, even for slow redox processes such as solid-phase autotrophy given the age of the water. In addition to having a mean age that pre-dates the intensification of agricultural activities, especially with regards to fertilizer usage and manure production, the deep aquifer groundwater has a chemical composition that indicates the absence of significant agricultural input. Salinity, dissolved organic C, nitrate and excess nitrogen are all low.

The perched aquifer is impacted by agricultural operations. Total inorganic nitrogen ($\text{NO}_3 + \text{NO}_2 + \text{excess N}_2$) shows a secular trend with apparent groundwater age, with the highest concentrations in the young water. The isotopic composition of high-nitrate waters indicates a wastewater source. Groundwater transport modeling indicates that irrigation dominates recharge in the system, and results in the deep penetration of young oxic water with high nitrate from application of manure lagoon water to field crops.

Denitrification under irrigated fields occurs where oxic high-nitrate irrigation water mixes with older anoxic water. The mixing zone is sharp and at constant depth, and may be controlled by pumping. The availability of dissolved and sedimentary organic carbon and the lack of evidence for widespread distribution of autotrophic denitrifying bacteria or sedimentary sulfide in the perched aquifer are consistent with heterotrophic denitrification being operative in the agriculturally impacted perched aquifer.

DRAFT - DO NOT DISTRIBUTE OR CIRCULATE

References

- Aeschbach-Hertig W., Peeters F., Beyerle U., and Kipfer R. (1999) Interpretation of dissolved atmospheric noble gases in natural waters. *Water Resources Research* **35**(9), 2779-2792.
- Aeschbach-Hertig W., Peeters F., Beyerle U., and Kipfer R. (2000) Palaeotemperature reconstruction from noble gases in ground water taking into account equilibration with entrapped air. *Nature* **405**(6790), 1040-1044.
- An S. M., Gardner W. S., and Kana T. (2001) Simultaneous measurement of denitrification and nitrogen fixation using isotope pairing with membrane inlet mass spectrometry analysis. *Applied and Environmental Microbiology* **67**(3), 1171-1178.
- Beller H. R., Madrid V., Hudson G. B., McNab W. W., and Carlsen T. (2004) Biogeochemistry and natural attenuation of nitrate in groundwater at an explosives test facility. *Applied Geochemistry* **19**(9), 1483-1494.
- Bohlke J. K. and Denver J. M. (1995) Combined use of groundwater dating, chemical, and isotopic analyses to resolve the history and fate of nitrate contamination in two agricultural watersheds, Atlantic Coastal Plain, Maryland. *Water Resources Research* **31**(9), 2319-2339.
- Burow K. R., Shelton K. R., and Dubrovsky N. M. (1998a) Nitrate and pesticides in ground water in the eastern San Joaquin Valley, California: Occurrence and trends. U.S. Geological Survey Water-Resources Investigations Report 98-4040A, 33 pp.
- Burow K. R., Shelton K. R., and Dubrovsky N. M. (1998b) Occurrence of nitrate and pesticides in ground water beneath three agricultural land-use settings in the eastern San Joaquin Valley, California, 1993-1995. U.S. Geological Survey Water-Resources Investigations Report 97-4284, 51 pp.
- Burrow K. R., Shelton K. R., and Dubrovsky N. M. (1998) Occurrence of nitrate and pesticides in ground water beneath three agricultural land-use settings in the eastern San Joaquin Valley, California, 1993-1995. United States Geological Survey Water-Resources Investigations Report 97-4284, 51 pp.
- California DWR. (2003) California's Groundwater. California Department of Water Resources Bulletin 118 (2003 Update Public Review Draft).
- Carle S. F., Esser B. K., McNab W. W., Moran J. E., and Singleton M. J. (2005) Simulation of canal recharge, pumping, and irrigation in a heterogeneous perched aquifer: Effects on nitrate transport and denitrification (abstr.). *25th Biennial Groundwater Conference and 14th Annual Meeting of the Groundwater Resources Association of California (Sacramento, CA; October 25-26, 2005)*.
- Casciotti K. L., Sigman D. M., Hastings M. G., Bohlke J. K., and Hilkert A. (2002) Measurement of the oxygen isotopic composition of nitrate in seawater and freshwater using the denitrifier method. *Analytical Chemistry* **74**(19), 4905-4912.
- Coleman M. L., Shepherd T. J., Durham J. J., Rouse J. E., and Moore G. R. (1982) Reduction of water with zinc for hydrogen isotope analysis. *Analytical Chemistry* **54**(6), 993-995.
- Ekwrzel B. (2004) LLNL Isotope Laboratories Data Manual. Lawrence Livermore National Laboratory, 133 pp.

DRAFT - DO NOT DISTRIBUTE OR CIRCULATE

- Ekwurzel B., Schlosser P., Smethie W. M., Plummer L. N., Busenberg E., Michel R. L., Weppernig R., and Stute M. (1994) Dating of shallow groundwater - comparison of the transient tracers H-3/He-3, chlorofluorocarbons, and Kr-85. *Water Resources Research* **30**(6), 1693-1708.
- Epstein S. and Mayeda T. K. (1953) Variation of O-18 content of waters from natural sources. *Geochim. Cosmochim. Acta* **4**, 213-224.
- Gibson U. E. M., Heid C. A., and Williams P. M. (1996) A novel method for real time quantitative RT-PCR. *PCR Methods & Applications* **6**(10), 995-1001.
- Harter T., Davis H., Mathews M. C., and Meyer R. D. (2002) Shallow groundwater quality on dairy farms with irrigated forage crops. *Journal of Contaminant Hydrology* **55**(3-4), 287-315.
- Heid C. A., Stevens J., Livak K. J., and Williams P. M. (1996) Real time quantitative PCR. *PCR Methods & Applications* **6**(10), 986-994.
- Holland P., Abramson R., Watson R., and Gelfand D. (1991) Detection of Specific Polymerase Chain Reaction Product by Utilizing the 5' \rightarrow 3' Exonuclease Activity of *Thermus aquaticus* DNA Polymerase. *PNAS* **88**(16), 7276-7280.
- Hristova K. R., Lutenegger C. M., and Scow K. M. (2001) Detection and quantification of methyl tert-butyl ether-degrading strain PM1 by real-time TaqMan PCR. *Applied & Environmental Microbiology* **67**(11), 5154-5160.
- Kana T. M., Darkangelo C., Hunt M. D., Oldham J. B., Bennett G. E., and Cornwell J. C. (1994) Membrane inlet mass spectrometer for rapid high precision determination of N₂, O₂, and Ar in environmental water samples. *Analytical Chemistry* **66**(23), 4166-4170.
- Ketola R. A., Kotiaho T., Cisper M. E., and Allen T. M. (2002) Environmental applications of membrane introduction mass spectrometry. *Journal of Mass Spectrometry* **37**(5), 457-476.
- Lowry P. (1987) Hilmar Ground Water Study. California EPA Regional Water Quality Control Board - Central Valley Region, 56 pp.
- McMahon P. B. and Bohlke J. K. (1996) Denitrification and mixing in a stream-aquifer system: Effects on nitrate loading to surface water. *Journal of Hydrology* **186**(1-4), 105-128.
- Moran J. E. (2006) California GAMA Program: Fate and Transport of WasteWater Indicators: Results from Ambient Groundwater and from Groundwater Directly Influenced by Wastewater. Lawrence Livermore National Laboratory, 58 pp.
- Page R. W. and Balding G. O. (1973) Geology and quality of water in the Modesto-Merced Area, San Joaquin Valley, California. U. S. Geological Survey Water Resources Investigation 6-73, 85 pp.
- Parkhurst D. L. and Appelo C. A. J. (2002) User's Guide to PHREEQC (Version 2) - A Computer Program for Speciation, Batch Reaction One-Dimensional Transport, and Inverse Geochemical Calculations. U. S. Geological Survey Water-Resources Investigations Report 99-4259.
- Poreda R. J., Cerling T. E., and Solomon D. K. (1988) Tritium and helium-isotopes as hydrologic tracers in a shallow unconfined aquifer. *Journal of Hydrology* **103**(1-2), 1-9.

DRAFT - DO NOT DISTRIBUTE OR CIRCULATE

- Robertson P. K., Campanella R. G., and Wightman A. (1983) SBT-CPT Correlations. *Journal Of Geotechnical Engineering-ASCE* **109**(11), 1449-1459.
- Schlosser P., Stute M., Dorr H., Sonntag C., and Munnich K. O. (1988) Tritium He-3 dating of shallow groundwater. *Earth and Planetary Science Letters* **89**(3-4), 353-362.
- Silva S. R., Kendall C., Wilkison D. H., Ziegler A. C., Chang C. C. Y., and Avanzino R. J. (2000) A new method for collection of nitrate from fresh water and the analysis of nitrogen and oxygen isotope ratios. *Journal of Hydrology* **228**(1-2), 22-36.
- Singleton M. J., Woods K. N., Conrad M. E., Depaolo D. J., and Dresel P. E. (2005) Tracking sources of unsaturated zone and groundwater nitrate contamination using nitrogen and oxygen stable isotopes at the Hanford Site, Washington. *Environmental Science & Technology* **39**(10), 3563-3570.
- Solomon D. K., Poreda R. J., Schiff S. L., and Cherry J. A. (1992) Tritium and He-3 as groundwater age tracers in the Borden Aquifer. *Water Resources Research* **28**(3), 741-755.
- Suzuki M. T., Taylor L. T., and DeLong E. F. (2000) Quantitative analysis of small-subunit rRNA genes in mixed microbial populations via 5'-nuclease assays. *Applied & Environmental Microbiology* **66**(11), 4605-4614.
- Takai K. and Horikoshi K. (2000) Rapid detection and quantification of members of the archaeal community by quantitative PCR using fluorogenic probes. *Applied & Environmental Microbiology* **66**(11), 5066-+.
- Tiedje J. M. (1988) Ecology of denitrification and dissimilatory nitrate reduction to ammonium. In *Biology of Anaerobic Microorganisms* (ed. A. J. B. Zehnder), pp. 179-244. John Wiley & Sons.
- USDA National Resource Conservation Service. (2006) Soil Survey Geographic (SSURGO) Database. <http://www.ncgc.nrcs.usda.gov/products/datasets/ssurgo/>.
- Van der Schans M. (2001) Nitrogen Leaching from Irrigated Dairy Farms in Merced County, California: Case Study and Regional Significance, MS Thesis, Wageningen University (advisors, A. Leijnse and T. Harter), 58 p.
- Vogel J. C., Talma A. S., and Heaton T. H. E. (1981) Gaseous nitrogen as evidence for denitrification in groundwater. *Journal of Hydrology* **50**, 191-200.
- Weissmann G. S., Bennett G. L., V, and Fogg G. E. (2003) Appendix 2: Stratigraphic sequences of the Kings River alluvial fan formed in response to Sierra Nevada glacial cyclicity. In *Tectonics, Climate Change, and Landscape Evolution in the Southern Sierra Nevada, California (Friends of the Pleistocene Pacific Cell, 2003 Fall Field Trip, October 3-5)* (ed. G. Stock), pp. 41-50.
- Weissmann G. S., Carle S. F., and Fogg G. E. (1999) Three dimensional hydrofacies modeling based on soil surveys and transition probability geostatistics. *Water Resources Research* **35**(6), 1761-1770.
- Weissmann G. S. and Fogg G. E. (1999) Multi-scale alluvial fan heterogeneity modeled with transition probability geostatistics in a sequence stratigraphic framework. *Journal of Hydrology* **226**(1-2), 48-65.
- Weissmann G. S., Mount J. F., and Fogg G. E. (2002a) Glacially driven cycles in accumulation space and sequence stratigraphy of a stream-dominated alluvial fan, San Joaquin valley, California, USA. *Journal of Sedimentary Research* **72**(2), 240-251.

DRAFT - DO NOT DISTRIBUTE OR CIRCULATE

- Weissmann G. S., Zhang Y., LaBolle E. M., and Fogg G. E. (2002b) Dispersion of groundwater age in an alluvial aquifer system. *Water Resources Research* **38**(10), art. no.-1198.
- Wilson G. B., Andrews J. N., and Bath A. H. (1990) Dissolved gas evidence for denitrification in the Lincolnshire limestone groundwaters, Eastern England. *Journal of Hydrology* **113**, 51-60.
- Wilson G. B., Andrews J. N., and Bath A. H. (1994) The nitrogen isotope composition of groundwater nitrates from the East Midlands Triassic Sandstone Aquifer, England. *Journal of Hydrology* **157**(1-4), 35-46.

DRAFT

DRAFT - DO NOT DISTRIBUTE OR CIRCULATE

Table 1: KCD2, KCD3, & SCD Site Data
Field Parameters, chemical composition, groundwater age, recharge temperature, excess air, stable isotopic composition, excess nitrogen
 (Unless otherwise indicated, all analytes are reported as mg/L; nitrate is reported as nitrate)

Name	Collection date	pH	DO	TOC	Na ⁺	K ⁺	Ca ⁺	Mg ⁺⁺	Cl ⁻	SO ₄ ⁻	NO ₃ ⁻	NO ₂ ⁻	NH ₄ ⁺	excess N ₂ (NO ₃ ⁻ equiv)	Br ⁻	F ⁻	Li ⁻	PO ₄ ⁻	³ H/ ³ He age (yr)	Recharge T (°C)	Excess air (cc STP/g)	H ₂ O-δ ¹⁸ O (‰ SMOW)	NO ₃ ⁻ -δ ¹⁵ N (‰ Air)	NO ₃ ⁻ -δ ¹⁸ O (‰ SMOW)
KCD2 DW-1	2005/04/26	8.2	0.2		105	1	10	0	64	41	7	0.11	<0.02	2	0.21	0.06	0.005	0.99		15	8.8E-03	-11.1		
KCD3 DW-1	2003/08/21				87	0	54	1	134	57	9	1.22	nd		0.05	0.14	nd					-11.7	17.7	10.6
SCD1 Y-03	2005/03/08	6.8	0.6	18	215	4	124	55	59	199	185	0.41	<0.02	37	0.36	0.11	0.007	<0.04			2.5E-01	-9.8		
SCD1 Y-10	2005/03/08	7.0	5.3	3	82	137	110	81	143	16	42	1.31	137	nd	0.54	0.17	0.008	<0.04		18	9.8E-04	-9.1		
SCD1 Y-13	2003/08/26	7.5			28	5	146	41	48	169	58		<0.02		0.15	0.43	0.005	0.22	>50	16	2.0E-02	-11.0		
SCD1 Y-14	2003/08/26	7.3			63	5	146	55	57	233	167	0.05	<0.02	nd	0.12	0.26	0.003	0.22				-11.5		
SCD1 Y-15	2003/08/26	7.3			50	5	44	54	50	98	62	0.01	<0.02		0.12	0.23	0.006	0.24				-9.7		
SCD1 Y-16	2003/08/26	7.0			48	3	181	43	34	172	201	0.02	<0.02	nd		0.07	0.009	0.29	9	17	1.4E-02	-10.3		
SCD1 Y-17	2003/08/26	7.2			145	6	223	69	75	488	178		<0.02	nd	0.40	0.15	0.004	0.24	9		1.6E-03	-10.5		
SCD1 Y-18	2003/08/26	7.1			132	7	138	45	52	205	207	0.07	<0.02	nd		0.17	0.009	4.44	8	17	8.0E-03	-9.6		

DRAFT - DO NOT DISTRIBUTE OR CIRCULATE

Table 2: KCD1 Site Sediment C, S Data

KCD well cluster	Texture	Depth (ft)	Total C Tot C (wt%) (2sd)	Carb C Carb C (wt%) (2sd)	Org C Org C (wt%) (2sd)	Total S Total S (wt%) (2sd)	Sulfate S Sulfate S (wt%) (2sd)	Reduced S Reduced S (wt%) (2sd)
Site 1	Silty Sand	18	0.079 0.008	0.007 0.002	0.072 0.008	0.057 0.006	0.054 0.011	
Site 1	Clayey Silt	21	0.065 0.007		0.065 0.007	0.009 0.004		
Site 1	Sandy Silt	24	0.042 0.005		0.042 0.005	0.011 0.004		
Site 1	Clayey Silt	26	0.044 0.005		0.044 0.005	0.013 0.004		
Site 1	Sand	33	0.064 0.006		0.064 0.006	0.012 0.004		
Site 1	Sand	38	0.138 0.014	0.006 0.002	0.132 0.014	0.011 0.004	0.017 0.011	
Site 1	Sand	48	0.108 0.011	0.002 0.001	0.107 0.011	0.070 0.007	0.022 0.011	0.047 0.013
Site 1	Silt	61	0.050 0.005		0.050 0.005	0.011 0.004		
Site 1	Sandy Silt	69	0.066 0.007		0.066 0.007	0.022 0.004	0.019 0.011	
Site 1	Silty Sand	76	1.299 0.130		1.299 0.130	0.155 0.016	0.077 0.011	0.078 0.019
Site 1	Sand	77	0.207 0.021		0.207 0.021	0.181 0.018	0.034 0.011	0.147 0.021
Site 1	Sandy Silt	171	0.074 0.007	0.011 0.002	0.064 0.008	0.012 0.004	0.019 0.011	
Site 1	Sand	178	0.072 0.007	0.003 0.002	0.069 0.007	0.016 0.004	0.015 0.011	
Site 1	Silt	185	0.037 0.005		0.037 0.005	0.025 0.004		
Site 2	Sand	16	0.101 0.010		0.101 0.010	0.012 0.004		
Site 2	Sand	21	0.107 0.011		0.107 0.011	0.009 0.004		
Site 2	Silt	22	0.040 0.005		0.040 0.005	0.010 0.004		
Site 2	Sandy Silt	26	0.036 0.005		0.036 0.005	0.009 0.004		
Site 2	Sand	31	0.061 0.006		0.061 0.006	0.009 0.004	0.017 0.011	
Site 2	Clayey Silt	32	0.052 0.005		0.052 0.005	0.010 0.004		
Site 2	Sand	37	0.037 0.005		0.037 0.005	0.010 0.004	0.022 0.011	
Site 2	Sandy Silt	41	0.080 0.008		0.080 0.008	0.007 0.004		
Site 2	Sand	43	0.028 0.005		0.028 0.005	0.012 0.004	0.020 0.011	
Site 3	Sandy Silt	11	0.043 0.005		0.043 0.005	0.011 0.004	0.021 0.011	
Site 3	Silt	14	0.035 0.005		0.035 0.005	0.011 0.004		
Site 3	Sandy Silt	17	0.045 0.005		0.045 0.005	0.041 0.007	0.038 0.005	
Site 3	Sand	20	0.083 0.008		0.083 0.008	0.011 0.004		
Site 3	Sand	27	0.080 0.008		0.080 0.008	0.015 0.004		
Site 3	Sand	32	0.147 0.015	0.014 0.002	0.132 0.015	0.025 0.004	0.035 0.011	
Site 3	Sand	36	0.073 0.007	0.004 0.002	0.068 0.007	0.019 0.004	0.023 0.011	
Site 3	Sand	40	0.059 0.006	0.002 0.001	0.057 0.006	0.018 0.004	0.016 0.011	
Site Temp	Clayey Silt	5	0.187 0.019		0.187 0.019	0.010 0.004	0.019 0.011	
Site Temp	Clayey Silt	8	0.107 0.011	0.001 0.001	0.106 0.011	0.008 0.004	0.016 0.011	
Site Temp	Clayey Silt	8	0.181 0.018		0.181 0.018	0.020 0.004	0.015 0.011	
Site Temp	Sandy Silt	14	0.070 0.007		0.070 0.007	0.009 0.004	0.023 0.011	
Site Temp	Clayey Silt	16	0.058 0.006		0.058 0.006	0.011 0.004	0.021 0.011	
Site Temp	Clayey Silt	23	0.035 0.005		0.035 0.005	0.008 0.004	0.019 0.011	
Site Temp	Sand	27	0.029 0.005		0.029 0.005	0.007 0.004	0.017 0.011	
Site Temp	Clayey Silt	28	0.050 0.005		0.050 0.005	0.008 0.004		
Site Temp	Sand	36	0.057 0.006	0.003 0.002	0.053 0.006	0.008 0.004	0.016 0.011	

Table 3. KCD1 Sediment PCR Data

KCD1 Well Cluster	Depth (ft)	Total <i>Nir</i> (gene copies/ 5 g sediment)	Total eubacteria (cells/ 5 g sediment)
Site 1	21	7.9E+03	1.1E+06
Site 1	27	nd	3.9E+06
Site 1	29	1.1E+04	1.0E+06
Site 1	30	5.1E+03	3.9E+05
Site 1	32	3.8E+03	1.9E+06
Site 1	36	1.1E+05	6.7E+06
Site 1	45	9.5E+03	6.9E+05
Site 2	29	9.6E+04	2.0E+06
Site 2	31	1.1E+04	5.4E+05
Site 2	34	1.6E+05	3.8E+06
Site 2	36	2.8E+05	1.2E+07
Site 2	38	2.2E+07	1.7E+08
Site 2	40	1.3E+06	1.9E+07
Site 2	44	5.6E+03	1.4E+05
Site 3	30	6.6E+03	5.9E+05
Site 3	38	3.6E+04	9.6E+05
Site 3	40	3.4E+04	2.6E+06
Site 3	42	9.6E+04	2.1E+06
Site 3	44	3.7E+04	7.4E+05
Site 3	46	1.9E+05	7.5E+06
Site 3	48	1.4E+05	6.9E+06
Site 4	28	2.5E+04	6.9E+05
Site 4	33	3.0E+04	1.1E+06
Site 4	43	1.9E+05	1.8E+06
Site 4	45	9.1E+04	4.9E+05
Site 4	47	7.2E+04	5.2E+05
Site 4	49	4.6E+04	1.7E+06

APPENDIX A

Saturated zone denitrification: potential for natural attenuation of nitrate contamination in shallow groundwater under dairy operations

M. J. Singleton^{1*}, B. K. Esser¹, J. E. Moran¹, G. B. Hudson¹, W. W. McNab², T. Harter³

¹*Chemical Biology & Nuclear Science Division, Lawrence Livermore National Laboratory*

²*Environmental Restoration Division, Lawrence Livermore National Laboratory*

³*Department of Land, Air, and Water Resources, University of California at Davis*

* *Corresponding Author, P.O. Box 808, L-231, Livermore, California, 94551; Telephone (925) 424-2022; Fax (925) 422-3160; Email singleton20@llnl.gov*

Abstract

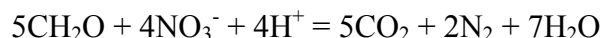
We present results from field studies at two central California dairies that demonstrate the prevalence of saturated-zone denitrification in shallow groundwater with $^3\text{H}/^3\text{He}$ apparent ages of 30 years or younger. Confined animal feeding operations are suspected to be major contributors of nitrate to groundwater but saturated zone denitrification could effectively mitigate their impact to groundwater quality. Denitrification is identified and quantified using stable isotope compositions of nitrate coupled with measurements of excess N_2 and residual NO_3^- . Nitrate in dairy groundwater from this study has $\delta^{15}\text{N}$ values (4.3–61 ‰), and $\delta^{18}\text{O}$ values (-4.5–24.5 ‰) that plot with a $\delta^{18}\text{O}/\delta^{15}\text{N}$ slope of 0.5, consistent with denitrification. Dissolved gas compositions, determined by noble gas mass spectrometry and membrane inlet mass spectrometry, are combined to document denitrification and to determine recharge temperature and excess air content. Dissolved N_2 is found at concentrations well above those expected for equilibrium with air or incorporation of excess air, consistent with reduction of nitrate to N_2 . Fractionation factors for oxygen and nitrogen isotopes appear to be smaller ($\epsilon_{\text{N}} \approx -10\text{‰}$; $\epsilon_{\text{O}} \approx -5\text{‰}$) at a location where denitrification is found in a laterally extensive anoxic zone 5 m below the water table, compared with a site where denitrification occurs near the water table and is strongly influenced by localized lagoon seepage ($\epsilon_{\text{N}} \approx -50\text{‰}$; $\epsilon_{\text{O}} \approx -25\text{‰}$).

Introduction

High concentrations of nitrate, a cause of methemoglobinemia in infants (1), are a national problem in the United States (2), and nearly 10% of public drinking water wells in the state of California are polluted with nitrate at concentrations above the maximum contaminant level (MCL) for drinking water set by the US Environmental Protection Agency (California Department of Health Services, August 2003 data from the online Geotracker database maintained by the California State Water Resources Control Board, <http://geotracker.swrcb.ca.gov/>). The federal MCL is 10 mg/L as N, equivalent to the California EPA limit of 45 mg/L as NO₃⁻ (all nitrate concentrations are hereafter given as NO₃⁻). Nearly 25% of California's remaining public drinking water wells have reported maximum nitrate levels (20 to 45 mg/L NO₃⁻) that are elevated or close to the MCL and in the range considered to indicate anthropogenic impact (>13-18 mg/L) (3-5). In the agricultural areas of California's Central Valley, it is not uncommon to have nearly half the active drinking water wells produce groundwater close to or above the MCL for nitrate. The major sources of this nitrate are septic discharge, fertilization using natural (e.g. manure) or synthetic nitrogen sources, and confined animal feeding operations. Dairies are the largest confined animal operations in California, with a total herd size of 1.7 million milking cows (6).

Denitrification is the microbially mediated reduction of nitrate to gaseous N₂. Denitrification in the unsaturated zone has been recognized as an important process in manure and fertilizer management (7). Although a number of field studies have shown the impact of denitrification in the saturated zone (e.g., 8, 9-13), prior to this study it was not known whether saturated zone denitrification could mitigate the impact of nitrate loading at dairy operations. The combined use of tracers of denitrification and groundwater dating allows us to distinguish between nitrate dilution and denitrification, and to detect the presence of pre-modern water.

Heterotrophic denitrification requires a bioavailable carbon source to be used as an electron donor:



In addition, the dissolved O₂ must be low in the system since most denitrifying bacteria are facultative anaerobes, and will respire using O₂ preferentially to NO₃⁻ (14). Denitrification may occur in both unsaturated soils and below the water table where the presence of NO₃⁻, low O₂ concentrations, and electron donor availability exist. In groundwater systems, the lack of an electron donor is often the limiting factor for heterotrophic denitrification (12, 13).

The two detectable products of heterotrophic denitrification are the gases N₂ and CO₂. Nitrogen gas, the more conservative product, has been used as a natural tracer to detect denitrification in the subsurface (15-17). Groundwater often also contains N₂ beyond equilibrium concentrations due to incorporation of excess air from physical processes at the water table interface (18-21). In the saturated zone, total dissolved N₂ is a sum of these three sources:

$$(N_2)_{dissolved} = (N_2)_{equilibrium} + (N_2)_{excess_air} + (N_2)_{denitrification}$$

The dissolved excess N_2 produced by saturated zone denitrification is likely transported conservatively in groundwater. However, quantification of excess N_2 is complicated since the concentrations of excess air and the recharge temperature (which is a control on equilibrium solubility of atmospheric gases) are often unknown. Noble gas compositions have been vital for determining paleo-recharge conditions that are used to demonstrate climate change (22, 23). This study uses dissolved noble gas compositions to constrain recharge conditions in young, shallow aquifers. Quantifying the recharge conditions of groundwater at dairy sites allows for the first robust calculations of nitrogen produced by saturated zone denitrification based on independent determinations of recharge temperature and amount of excess air. These results are combined with N and O isotopic compositions of nitrate to document saturated zone denitrification at two dairy operations referred to here as the Kings County Dairy (KCD) and the Merced County Dairy (Figure 1). Detailed descriptions of the hydrogeologic settings and dairy operations at each site are included as Supporting Material.

Materials and Methods:

Concentrations and nitrate isotopic compositions.

Samples for nitrate N and O isotopic compositions are filtered in the field to 0.45 μm , and stored cold and dark until analysis. Anion and cation concentrations are determined by ion chromatography using a Dionex DX-600. Field measurements of dissolved oxygen and oxidation reduction potential (using Ag/AgCl with 3.33 mol/L KCl as the reference electrode) were carried out using a Horiba U-22 $\text{\textcircled{R}}$ water quality analyzer. The nitrogen and oxygen isotopic compositions ($\delta^{15}\text{N}$ and $\delta^{18}\text{O}$) of nitrate in 26 groundwater samples from KCD and MCD were measured at Lawrence Berkeley National Laboratory's Center for Isotope Geochemistry using a version of the denitrifying bacteria procedure (24) as described in Singleton et al. (25). In addition, the nitrate from 34 samples were extracted by ion exchange procedure of (26) and analyzed for $\delta^{15}\text{N}$ at the University of Waterloo. Analytical uncertainty is 0.3 ‰ for $\delta^{15}\text{N}$ of nitrate and 0.5‰ for $\delta^{18}\text{O}$ of nitrate.

Isotopic composition of oxygen in water were determined on a VG Prism isotope ratio mass spectrometer at LLNL using the CO_2 equilibration method (27), and have an analytical uncertainty of 0.1‰.

Membrane inlet mass spectrometry

Previous studies have used gas chromatography and/or mass spectrometry to measure dissolved N_2 gas (15-17, 28, 29). Both methods require extraction of a gas sample, which adds time and can limit precision. Membrane inlet mass spectrometry (MIMS) allows precise and fast determination of the concentrations of nitrogen, oxygen and argon dissolved in groundwater samples without a separate extraction step. This method has been used to document denitrification in estuarine and ocean settings (30, 31), as well as for detection of volatile organic compounds in water (32). The MIMS technique has also proven useful for determining excess N_2 from denitrification in groundwater systems (33).

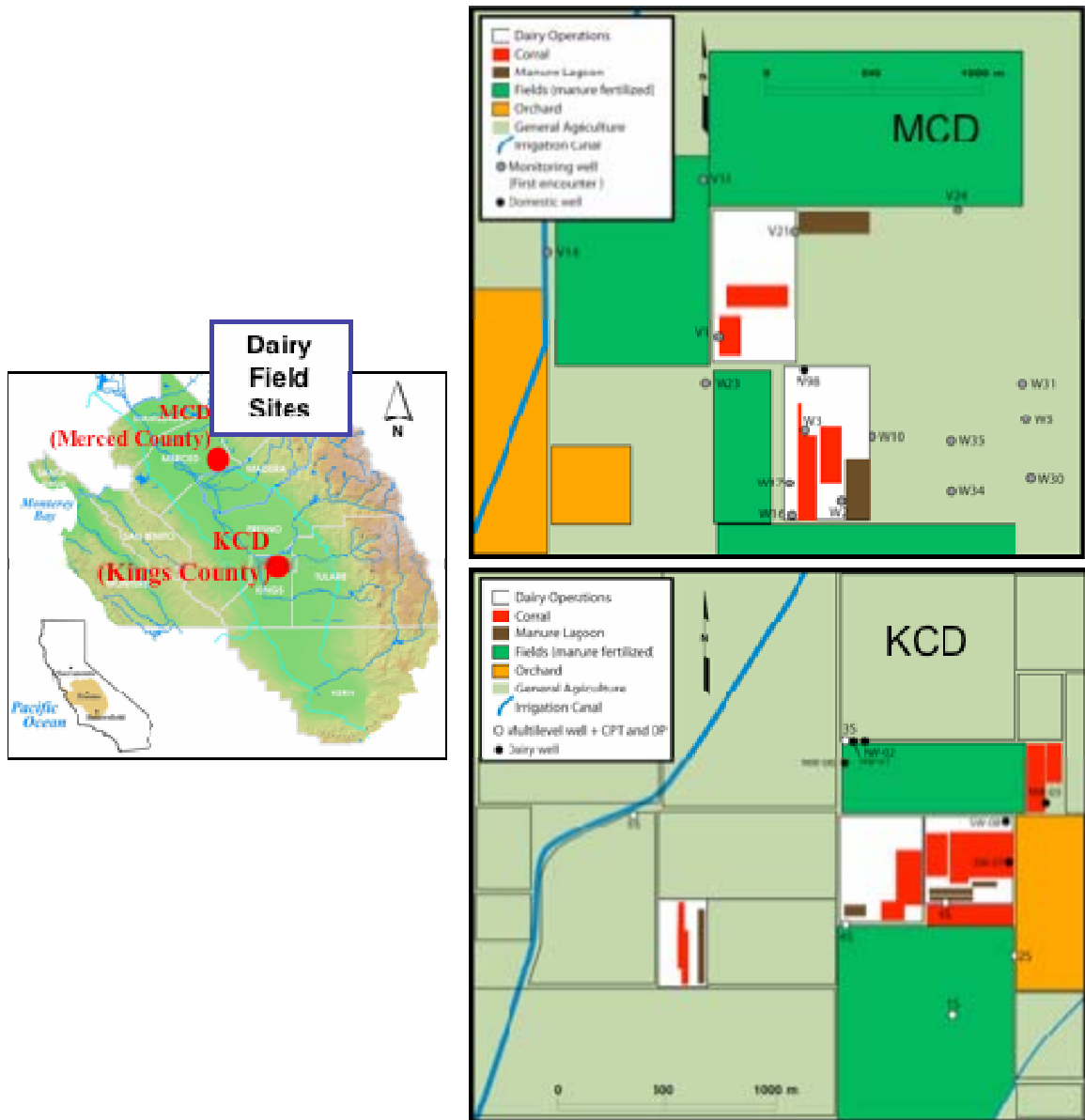


Figure 1. Location of dairy study sites, and generalized maps of each dairy showing sample locations relative to lagoons and dairy operations.

DRAFT - DO NOT DISTRIBUTE OR RELEASE

Samples for N₂, O₂, Ar, CO₂ and CH₄ concentration were analyzed by MIMS. A water sample at atmospheric pressure is drawn into the MIMS through a thin silicone rubber tube inside a vacuum manifold. Dissolved gases readily permeate through the tubing into the analysis manifold, and are analyzed using a quadrupole mass spectrometer. Water vapor that permeates through the membrane is frozen in a dry ice cold trap before reaching the quadrupole. The gas abundances are calibrated using water equilibrated with air under known conditions of temperature, altitude and humidity (typically 18 °C, 183 m, and 100% relative humidity). A small isobaric interference from CO₂ at mass 28 (N₂) is corrected based on calibration with CO₂-rich waters with known dissolved N₂, but is negligible for most samples. Typical sample size is 5 mL, and each analysis takes approximately 3 minutes. Dissolved oxygen, methane, carbon dioxide and argon content are measured at the same time as nitrogen. Samples are collected for MIMS analysis in 40 mL amber glass VOA vials, with no headspace, and kept cold during transport. Samples are analyzed within 24 hours to minimize the risk of gas loss or biological fractionation of gas in the sample container. The MIMS is field portable, and can be used on site when fieldwork requires extended time away from the laboratory, or when samples cannot be readily transported to the laboratory.

Noble gases and ³H/³He dating.

Dissolved noble gas samples are collected in copper tubes, which are filled without bubbles and sealed with a cold weld in the field. Dissolved noble gas concentrations were measured at LLNL after gas extraction on a vacuum manifold and cryogenic separation of the noble gases. Concentrations of He, Ne, Ar and Xe were measured on a quadrupole mass spectrometer. Calculations of excess air and recharge temperature from Ne and Xe measurements are described in detail in Ekwurzel (34), using an approach similar to that of Aeschbach-Hertig et al. (19). The ratio of ³He to ⁴He was measured on a VG5400 mass spectrometer.

Tritium samples are collected in 1 L glass bottles. Tritium was determined by measuring ³He accumulation after vacuum degassing each sample and allowing three to four weeks accumulation time. After correcting for sources of ³He not related to ³H decay (35, 36), the measurement of both tritium and its daughter product ³He allows calculation of the initial tritium present at the time of recharge, and apparent ages can be determined from the following relationship based on the production of tritiogenic helium (³He_{trit}):

$$\text{Groundwater Apparent Age (years)} = -17.8 \times \ln(1 + {}^3\text{He}_{\text{trit}}/{}^3\text{H})$$

The reported groundwater age is the mean age of the mixed sample, and furthermore, is only the age of the portion of the water that contains measurable tritium. Average analytical error for the age determinations is ±1 year, and samples with ³H that is too low for accurate age determination (<1 pCi/L) are reported as >50 years. Loss of ³He from groundwater is not likely in this setting given the relatively short residence times, lack of water table fluctuations, and high infiltration rates from irrigation. Groundwater age dating has been applied in several studies of basin-wide flow and transport (36-39). Mean ³H-³He apparent ages are determined for water produced from 20 KCD monitor wells at depths of 6 m to 54 m, and from 14 sites at MCD. The apparent ages give a measure of the time elapsed since water entered the saturated zone, but only of tritium-containing portion of the groundwater sample. Apparent ages therefore give the mean residence

DRAFT - DO NOT DISTRIBUTE OR RELEASE

time of the fraction of recently recharged water in a sample, and are especially useful for comparing relative ages of water from different locations at each site. The absolute mean age of groundwater may be obscured by mixing along flow paths due to heterogeneity in the sediments (40).

Results and Discussion

Groundwater flow and apparent age

The upper aquifer below KCD has $^3\text{H}/^3\text{He}$ apparent ages that range from 1 to 35 years. In general, apparent ages are lowest near the water table and increase regularly with depth in the monitoring wells (Figure 2), consistent with recharge by infiltration of irrigation water. At well 1D1 (54m BGS), the lower aquifer has no measurable NO_3^- and tritium below 1 pCi/L, indicating a groundwater age of more than 50 years. Modern water (i.e. water containing measurable tritium) is found at all multi-level wells completed in the upper aquifer at KCD, the deepest of which is 20 m BGS. Sites 2S and 5S are seasonally influenced by recharge from unlined irrigation canals, and have particularly young apparent ages. Site 3S has an observed high vertical flow rate since there is no measurable increase in apparent age with depth, except for a localized low-yield clay-rich zone at 12m BGS that has an older apparent age than the water sampled at 14 m BGS. The clay-rich zone is thought to impede flow around the 12 m monitor well screen, and also has lower nitrate concentrations than samples from surrounding depths.

At the MCD site, groundwater $^3\text{H}/^3\text{He}$ apparent ages indicate fast transit rates from the water table to the shallow monitoring wells. Most of the first encounter wells have apparent ages of <2 years, consistent with the hydraulic analysis presented by Harter et al. (6). The 57 m deep supply well (W98) has an apparent age of 31 years.

Nitrate in dairy groundwater

Nitrate concentrations at KCD range from below detection limit (BDL, <0.07 mg/L) to 274 mg/L. Within the upper aquifer, there is a sharp boundary between high nitrate waters near the surface and deeper, low nitrate waters. Nitrate concentrations are highest between 6 m and 13 m BGS at all multilevel wells (0.5 m screened intervals), with an average concentration of 98 mg/L. Groundwater below 15 m has low nitrate concentrations ranging from BDL to 2.8 mg/L, and also has low or nondetectable ammonium concentrations. The transition from high to low nitrate concentration corresponds to a change in field-measured Oxidation-Reduction Potential (ORP). ORP values of 0-107 mV are found above 10 m, defining an upper oxic zone (Figure 3). An anoxic zone is defined below 10 m by ORP values as low as -196 mV.

Nitrate concentrations at MCD monitoring wells sampled for this study range from 2-426 mg/L with an average of 230 mg/L. Several wells (W-02, W-16, and W-17) located next to a lagoon and corral have lower nitrate but high ammonium concentrations (Table 1 in Supporting Material). The MCD wells are all screened at the top of the unconfined aquifer except W98, a supply well that is pumped from approximately 57 m BGS. Nitrate concentrations observed for this deeper well are <1 mg/L.

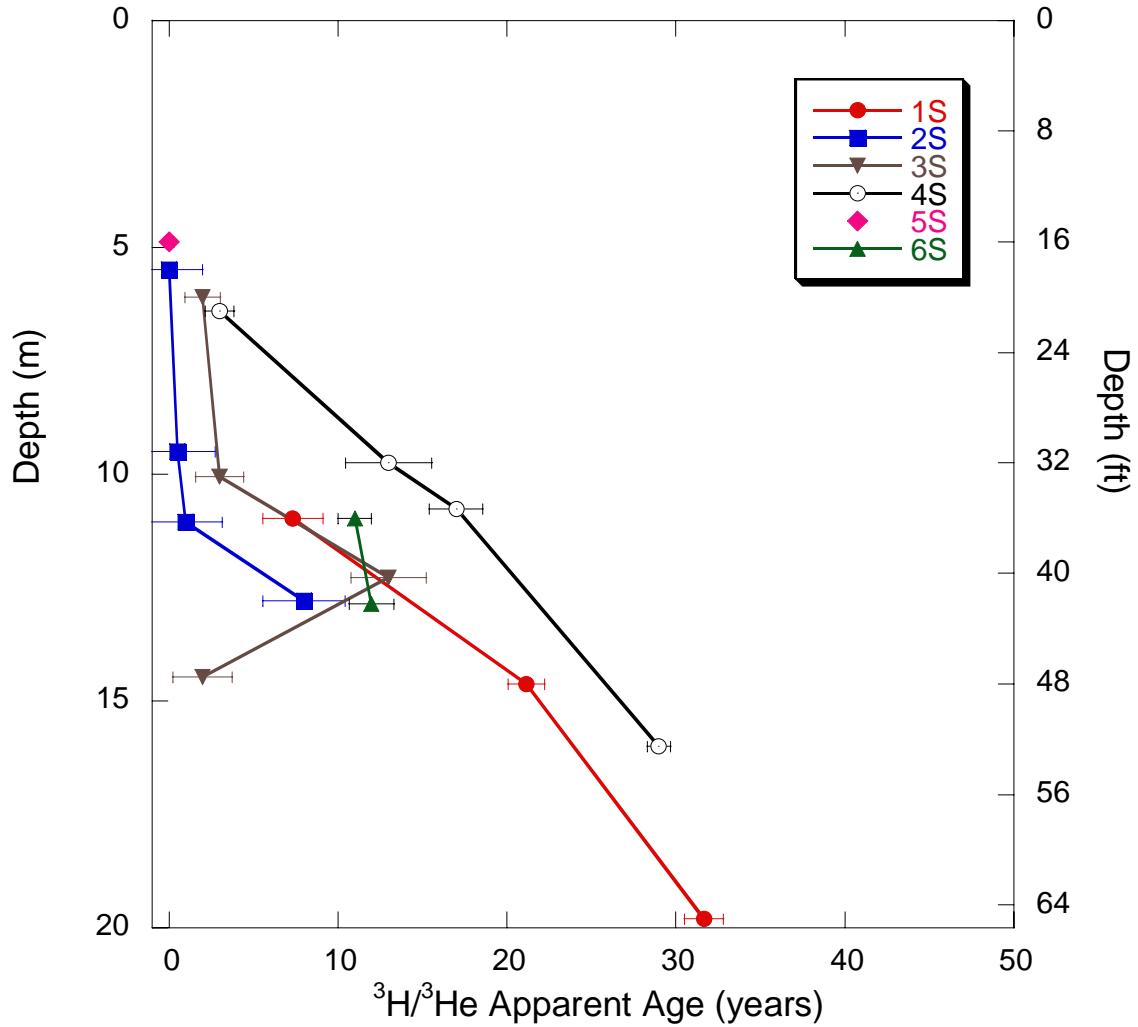
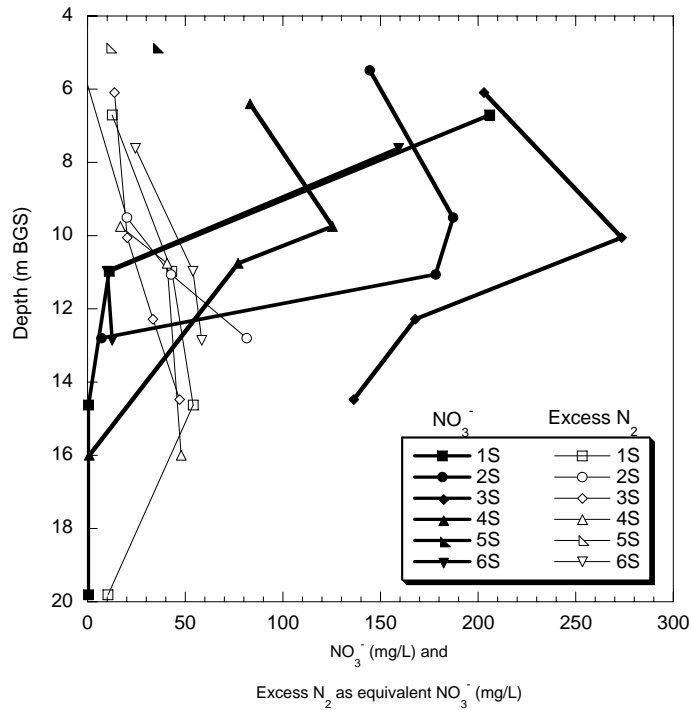


Figure 2. Groundwater $^3\text{H}/^3\text{He}$ apparent ages from multilevel monitoring wells at KCD. Error bars show analytical error. These ages represent the mean age of the tritium-containing portion of the sampled water.

A)



B)

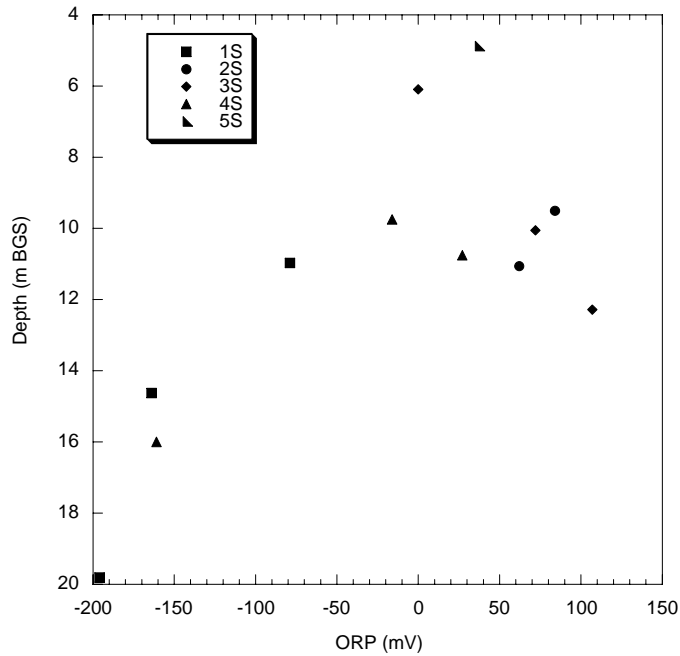


Figure 3. a) Average excess N_2 and nitrate concentrations and b) Oxidation-reduction potential (ORP) in multilevel monitoring wells at the KCD site. Excess N_2 has been calculated in units of equivalent reduced nitrate based on the stoichiometry of the denitrification reaction.

Dissolved gases

In this study, we use recharge temperature and excess air content determined using noble gas compositions to calculate excess N_2 . It is most practical to correct for excess air based on the amount of Ar in a sample, since Ar is non-reactive, and since Ar in air would dominate any potential subsurface sources such as decay of ^{40}K . By normalizing the measured dissolved concentrations as N_2/Ar ratios, the amount of excess N_2 can be calculated as:

$$(N_2)_{excess} = \left(\left(\frac{N_2}{Ar} \right)_{measured} - \left(\frac{N_{2, equilibrium} + N_{2, excess\ air}}{Ar_{equilibrium} + Ar_{excess\ air}} \right) \right) Ar_{measured}$$

where the N_2 and Ar terms for equilibrium are calculated by from equilibrium concentrations determined by gas solubility. The N_2/Ar ratio is relatively insensitive to recharge temperature, but the incorporation of excess air must be constrained in order to determine whether denitrification has shifted the ratio to higher values (29). Calculations of excess N_2 based on the N_2/Ar ratio assume that any excess air entrapped during recharge has the ratio of N_2/Ar in the atmosphere (83.5). Any partial dissolution of air bubbles would lower the N_2/Ar ratio (20, 21), thus decreasing the apparent amount of excess N_2 .

The temperature used to determine equilibrium gas concentrations and the amount of excess air must either be estimated or measured independently. Recharge temperature and excess air concentration can be determined independently using measurements of noble gases in the groundwater. Xenon, having the highest degree of temperature dependence, is used to calculate the recharge temperature, while excess air is best constrained by Ne concentrations, as Ne does not have subsurface sources and is measured with high accuracy and precision (19). Dissolved Ne concentrations have previously been used to determine the minimum N_2/Ar ratios necessary to demonstrate denitrification (29). For this study, Xe and Ne derived recharge temperature and excess air content were determined for 12 of the monitoring wells at KCD and 9 wells at MCD. For these sites, excess N_2 can be calculated directly, accounting for the contribution of excess air and recharge temperature. Based on the stoichiometry of denitrification, there are two moles of NO_3^- consumed for every mole of N_2 produced. Thus, the excess N_2 concentration can be expressed in terms of the equivalent reduced nitrate that it represents in mg/L NO_3^- .

Mean annual air temperature at the KCD and MCD sites is 16°C and 17°C respectively (www.giss.nasa.gov NOAA web site), and the Xe-derived average recharge temperatures for the KCD and MCD sites are 18°C and 19°C. Recharge temperatures are most likely higher than mean annual air temperature because most recharge is from excess irrigation during the summer months. The average amount of excess air is $2.2 \times 10^{-3} \text{ cm}^3(\text{STP})/\text{g H}_2\text{O}$ for KCD and $1.7 \times 10^{-3} \text{ cm}^3(\text{STP})/\text{g H}_2\text{O}$ for MCD. From these parameters, we estimate the initial N_2/Ar ratios including excess air to be 41.2 for KCD and 40.6 for MCD. Measured N_2/Ar ratios greater than these values are attributed to production of N_2 by denitrification.

Where Ne and Xe concentrations have not been measured, it is useful to compare excess N_2 concentrations calculated using the MIMS data and the site-representative recharge temperature and excess air content with the fully constrained calculations based on Xe and Ne concentrations.

DRAFT - DO NOT DISTRIBUTE OR RELEASE

This comparison indicates that the representative values result in only a small amount of added uncertainty (usually 1-2 mg/L equivalent NO_3^-) over the fully constrained system. This relation is encouraging since it is much more difficult and expensive to determine noble gas compositions for every well. However, without taking any excess air into account, calculations of excess N_2 would be systematically overestimated by 5 to 10 mg/L equivalent NO_3^- .

Considering excess N_2 in terms of equivalent NO_3^- provides a test to determine whether there is a mass balance between nitrate concentrations and excess N_2 . From Figure 3, there does not appear to be a balance between nitrate concentrations and excess N_2 in KCD groundwater, since nitrate concentrations in the shallow wells are more than twice that of equivalent excess N_2 concentrations in the anoxic zone. There are multiple possible causes of the discrepancy between NO_3^- concentrations and excess N_2 concentrations including 1) the NO_3^- loading at the surface has increased over time, 2) denitrification is limited by slow vertical transport into the anoxic zone, or 3) mixing with deeper, low initial NO_3^- waters has diluted both the NO_3^- and excess N_2 concentrations. All three processes may play a role in N cycling at the dairies, but we can shed some light on their relative importance by first considering the extent of denitrification and then constraining the time scale of denitrification as discussed in the following sections.

Isotopic compositions of nitrate

Both dairies have large ranges of $\delta^{15}\text{N}$ and $\delta^{18}\text{O}$ values, which can be attributed to various processes in the N cycle (Figure 4). Nitrate from KCD has $\delta^{15}\text{N}$ values of 4.5–61.1 ‰, and $\delta^{18}\text{O}$ values of -4.5–24.5 ‰. At MCD, nitrate $\delta^{15}\text{N}$ values range from 5.3–30.2‰, and $\delta^{18}\text{O}$ values range from -0.7–13.1‰. The extensive monitoring well network at these sites increases the probability that water containing residual nitrate from denitrification can be sampled.

Nitrate $\delta^{15}\text{N}$ and $\delta^{18}\text{O}$ values at both dairies are consistent with nitrification of ammonium and mineralized organic N compounds from manure-rich wastewater, in some cases followed by denitrification. Prior to nitrification, cow manure likely starts out with a bulk $\delta^{15}\text{N}$ value close to 5 ‰, but is enriched in ^{15}N to varying degrees due to volatile loss of ammonia, resulting in $\delta^{15}\text{N}$ values of 10–22 ‰ in nitrate derived from manure (41, 42). Culture experiments have shown that nitrification reactions typically combine 2 oxygen atoms from the local pore water and one oxygen atom from atmospheric O_2 (43, 44), which has a $\delta^{18}\text{O}$ of 23.5‰ (45). Different ratios of oxygen from water and atmospheric O_2 are possible for very slow nitrification rates and low ammonia concentrations (46), however for dairy waste water we assume that the 2:1 relation gives a reasonable prediction of the starting $\delta^{18}\text{O}$ values for nitrate at the two dairies based on the average values for $\delta^{18}\text{O}$ of groundwater at each site (-12.6‰ at KCD and -9.9‰ at MCD). Based on this approach, the predicted initial values for $\delta^{18}\text{O}$ in nitrate are -0.7 ‰ at KCD and 1.1‰ at MCD. Samples with the lowest nitrate $\delta^{15}\text{N}$ values have $\delta^{18}\text{O}$ values in this range, and are consistent with nitrate derived from manure. There is no strong evidence for mixing with nitrate from synthetic nitrogen fertilizers, which are used occasionally at both sites, but typically have low $\delta^{15}\text{N}$ values (0–5 ‰) and $\delta^{18}\text{O}$ values around 23 ‰ (47).

Denitrification drives the isotopic composition of the residual nitrate to higher $\delta^{15}\text{N}$ and $\delta^{18}\text{O}$ values. The stable isotopes of nitrogen are more strongly fractionated during denitrification than those of oxygen, leading to a trajectory on a $\delta^{18}\text{O}$ vs. $\delta^{15}\text{N}$ diagram with slope of 0.5 (42). At

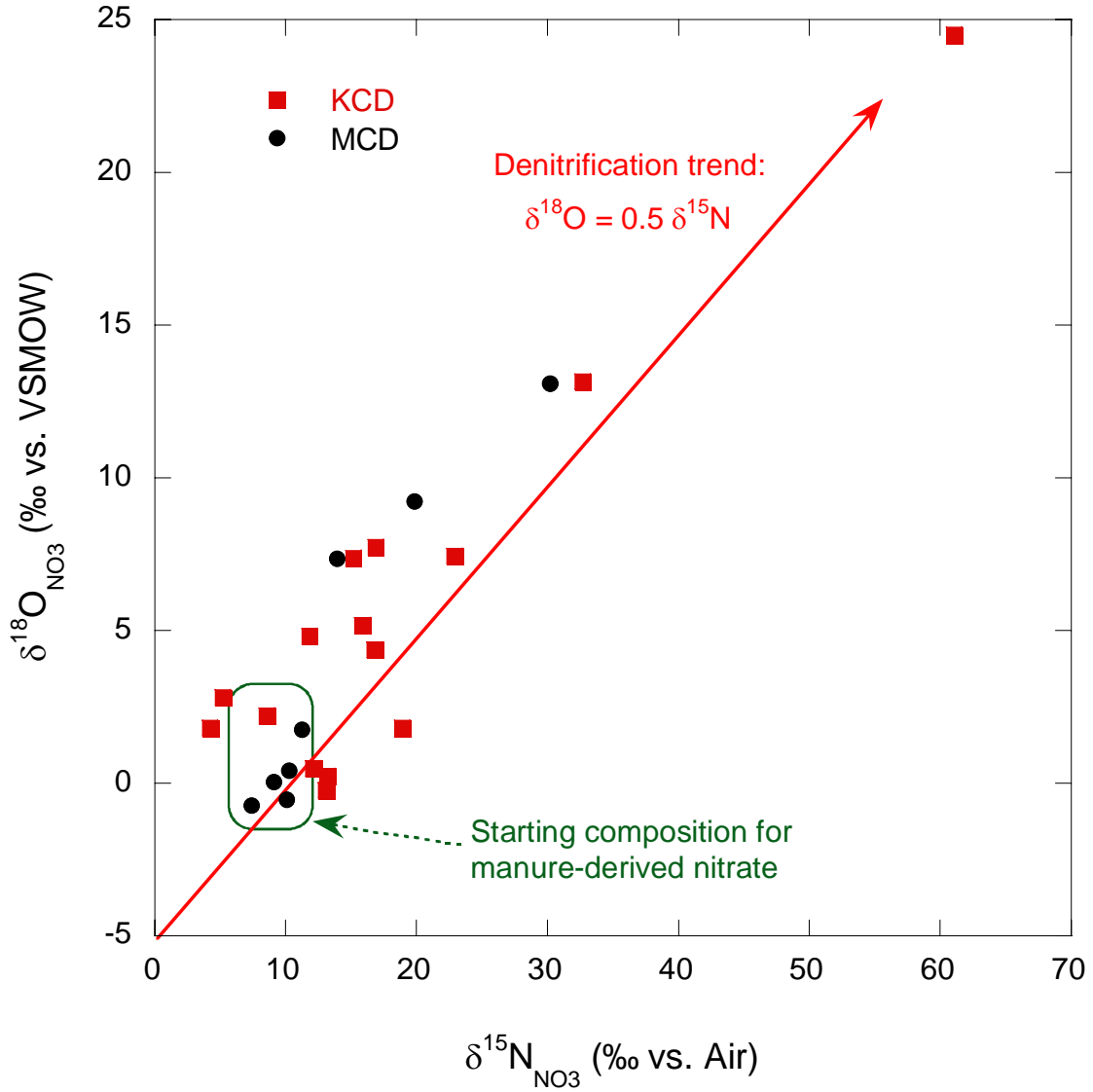


Figure 4. Oxygen and Nitrogen isotopic composition of nitrate in dairy groundwater at KCD and MCD.

both dairy sites, nitrate $\delta^{15}\text{N}$ and $\delta^{18}\text{O}$ are positively correlated with a slope close to 0.5 (Figure 4), which suggests that denitrification is occurring at both dairies. However, because a wide range of fractionation factors are known to exist for this process (48), it is not possible to determine the extent of denitrification using only the isotopic compositions of nitrate along a denitrification trend, even when the initial value for manure-derived nitrate can be measured or calculated.

Extent of denitrification

The concentrations of excess N_2 and residual nitrate can be combined with the isotopic composition of nitrate in order to characterize the extent of denitrification. In an ideal system, denitrification leads to a regular decrease in nitrate concentrations, an increase in excess N_2 , and a Rayleigh-type fractionation of N and O isotopes in the residual nitrate (Figure 5). In the Rayleigh fractionation model (49) the isotopic composition of residual nitrate depends on the fraction of initial nitrate remaining in the system ($f = C/C_{\text{initial}}$), the initial $\delta^{15}\text{N}$, and the fractionation factor (α) for denitrification:

$$\delta^{15}\text{N} = (1000 + \delta^{15}\text{N}_{\text{initial}}) f^{(\alpha-1)} - 1000$$

The fractionation factor α is defined from the isotopic ratios of interest ($R = {}^{15}\text{N}/{}^{14}\text{N}$ and ${}^{18}\text{O}/{}^{16}\text{O}$):

$$\alpha = \frac{(R)_{\text{N}_2}}{(R)_{\text{NO}_3^-}}$$

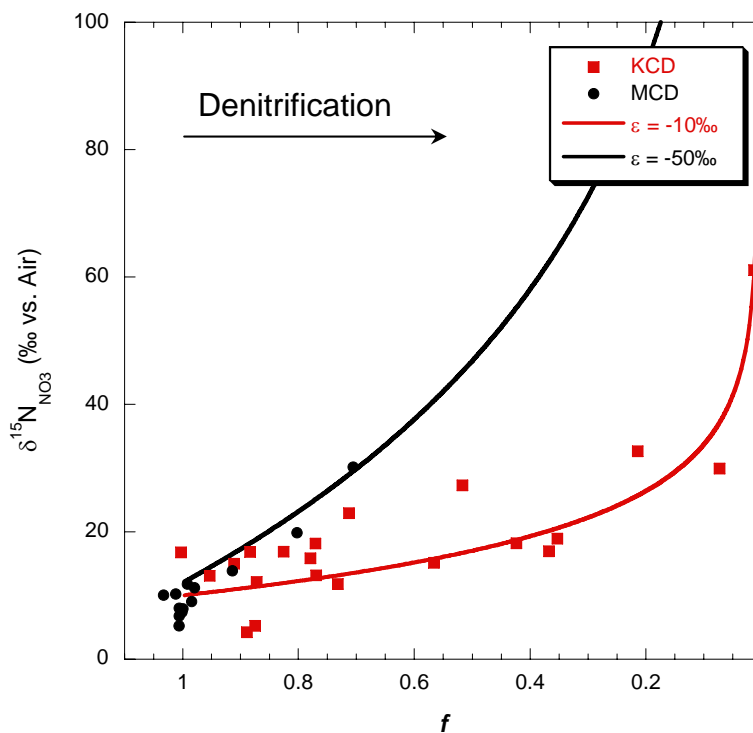
This fractionation can also be considered as an enrichment factor (ϵ) in ‰ units using the approximation $\epsilon \approx 1000 \ln \alpha$. Rather than relying on an estimate of initial nitrate concentration, the parameter f is determined directly using field measurements of excess N_2 in units of equivalent reduced NO_3^- :

$$f = C_{\text{NO}_3^-} / (C_{\text{NO}_3^-} + C_{\text{excess N}_2})$$

Values of $\delta^{15}\text{N}$ and f calculated from nitrate and excess N_2 fall along Rayleigh fractionation curves with enrichment factors (ϵ) of approximately -50 ‰ for MCD and -10 ‰ for KCD (Figure 5a). The enrichment factor for residual nitrate at MCD is one of the highest reported for denitrification, which range from -40 ‰ to -5 ‰ (42, 48). As expected for denitrification, the enrichment factors for oxygen are roughly half of those for nitrogen (Figure 5b). Considering the large differences observed for denitrification fractionation factors between the two dairy sites, it is not sufficient to estimate fractionation factors for denitrification at dairies based on laboratory-derived values or field-derived values from other sites. The appropriate fractionation factors must be determined for each site, and even then there are a number of complications that can obscure the relation between isotopic values and the extent of denitrification.

At the KCD site, several samples have $\delta^{15}\text{N}$ compositions that plot above or below an ideal Rayleigh fractionation trend with a constant enrichment factor. Heterogeneity in groundwater systems can often complicate the interpretation of contaminant degradation using a Rayleigh

A)



B)

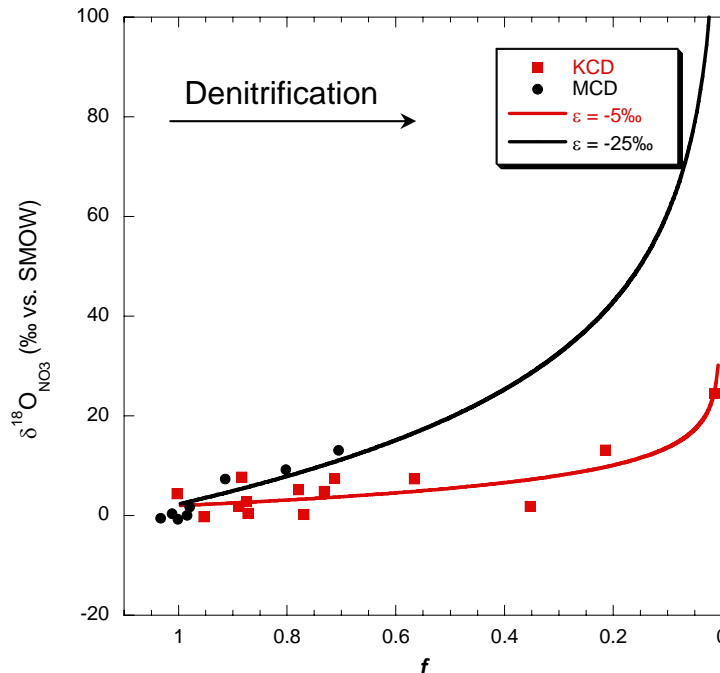


Figure 5. Nitrate $\delta^{15}\text{N}$ (a) and $\delta^{18}\text{O}$ (b) values plotted against the fraction of original nitrate remaining (f). The initial concentration of nitrate is calculated as the sum of excess N_2 and residual nitrate. Model curves are calculated based on Rayleigh fractionation during denitrification as discussed in the text.

model (50). Mixing with water that has experienced different degrees of denitrification, that has undergone unsaturated zone denitrification, or that has undergone reactions other than denitrification that affect nitrogen and/or nitrate concentrations can also account for these deviations. Mixing along groundwater flow paths with infiltrating water that has experienced some degree of denitrification in the unsaturated zone (field-applied manure wastewater, for example) will tend to move points above the fractionation line. Denitrification in the unsaturated zone during infiltration with partial or complete equilibration of atmospheric gases will in effect produce water with a low apparent degree of denitrification (low excess N_2 /residual nitrate ratio) and high initial $\delta^{15}N$ isotopic composition. Dissimilatory reduction of nitrate to ammonia, which fractionates residual nitrate to heavier values without producing excess nitrogen, would also shift $\delta^{15}N$ of residual nitrate above the Rayleigh curve. Mixing between waters that have experienced different degrees of denitrification will cause samples to plot below the expected Rayleigh fractionation curve when initial nitrate- $\delta^{15}N$ and fractionation factors are the same. Denitrified water retains a proportion of its excess N_2 concentration (and low values of f) during mixing, but the isotopic compositions of nitrate are easily disturbed by mixing since denitrified waters contain extremely low concentrations of nitrate (<1 mg/L).

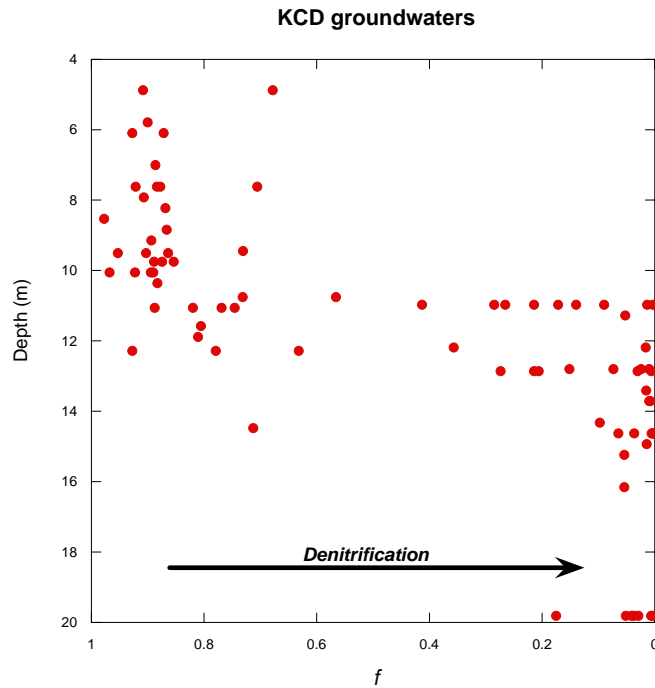
Time scale of denitrification

The extent of denitrification at KCD is related to both depth and groundwater residence times based on $^3H/^3He$ apparent ages (Figure 6). There is a sharp transition from high nitrate waters to denitrified waters between 11 and 13 m depth across the KCD site. This transition is also related to the apparent age of the groundwater, as the high nitrate waters typically have apparent ages of between 0 and 5 years, and most samples with ages greater than 8 years are significantly or completely denitrified. There are five samples that do not follow this pattern. These outliers are from sites 3S and 4S where the shallow groundwater has much higher $^3H/^3He$ apparent ages due to slow movement around clay zones at the screened intervals for these samples. The existence of older water that is not significantly impacted by denitrification indicates that it is the physical transport of water below the transition from oxic to anoxic conditions rather than the residence time that governs denitrification in this system.

The very fast transit times to the shallow monitoring wells at MCD allow for some constraints on minimum denitrification rates at this site. Based on the comparison of the calculated ages with the initial tritium curve, these shallow wells contain a negligible amount of old, 3H -decayed water. In shallow wells near lagoons (e.g. W-16 and V-21), the observed excess N_2 (equivalent to 71 and 40 mg/L of reduced NO_3^-) accumulated over a duration of less than one year, indicating that denitrification rates may be very high at these sites. Complete denitrification of groundwater collected from well W-98 (excess N_2 equivalent to 51 mg/L NO_3^-) was attained within approximately 31 years, but may have occurred over a short period of time relative to the mean age of the water. Based on excess N_2 in the young groundwater at MCD, denitrification rates in the anoxic zones around lagoons are relatively fast, and would reduce the high nitrate concentrations observed near the water table to background levels in less than 10 years in the absence of additional nitrate loading.

Mariotti et al. (51) found that faster denitrification rates in soil incubation experiments result in smaller kinetic isotope fractionation factors. This relation would appear to be at odds with the

A)



B)

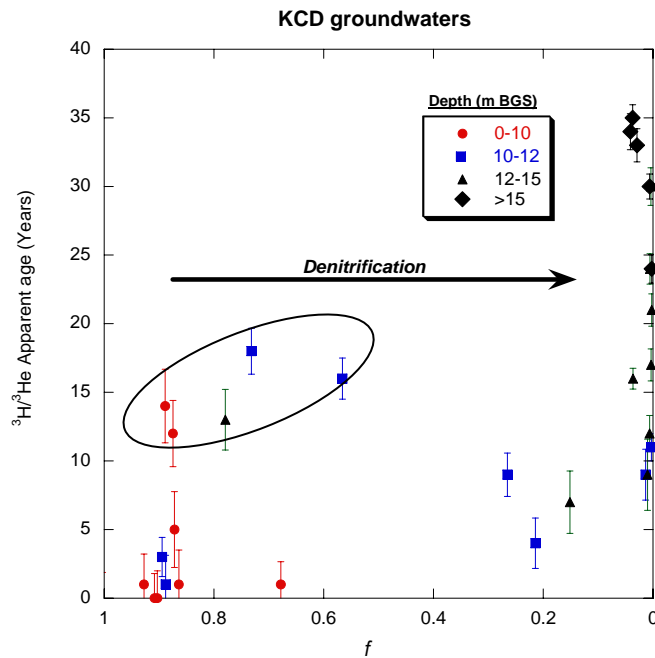


Figure 6. Sample depth (a) and $^3\text{H}/^3\text{He}$ apparent age (b) plotted against the fraction of original nitrate remaining from denitrification. In general, denitrification is mostly complete below 13 m depth and in groundwater with $^3\text{H}/^3\text{He}$ apparent ages greater than 8 years. Samples at two sites have experienced less denitrification than is typical for samples with $^3\text{H}/^3\text{He}$ apparent age > 8 years (circled, see text).

DRAFT - DO NOT DISTRIBUTE OR RELEASE

higher apparent isotopic enrichment factors from denitrification in the younger groundwaters at MCD relative to the older waters with a smaller enrichment at KCD. However, the denitrification observed at KCD may have happened quickly once nitrate reached the anoxic zone that exists below about 10 m BGS.

The fraction of 'pre-modern' (^3H -dead) component can be estimated from a comparison of the tritium measured in a sample with the predicted tritium based on tritium measured in precipitation at the time of recharge (52). In KCD samples, estimated fractions of pre-modern water are generally less than 10%, but become more significant at depths below 10m. The ^3H -dead water at this field site pre-dates most dairy operations and thus would not contribute significantly to the nitrate concentration. However, water that contains a significant fraction of older ^3H -dead water can dilute both the nitrate and excess N_2 concentrations of younger groundwater. Addition of this older water may offer a partial explanation of the lower excess N_2 concentrations at depth relative to shallow nitrate concentrations.

Occurrence of denitrification at dairy sites

The presence of excess N_2 , a characteristic shift in $\delta^{15}\text{N}$ and $\delta^{18}\text{O}$ values, and a decrease in nitrate concentration demonstrate the occurrence of saturated zone denitrification at the two dairy sites. At KCD, samples with excess N_2 indicative of denitrification are primarily confined to depths below 10 m BGS. The depth at which denitrified waters are encountered is remarkably similar across the dairy site. This transition is not strongly correlated with a change in sediment texture. The denitrified waters at all KCD wells coincide with negative ORP values and generally low O_2 concentrations. Total organic carbon (TOC) concentration in the shallow groundwaters range from 1.1 to 15.7 mg/L at KCD, with the highest concentrations of TOC found in wells adjacent to lagoons. The highest concentrations of excess N_2 are found in nested well-set 2S, which is located in a field downgradient from the lagoons. However, sites distal to the lagoons that are apparently not impacted by lagoon seepage (sites 3S and 4S) also show evidence of denitrification, suggesting that direct lagoon seepage is not the sole driver for this process.

The chemical stratification observed in multilevel wells at the KCD site demonstrates the importance of characterizing vertical variations within aquifers for nitrate monitoring studies. Groundwater nitrate concentrations are integrated over the high and low nitrate concentration zones by dairy water supply wells, which have long screened intervals from 9 to 18 meters BGS. Water quality samples from these supply wells underestimate the actual nitrate concentrations present in the uppermost oxic aquifer. Similarly, first encounter monitoring wells give an overestimate of nitrate concentrations found deep in the aquifer, and thus would miss entirely the impact of saturated zone denitrification in mitigating nitrate transport to the deep aquifer.

Monitoring wells at MCD sample only the top of the aquifer, so the extent of denitrification at depth is unknown, except for the one deep domestic well (W98), which has less than 1 mg/L nitrate and an excess N_2 content consistent with reduction of 51 mg/L NO_3^- to N_2 . This supply well would be above the MCL for nitrate without the attenuation of nitrate by denitrification. In the shallow first-encounter wells, denitrification is spatially linked to lagoons and corrals, where mixing of oxic high nitrate waters and anoxic lagoon seepage may induce both nitrification and

denitrification. The presence of ammonium at several of the wells with denitrified water indicates a component of wastewater seepage in wells located near lagoons. First-encounter wells that are located in the surrounding fields have high NO_3^- concentrations, and do not have any detectable excess N_2 , a result consistent with mass-balance models of nitrate loading and groundwater nitrate concentration (6).

While dairy operations seem likely to establish conditions conducive to saturated zone denitrification, the prevalence of the phenomenon at dairies is not known. Major uncertainties include the spatial extent of anaerobic conditions, and transport of organic carbon under differing hydrogeologic conditions and differing nutrient management practices. However, denitrification is more likely to be a major factor in the fate of subsurface nitrate under manure-fertilized fields than it is beneath fields fertilized with synthetic fertilizer, where organic carbon sources are scarce and dissolved oxygen is often present. Lagoon seepage may also increase the likelihood of denitrification in dairy aquifers. The extent to which dairy animal and field operations affect saturated zone denitrification is an important consideration in determining the assimilative capacity of underlying groundwater to nitrogen loading associated with dairy operations.

Acknowledgements

This work was performed under the auspices of the U.S. Department of Energy by University of California, Lawrence Livermore National Laboratory under Contract W-7405-Eng-48. Funding for this project was from the California State Water Resources Control Board Groundwater Ambient Monitoring and Assessment Program and from the LLNL Laboratory Directed Research and Development Program. We thank Mark Conrad for use of the LBNL Center for Isotope Geochemistry's stable isotope lab, and Katharine Woods for help with analyses.

References

- (1) Fan, A. M.; Steinberg, V. E., Health implications of nitrate and nitrite in drinking water - an update on methemoglobinemia occurrence and reproductive and developmental toxicity. *Regulatory Toxicology and Pharmacology* **1996**, *23*, 35-43.
- (2) Nolan, B. T.; Stoner, J. D., Nutrients in groundwaters of the conterminous United States 1992-1995. *Environmental Science & Technology* **2000**, *34*, 1156-1165.
- (3) Nolan, B. T.; Hitt, K. J.; Ruddy, B. C., Probability of nitrate contamination of recently recharged groundwaters in the conterminous United States. *Environmental Science & Technology* **2002**, *36*, 2138-2145.
- (4) Squillace, P. J.; Scott, J. C.; Moran, M. J.; Nolan, B. T.; Kolpin, D. W., VOCs, pesticides, nitrate, and their mixtures in groundwater used for drinking water in the United States. *Environmental Science & Technology* **2002**, *36*, 1923-1930.
- (5) Tesoriero, A. J.; Voss, F. D., Predicting the probability of elevated nitrate concentrations in the Puget Sound Basin: Implications for aquifer susceptibility and vulnerability. *Ground Water* **1997**, *35*, 1029-1039.
- (6) Harter, T.; Davis, H.; Mathews, M. C.; Meyer, R. D., Shallow groundwater quality on dairy farms with irrigated forage crops. *Journal of Contaminant Hydrology* **2002**, *55*, 287-315.
- (7) Cameron, K. C.; Di, H. J.; Reijnen, B. P. A.; Li, Z.; Russell, J. M.; Barnett, J. W., Fate of nitrogen in dairy factory effluent irrigated onto land. *New Zealand Journal of Agricultural Research*, **2002**, *45*, 217-216.
- (8) Mariotti, A.; Landreau, A.; Simon, B., ¹⁵N isotope biogeochemistry and natural denitrification process in groundwater: Application to the chalk aquifer of northern France. *Geochimica et Cosmochimica Acta* **1988**, *52*, 1869-1878.
- (9) Puckett, L. J.; Cowdery, T. K.; Lorenz, D. L.; Stoner, J. D., Estimation of nitrate contamination of an agro-ecosystem outwash aquifer using a nitrogen mass-balance budget. *Journal of Environmental Quality* **1999**, *28*, 2015-2025.
- (10) Puckett, L. J.; Cowdery, T. K., Transport and fate of nitrate in a glacial outwash aquifer in relation to ground water age, land use practices, and redox processes. *Journal of Environmental Quality* **2002**, *31*, 782-796.
- (11) Korom, S. F., Natural denitrification in the saturated zone - a review. *Water Resources Research* **1992**, *28*, 1657-1668.
- (12) DeSimone, L. A.; Howes, B. L., Nitrogen transport and transformations in a shallow aquifer receiving wastewater discharge: A mass balance approach. *Water Resources Research* **1998**, *34*, 271-285.
- (13) Desimone, L. A.; Howes, B. L., Denitrification and nitrogen transport in a coastal aquifer receiving wastewater discharge. *Environmental Science & Technology* **1996**, *30*, 1152-1162.
- (14) Tiedje, J. M., Ecology of denitrification and dissimilatory nitrate reduction to ammonium. In *Biology of Anaerobic Microorganisms*, Zehnder, A. J. B., Ed. John Wiley & Sons: New York, 1988; pp 179-244.
- (15) Vogel, J. C.; Talma, A. S.; Heaton, T. H. E., Gaseous nitrogen as evidence for denitrification in groundwater. *Journal of Hydrology* **1981**, *50*, 191-200.
- (16) Bohlke, J. K.; Denver, J. M., Combined use of groundwater dating, chemical, and isotopic analyses to resolve the history and fate of nitrate contamination in two agricultural

- watersheds, Atlantic Coastal Plain, Maryland. *Water Resources Research* **1995**, *31*, 2319-2339.
- (17) McMahon, P. B.; Bohlke, J. K., Denitrification and mixing in a stream-aquifer system: Effects on nitrate loading to surface water. *Journal of Hydrology* **1996**, *186*, 105-128.
 - (18) Heaton, T. H. E.; Vogel, J. C., Excess air in groundwater. *Journal of Hydrology* **1981**, *50*, 201-216.
 - (19) Aeschbach-Hertig, W.; Peeters, F.; Beyerle, U.; Kipfer, R., Palaeotemperature reconstruction from noble gases in ground water taking into account equilibration with entrapped air. *Nature* **2000**, *405*, 1040-1044.
 - (20) Holocher, J.; Peeters, F.; Aeschbach-Hertig, W.; Hofer, M.; Kipfer, R., Gas exchange in quasi-saturated porous media: Investigations on the formation of excess air using noble gases (abstr.). *Geochimica Et Cosmochimica Acta* **2002**, *66*, A338-A338.
 - (21) Holocher, J.; Peeters, F.; Aeschbach-Hertig, W.; Hofer, M.; Brennwald, M.; Kinzelbach, W.; Kipfer, R., Experimental investigations on the formation of excess air in quasi-saturated porous media. *Geochimica Et Cosmochimica Acta* **2002**, *66*, 4103-4117.
 - (22) Aeschbach-Hertig, W.; Stute, M.; Clark, J. F.; Reuter, R. F.; Schlosser, P., A paleotemperature record derived from dissolved noble gases in groundwater of the Aquia Aquifer (Maryland, USA). *Geochimica Et Cosmochimica Acta* **2002**, *66*, 797-817.
 - (23) Clark, J. F.; Stute, M.; Schlosser, P.; Drenkard, S., A tracer study of the Floridan aquifer in southeastern Georgia: Implications for groundwater flow and paleoclimate. *Water Resources Research* **1997**, *33*, 281-289.
 - (24) Casciotti, K. L.; Sigman, D. M.; Hastings, M. G.; Bohlke, J. K.; Hilkert, A., Measurement of the oxygen isotopic composition of nitrate in seawater and freshwater using the denitrifier method. *Analytical Chemistry* **2002**, *74*, 4905-4912.
 - (25) Singleton, M. J.; Woods, K. N.; Conrad, M. E.; Depaolo, D. J.; Dresel, P. E., Tracking sources of unsaturated zone and groundwater nitrate contamination using nitrogen and oxygen stable isotopes at the Hanford Site, Washington. *Environmental Science & Technology* **2005**, *39*, 3563-3570.
 - (26) Silva, S. R.; Kendall, C.; Wilkison, D. H.; Ziegler, A. C.; Chang, C. C. Y.; Avanzino, R. J., A new method for collection of nitrate from fresh water and the analysis of nitrogen and oxygen isotope ratios. *Journal of Hydrology* **2000**, *228*, 22-36.
 - (27) Epstein, S.; Mayeda, T. K., Variation of O-18 content of waters from natural sources. *Geochim. Cosmochim. Acta* **1953**, *4*, 213-224.
 - (28) Wilson, G. B.; Andrews, J. N.; Bath, A. H., Dissolved gas evidence for denitrification in the Lincolnshire limestone groundwaters, Eastern England. *Journal of Hydrology* **1990**, *113*, 51-60.
 - (29) Wilson, G. B.; Andrews, J. N.; Bath, A. H., The nitrogen isotope composition of groundwater nitrates from the East Midlands Triassic Sandstone Aquifer, England. *Journal of Hydrology* **1994**, *157*, 35-46.
 - (30) Kana, T. M.; Darkangelo, C.; Hunt, M. D.; Oldham, J. B.; Bennett, G. E.; Cornwell, J. C., Membrane inlet mass spectrometer for rapid high precision determination of N₂, O₂, and Ar in environmental water samples. *Analytical Chemistry* **1994**, *66*, 4166-4170.
 - (31) An, S. M.; Gardner, W. S.; Kana, T., Simultaneous measurement of denitrification and nitrogen fixation using isotope pairing with membrane inlet mass spectrometry analysis. *Applied and Environmental Microbiology* **2001**, *67*, 1171-1178.

- (32) Ketola, R. A.; Kotiaho, T.; Cisper, M. E.; Allen, T. M., Environmental applications of membrane introduction mass spectrometry. *Journal of Mass Spectrometry* **2002**, *37*, 457-476.
- (33) Beller, H. R.; Madrid, V.; Hudson, G. B.; McNab, W. W.; Carlsen, T., Biogeochemistry and natural attenuation of nitrate in groundwater at an explosives test facility. *Applied Geochemistry* **2004**, *19*, 1483-1494.
- (34) Ekwurzel, B. *LLNL Isotope Laboratories Data Manual*; Lawrence Livermore National Laboratory: April 1, 2004, 2004; p 133.
- (35) Aeschbach-Hertig, W.; Peeters, F.; Beyerle, U.; Kipfer, R., Interpretation of dissolved atmospheric noble gases in natural waters. *Water Resources Research* **1999**, *35*, 2779-2792.
- (36) Ekwurzel, B.; Schlosser, P.; Smethie, W. M.; Plummer, L. N.; Busenberg, E.; Michel, R. L.; Weppernig, R.; Stute, M., Dating of shallow groundwater - comparison of the transient tracers H-3/He-3, chlorofluorocarbons, and Kr-85. *Water Resources Research* **1994**, *30*, 1693-1708.
- (37) Poreda, R. J.; Cerling, T. E.; Solomon, D. K., Tritium and helium-isotopes as hydrologic tracers in a shallow unconfined aquifer. *Journal of Hydrology* **1988**, *103*, 1-9.
- (38) Schlosser, P.; Stute, M.; Dorr, H.; Sonntag, C.; Munnich, K. O., Tritium He-3 dating of shallow groundwater. *Earth and Planetary Science Letters* **1988**, *89*, 353-362.
- (39) Solomon, D. K.; Poreda, R. J.; Schiff, S. L.; Cherry, J. A., Tritium and He-3 as groundwater age tracers in the Borden Aquifer. *Water Resources Research* **1992**, *28*, 741-755.
- (40) Weissmann, G. S.; Zhang, Y.; LaBolle, E. M.; Fogg, G. E., Dispersion of groundwater age in an alluvial aquifer system. *Water Resources Research* **2002**, *38*, art. no.-1198.
- (41) Kreitler, C. W., Nitrogen-isotope ratio studies of soils and groundwater nitrate from alluvial fan aquifers in Texas. *Journal of Hydrology* **1979**, *42*, 147-170.
- (42) Kendall, C., Tracing nitrogen sources and cycling in catchments. In *Isotope Tracers in Catchment Hydrology*, Kendall, C.; McDonnell, J. J., Eds. Elsevier: New York, 1998; pp 519-576.
- (43) Andersson, K. K.; Hooper, A. B., O₂ and H₂O are each the source of one O in NO₂⁻ produced from NH₃ by Nitrosomonas - N15-NMR evidence. *FEBS Letters* **1983**, *164*, 236-240.
- (44) Hollocher, T. C., Source of the oxygen atoms of nitrate in the oxidation of nitrite by *Nitrobacter agilis* and evidence against a P-O-N anhydride mechanism in oxidative phosphorylation. *Archives of Biochemistry and Biophysics* **1984**, *233*, 721-727.
- (45) Kroopnick, P. M.; Craig, H., Atmospheric oxygen: Isotopic composition and solubility fractionation. *Science* **1972**, *175*, 54-55.
- (46) Mayer, B.; Bollwerk, S. M.; Mansfeldt, T.; Hutter, B.; Veizer, J., The oxygen isotope composition of nitrate generated by nitrification in acid forest floors. *Geochimica et Cosmochimica Acta* **2001**, *65*, 2743-2756.
- (47) Kendall, C.; Aravena, R., Nitrate isotopes in groundwater systems. In *Environmental Tracers in Subsurface Hydrology*, Cook, P. G.; Herczeg, A. L., Eds. Kluwer Academic Publishers: Norwell, Massachusetts, 2000; pp 261-297.
- (48) Hubner, H., Isotope effects of nitrogen in the soil and biosphere. In *Handbook of Environmental Isotope Geochemistry: Volume 2b, The Terrestrial Environment*, Fritz, P.; Fontes, J. C., Eds. Elsevier: New York, 1986; pp 361-425.

DRAFT - DO NOT DISTRIBUTE OR RELEASE

- (49) Criss, R. E., *Principles of Stable Isotope Distribution*. Oxford University Press: New York, 1999; p 254.
- (50) Abe, Y.; Hunkeler, D., Does the Rayleigh equation apply to evaluate field isotope data in contaminant hydrogeology? *Environmental Science & Technology* **2006**, *40*, 1588-1596.
- (51) Mariotti, A.; Germon, J. C.; Leclerc, A., Nitrogen isotope fractionation associated with the NO_2^- - N_2O step of denitrification in soils. *Canadian Journal of Soil Science* **1982**, *62*, 227-241.
- (52) Manning, A. H.; Thiros, S. A., H-3/He-3 age data in assessing the susceptibility of wells to contamination. *Ground Water* **2005**, *43*, 353-367.

Supporting Materials

Site Description

Study Site 1:

Study Site #1 is located at a dairy operation in Kings County, CA (KCD, Figure 1). Manure management practices employed at KCD, with respect to corral design, runoff capture and lagoon management are typical of practices employed at other dairies in the region. KCD has close to the 1000-cow average for dairies in the area, and operates three clay-lined wastewater lagoons that receive wastewater after solids separation. Wastewater is used for irrigation of 500 acres of forage crops (corn and alfalfa) on the dairy and on neighboring farms; dry manure is exported to neighboring farms.

KCD is located in the Kings River alluvial fan, a sequence of layered sediments transported by the Kings River from the Sierra Nevada to the low lying southern San Joaquin Valley of California (1, 2). The site overlies an unconfined aquifer, which has been split into an upper aquifer from 3m to 24m below ground surface (BGS) and a lower aquifer (>40 m BGS) that are separated by a gap of unsaturated sediments. Both aquifers are predominantly composed of unconsolidated sands with minor clayey sand layers. The lower unsaturated gap was likely caused by intense regional groundwater pumping, and a well completed in this unsaturated zone has very low gas pressures. There are no persistent gradients in water table levels across the KCD site, but in general, regional groundwater flow is from the NW to SE due to topographic flow on the Kings River fan. The water table is located about 5 m BGS. Local recharge is dominated by vertical fluxes from irrigation, and to a lesser extent, leakage from adjacent unlined canals. Transient cones of depression are induced during groundwater pumping from dairy operation wells. The regional groundwater is highly impacted by agricultural activities and contains elevated concentrations of nitrate and pesticides (3, 4).

KCD was instrumented with five sets of multi-level monitoring wells and one “up-gradient” well near an irrigation canal. These wells were installed in 2002, and sampled between Feb. 2002 and Aug. 2005. The multi-level wells have short (0.5 m) screened intervals in order to detect heterogeneity and stratification in aquifer chemistry. One monitoring well was screened in the lower aquifer, 54m BGS. The remaining monitoring wells are screened in the upper aquifer from 5m to 20m BGS. In addition, there are eight dairy operation wells that were sampled over the course of this study. These production wells have long screens, generally between 9 to 18 meters below ground surface (BGS).

Study Site 2:

The second dairy field site is located in Merced County, CA. The Merced County dairy (MCD) lies within the northern San Joaquin Valley, approximately 160 km NNW from the KCD site. The site is located on the low alluvial fans of the Merced and Tuolumne Rivers, which drain the north-central Sierra Nevada. Soils at the site are sand to loamy

sand with rapid infiltration rates. The upper portion of the unconfined alluvial aquifer is comprised of arkosic sand and silty sand, containing mostly quartz and feldspar, with interbedded silt and hardpan layers. Hydraulic conductivities were measured with slug tests and ranged from 1×10^{-4} m/s to 2×10^{-3} m/s with a geometric mean of 5×10^{-4} m/s (5). Regional groundwater flow is towards the valley trough with a gradient of approximately 0.05% to 0.15%. Depth to groundwater is 2.5 m to 5 m BGS. The climate is Mediterranean with annual precipitation of 0.5 m, but groundwater recharge is on the order of 0.5–0.8 m per year with most of the recharge originating from excess irrigation water (3). Transit times in the unsaturated zone are relatively short due to the shallow depth to groundwater and due to low water holding capacity in the sandy soils. Shallow water tables are managed through tile drainage and groundwater pumping specifically for drainage. The MCD site is instrumented with monitoring wells that are screened from 2-3 m BGS to a depth of 7-9 m BGS. The wells access the upper-most part of the unconfined aquifer, hence, the most recently recharged groundwater (6). Recent investigations showed strongly elevated nitrate levels in this shallow groundwater originating largely from applications of liquid dairy manure to field crops, from corrals, and from manure storage lagoons (6). For this study, a subset of 18 wells was sampled. A deep domestic well was also sampled at MCD. This domestic well is completed to 57 m BGS, and thus samples a deeper part of the aquifer than the monitoring well network.

References

- (1) Weissmann, G. S.; Fogg, G. E., Multi-scale alluvial fan heterogeneity modeled with transition probability geostatistics in a sequence stratigraphic framework. *Journal of Hydrology* **1999**, *226*, 48-65.
- (2) Weissmann, G. S.; Mount, J. F.; Fogg, G. E., Glacially driven cycles in accumulation space and sequence stratigraphy of a stream-dominated alluvial fan, San Joaquin valley, California, USA. *Journal of Sedimentary Research* **2002**, *72*, 240-251.
- (3) Burrow, K. R.; Shelton, K. R.; Dubrovsky, N. M. *Occurrence of nitrate and pesticides in ground water beneath three agricultural land-use settings in the eastern San Joaquin Valley, California, 1993-1995*; Water-Resources Investigations Report 97-4284; U.S. Geological Survey: 1998; p 51.
- (4) Burrow, K. R.; Shelton, K. R.; Dubrovsky, N. M. *Occurrence of nitrate and pesticides in ground water beneath three agricultural land-use settings in the eastern San Joaquin Valley, California, 1993-1995*; Water-Resources Investigations Report 97-4284; United States Geological Survey: 1998; p 51.
- (5) Davis, H. H. In *Monitoring and evaluation of water quality under Central Valley dairy sites*, Proceedings of the California Plant and Soil Conference (California Chapter of American Society of Agronomy and California Fertilizer Association, Visalia, California), Visalia, California, 1995; California Chapter of American Society of Agronomy: Visalia, California, 1995; pp 158-164.
- (6) Harter, T.; Davis, H.; Mathews, M. C.; Meyer, R. D., Shallow groundwater quality on dairy farms with irrigated forage crops. *Journal of Contaminant Hydrology* **2002**, *55*, 287-315.

DRAFT - DO NOT DISTRIBUTE OR CIRCULATE

Table 1. KCD1 and MCD Groundwater Data

Site	Depth of multi-level well (m)	Cl (mg/L)	NO3- (mg/L)	NH4+ (mg/L)	ORP	DO (mg/L)	TOC (mg/L)	$\delta^{18}\text{O H}_2\text{O}$ (‰ SMOW)	$\text{d}^2\text{H H}_2\text{O}$ (‰ SMOW)	$\text{d}^{15}\text{N NO}_3^-$ (‰ Air)	$\text{d}^{18}\text{O NO}_3^-$ (‰ SMOW)	Excess N2 (as equiv. mg/L NO ₃ ⁻)	3H/3He age (yr)	3H/3He age error (yr)	Excess air determined from Ne (cc STP/g)	Recharge Temp. from Xe (deg C)	Number of times sampled	
KCD1 CANAL-1		2	1.2	0.2				-12.2	-94								5	
KCD1 LAGOON-1		305	29	361			480.0					1					3	
KCD1 LAGOON-2		265	14	292	170	9.5	490.0					4					3	
KCD1 LAGOON-3		212	22	214	141	2.9	420.0	-9.9	-87			0					5	
KCD1 LL-1D1	54	2	0.2	0.0	-164	0.7	0.8	-13.7	-103	7.1		1	>50		3.40E-03	15	5	
KCD1 LL-1S2	11	43	8	2.2	-63	0.3	2.5	-13.0		46.9	18.8	33	16.0	0.9			16	4
KCD1 LL-1S3	15	36	0.5	1.3	-186	0.6	1.3	-12.9	-96	7.6		44	21.1	0.8	2.82E-03		14	8
KCD1 LL-1S4	20	9	0.4	2.1	-149	0.5	1.1	-13.3	-102			7	31.0	0.9	4.21E-03		16	6
KCD1 LL-2S1	5	108	145				5.0					0			1.70E-03		19	2
KCD1 LL-2S2	10	95	187	0.6	80	0.2	4.1	-12.2		13.1	-0.2	9	1.0	0.9	1.78E-03		22	3
KCD1 LL-2S3	11	101	178	0.1	9	0.8	3.0	-12.1		13.2	0.2	36	1.0	0.6			21	4
KCD1 LL-2S4	13	73	7	1.0	-213	0.6	1.8	-12.4		29.9	4.2	121	4.0	1.4			23	3
KCD1 LL-3S1	6	170	203	0.4	62	1.7	5.3	-11.9		14.5	2.4	4	2.5	0.2	9.25E-04		19	3
KCD1 LL-3S2	10	256	274		113	0.5	14.0	-11.2				7	3.0	0.6			19	3
KCD1 LL-3S3	12	163	168	0.5	-91	0.6	9.0	-12.3		15.8	5.2	17	13.0	1.2	1.30E-03		18	3
KCD1 LL-3S4	14	194	136		-50	1.2	5.6	-11.8		22.9	7.4	30	2.0	0.7			20	2
KCD1 LL-4S1	6	127	83							8.6	2.2		3.0	0.4	3.35E-04		20	1
KCD1 LL-4S2	10	32	125	0.4	86	0.5	1.1	-11.8		4.7	2.3	15	13.0	1.1	5.07E-03		18	2
KCD1 LL-4S3	11	42	77	0.5	-16	0.8	1.0	-12.0		13.5	6.1	37	17.5	0.9	3.54E-03		19	2
KCD1 LL-4S4	16	35	0.9	1.8			3.5	-13.0				37	29.5	4.1	1.90E-01		18	2
KCD1 LL-5S1	5	15	35	1.3	-114	0.8	2.4	-14.1		18.9	1.8	5	0.0				18	4
KCD1 LL-TEMP-1	13	129	13	23	120	0.5	16.0	-11.8		12.1		36					6	6
KCD1 LL-TEMP-2	11	141	10	3.2	8	1.0	16.0	-11.9				31					5	5
KCD1 LL-TEMP-3	8	129	159	0.9	76	5.0	13.0	-11.9		19.0	9.2	8			2.13E-04		5	5
KCD1 NW-01		141	115	1.9				-12.0	-94	15.0	5.0	23					2	2
KCD1 NW-02		163	75	3.4				-12.0	-94	18.2	10.7	56					3	3
KCD1 NW-03		100	67														1	1
KCD1 NW-04		3	2	0.0				-13.7	-102				>50		7.72E-04		12	2
KCD1 NW-06		93	49	2.6				-12.2	-95	17.2	6.4	37					2	2
KCD1 RIVER		2	0.3	0.1				-12.2	-95								1	1
KCD1 SW-02		53	91	0.0				-12.7	-98	23.5	8.8						1	1
KCD1 SW-03		45	29	1.9		3.8		-12.4	-95	27.3	11.6	32					1	1
KCD1 SW-07		165	26														2	2
KCD1 SW-08		184	117	2.3		1.3		-10.9	-89	16.9	6.9	22					2	2
MCD1 LAGOON		514	0.0	692													1	1
MCD1 V-01		318	425	<0.02		5.6	13.0	-9.3		13.9	7.4	31	1.0	0.5	-4.36E-03		25	1
MCD1 V-14		71	316	<0.02			5.8			11.2	1.7	0	1.2	0.5	1.26E-03		18	2
MCD1 V-18		77	196	1.7		3.3	8.1			10.1	-0.5	0					2	2
MCD1 V-21		145	163	<0.02		1.4	23.0	-9.1		19.9	9.2	0	0.0		2.05E-02		1	1
MCD1 V-24		30	201	<0.02		7.0	5.4	-10.5		7.4	-0.7	0	0.0		4.31E-04		20	2
MCD1 V-99		73	303	2.4			12.0			10.3	0.4	0	0.9	0.5	-3.99E-05		19	1
MCD1 W-02		226	2	149		0.6	13.0	-9.1				138			2.00E-01		2	2
MCD1 W-03		82	342	0.7		0.8	15.0	-10.5				0			1.83E-03		18	1
MCD1 W-05		48	231					-10.7		6.8	-2.5	0	0.0		1.68E-02		1	1
MCD1 W-10		56	426	<0.02			12.0	-10.3		9.1	0.0	0			2.52E-03		19	2
MCD1 W-16		299	6	114		0.7	9.1	-8.1				154					2	2
MCD1 W-17		137	172	27		0.7	9.8	-9.4		30.2	13.1	84					2	2
MCD1 W-23		81	356	1.9		1.1	10.4	-10.2				0			1.65E-03		20	2
MCD1 W-30		49	325					-9.9		5.3	-1.6	0	1.1	0.4	1.23E-03		17	1
MCD1 W-31		41	188					-10.9		8.0	-1.1	0	0.0		1.82E-03		1	1
MCD1 W-34		63	186					-10.8		7.9	-2.6	0	1.6	0.5	2.77E-03		17	1
MCD1 W-35		160	304					-9.7		11.8	5.5	0	1.2	0.4	1.52E-03		17	1
MCD1 W-98		70	0.4	<0.02			2.1	-10.6				45	10.0	4.6	1.76E-03		18	2

APPENDIX B

Assessing the Impact of Animal Waste Lagoon Seepage on the Geochemistry of an Underlying Shallow Aquifer

Walt W. McNab, Jr.¹, Michael J. Singleton², Jean E. Moran², and Bradley K. Esser^{2*}

¹*Environmental Restoration Division, Lawrence Livermore National Laboratory*

²*Chemical Biology & Nuclear Science Division, Lawrence Livermore National Laboratory*

* *Corresponding Author, P.O. Box 808, L-231, Livermore, California, 94551; Telephone (925) 422-5247; Fax (925) 422-3160; Email bkesser@llnl.gov*

Abstract

Dairy facilities and similar confined animal operation settings pose a significant nitrate contamination threat to groundwater via oxidation of animal wastes and subsequent transport through the subsurface. While nitrate contamination resulting from application of animal manure as fertilizer to fields is well recognized, the impact of manure lagoon leakage on groundwater quality is less well characterized. For this study, a dairy facility located in the southern San Joaquin Valley of California has been instrumented with monitoring wells as part of a two-year multidisciplinary study to evaluate nitrate loading and denitrification associated with facility operations. Among the multiple types of data collected from the site, groundwater and surface water samples have been analyzed for major cations, anions, pH, oxidation-reduction potential, dissolved organic carbon, and selected dissolved gases (CO₂, CH₄, N₂, Ar, Ne). Modeling of geochemical processes occurring within the dairy site manure lagoons suggests substantial off-gassing of CO₂ and CH₄ in response to mineralization of organic matter. Evidence for gas ebullition is evident in low Ar and Ne concentrations in lagoon waters and in groundwaters downgradient of the lagoon, presumably as a result of gas “stripping”. Shallow groundwaters with Ar and Ne contents less than saturation with respect to atmosphere are extremely rare, making the fractionated dissolved gas signature an effective tracer for lagoon water in underlying shallow groundwater. Preliminary evidence suggests that lagoon water rapidly re-equilibrates with the atmosphere during furrow irrigation, allowing this tracer to also distinguish between seepage and irrigation as the source of lagoon water in underlying groundwater. Together with ion exchange and mineral equilibration reactions, identification of lagoon seepage helps to constrain key attributes of the local groundwater chemistry, including input and cycling of nitrogen, across the site.

Introduction

Background

Management of animal wastes at dairy facilities and similar confined animal operations often entails utilizing manure lagoons to store dairy wastewater which is rich in solids, organic nitrogen, and ammonia. Irrigation with manure lagoon water is a common practice as it provides the dairy operator with a readily available source of fertilizer while reducing the volume of waste stored in the lagoons. However, the transfer of anoxic manure lagoon water to aerated sandy unsaturated zone soils leads to the mineralization of organic nitrogen and nitrification of ammonia to nitrate and thus is a potential source of nitrate contamination to underlying groundwater when nitrogen is added to the fields in excess of the amount that can be assimilated by the crops (1-3).

The impact of direct seepage from anaerobic lagoons on the geochemistry of the underlying aquifer is a complex problem that depends upon a variety of geochemical and hydrological factors. As the majority of the nitrogen in manure lagoons exists in chemically reduced forms, water that seeps out of the bottom of lagoons may not necessarily directly increase nitrate concentrations if transport occurs under anoxic conditions. Moreover, ammonium ion (NH_4^+), a major constituent of such waters, may be adsorbed onto clay minerals in sediments during transport, further reducing the dissolved nitrogen load to groundwater (4). Finally, seepage waters rich in organic carbon may contribute significantly to the creation of anoxic conditions conducive to heterotrophic denitrification driven by microbial oxidation of organic material in the manure lagoon water.

Manure lagoons leak at measurable rates affected by soil type, construction, and operation. Unlined dairy lagoons constructed in coarse alluvial soils in Utah leak at rates ranging from 13 to 91 mm (5). Swine and cattle waste lagoons in southwestern Kansas leak at rates ranging from 0.2 to 2.4 mm/day (6). In the Kansas study, permeability in new lagoons constructed without clay liners decreased by a factor of five after addition of waste to the lagoons, indicating that organic sludge buildup over time does affect permeability (7). In the northern San Joaquin Valley of California, Harter et al. (8) inferred manure lagoon leaching rates on the order of 2 mm/day.

Site Description and Groundwater Analytical Suite

Given prior assessments indicating the potential for manure lagoon leakage, the goal of this study has been to expand upon the understanding of the impact of manure lagoon seepage on underlying groundwater in terms of (1) specific geochemical interactions, (2) alternative means for identifying groundwater affected by lagoon seepage, and (3) quantification of the lagoon water mixing fraction at various distances from an active manure lagoon system. The study has entailed evaluating data collected as part of a broader multi-disciplinary evaluation of saturated zone denitrification at a dairy facility located in Kings County, California in the southern portion of the San Joaquin Valley. The dairy facility operates in a typical fashion for older dairies in Kings County. It holds approximately 1,000 cows and three active manure lagoons, two of which have liners with a 10% clay content and the third unlined. The lagoons receive runoff water from animal stall flushing that utilizes water pumped from agricultural wells that are located onsite.

DRAFT - DO NOT DISTRIBUTE OR RELEASE

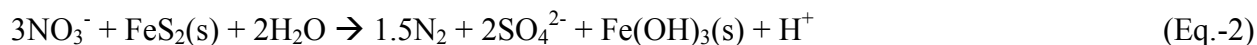
The largest of the lagoons measures approximately 200 m x 40 m (Figure 1). Water depth within the lagoons varies temporally but may range up to 3 m or more at certain times of the year.

The site is characterized by a shallow perched aquifer (to 10 m depth) and a deeper regional aquifer (greater than 40 m depth) that are separated by an unsaturated zone. Both aquifers consist of alluvial fan deposits which contain modest solid-phase concentrations of organic carbon (typically ~ 0.1% weight fraction) and reduced sulfur (1-10 $\mu\text{mol/gm}$). Recharge to the shallow aquifer is ultimately derived from one or more nearby unlined irrigation canals that carry water from the Kings River. However, local agricultural pumping from the shallow aquifer and infiltration from irrigation water appear to be dominant factors in shaping the shallow hydrologic system. The deeper aquifer is characterized by intensive regional pumping, rapidly decreasing water levels, and the apparent disposition of the shallow aquifer as a perched system for an area exceeding 1 km^2 in the vicinity of the dairy. The air gap separating the aquifers is depleted in oxygen and exhibits gas pressure changes in response to water level fluctuations in the deeper aquifer. Detailed vertical profiles of soil and microbial characteristics, groundwater chemistry, and dissolved excess nitrogen for the shallow aquifer were obtained at 5-ft (1.5-m) intervals at several locations using direct-push sampling technology as well as installed multi-level monitoring wells (Figure 1).

A variety of groundwater geochemical parameters were analyzed from water samples collected over several sampling events spanning a period of approximately two years. These include dissolved gases (O_2 , N_2 , CO_2 , CH_4 , Ar, Ne) measured by membrane inlet mass spectroscopy – MIMS (9), or noble gas mass spectrometry. Part of the rationale for collecting dissolved gas data was to quantify excess N_2 , or the concentration of nitrogen produced as a result of either heterotrophic denitrification,



or, alternatively, autotrophic denitrification,



Excess N_2 can be distinguished from atmospheric nitrogen by comparison with dissolved argon, the dominant source of which is atmospheric. In addition to the dissolved gases, major as well as trace cations (Ca^{2+} , Mg^{2+} , Na^+ , K^+ , Li^+ , NH_4^+) and anions (NO_3^- , SO_4^{2-} , Cl^- , F^- , Br^- , PO_4^{3-} , NO_2^-) were quantified by ion chromatography using a Dionex DX-600®. pH, DO, and oxidation-reduction potential were measured in the field using a Horiba U-22® water quality parameter field meter. Dissolved inorganic carbon (DIC) concentrations were estimated in the water samples by employing the PHREEQC geochemical model (10) to achieve charge balance in the samples by adjusting and speciating DIC at the measured pH values. This approach provides rough qualitative agreement between the implied equilibrium CO_2 partial pressures with those measured by MIMS (Figure 2). Dissolved organic carbon was measured in a subset of samples as CO_2 gas pressure after acidification with orthophosphoric acid. Finally, isotopic compositions of hydrogen and oxygen in water ($\delta^2\text{H}$ and $\delta^{18}\text{O}$) were determined using a VG Prism II® isotope ratio mass spectrometer, and are reported in per mil values relative to the Vienna Standard Mean Ocean Water (VSMOW). Oxygen isotope compositions were determined using the CO_2

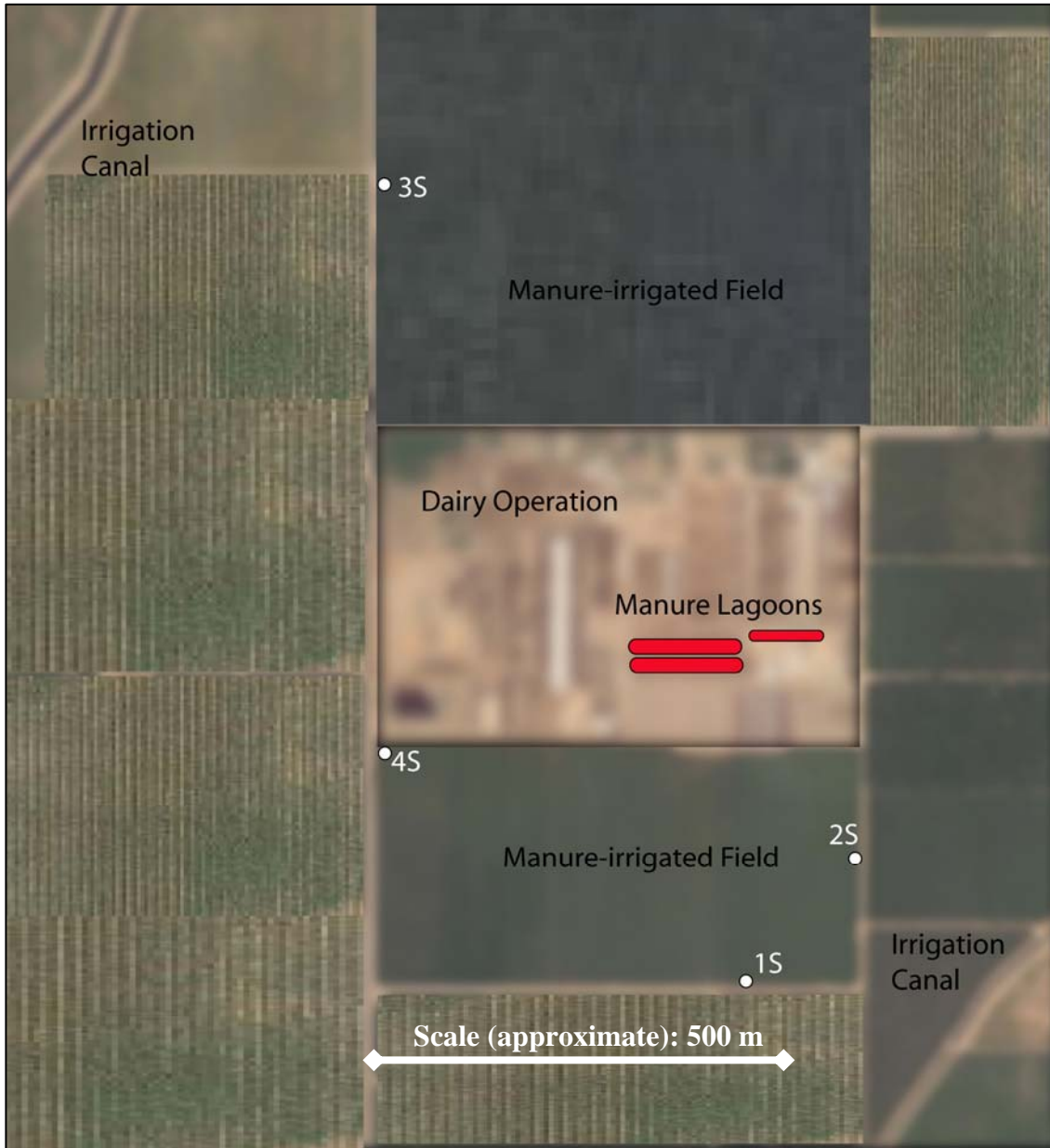


Figure 1. Site map of the instrumented dairy site indicating the locations of the manure lagoons and monitoring well locations.

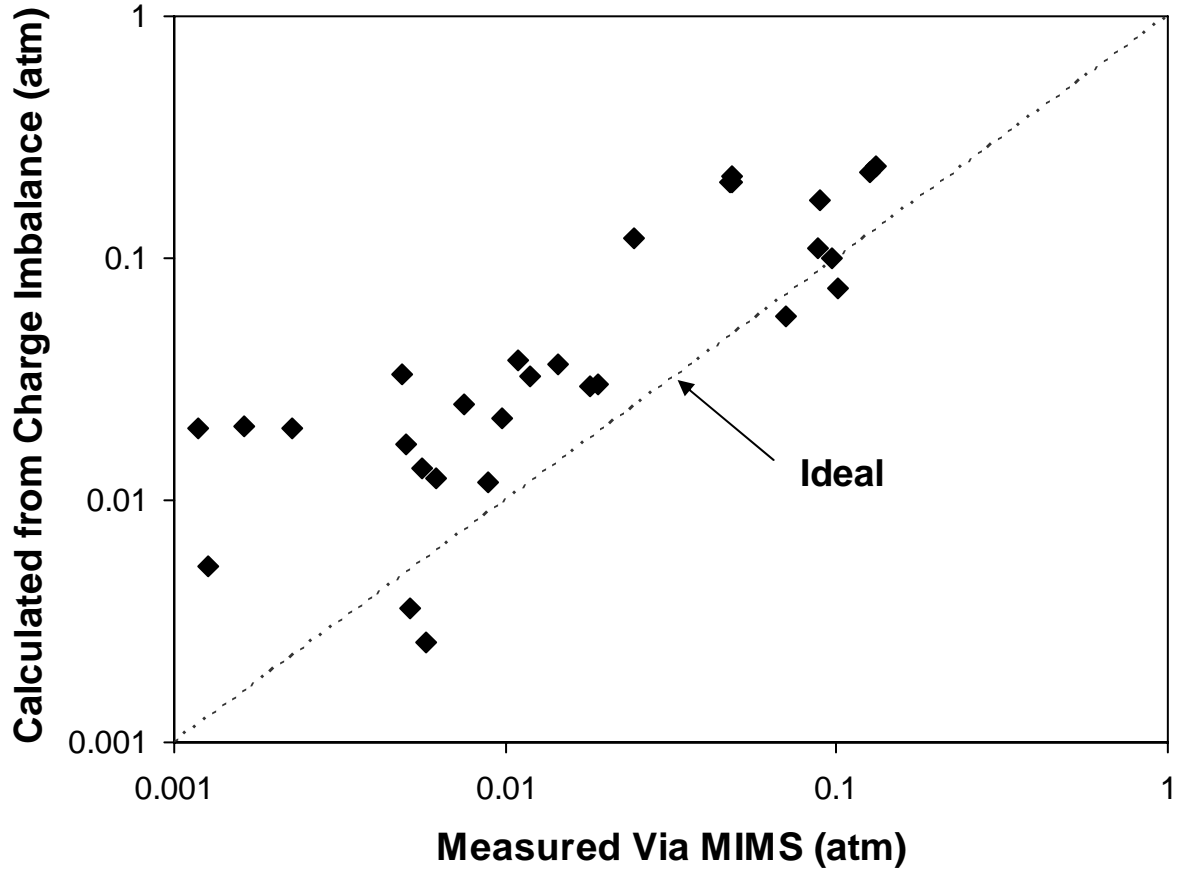


Figure 2. Correlation between carbon dioxide partial pressures calculated using PHREEQC from water sample charge imbalances and the assumption of thermodynamic equilibrium and partial pressures measured using MIMS (MIMS measurements at low concentrations may be characterized by low accuracy).

equilibration method (11), and hydrogen isotope compositions were determined using the Zn reduction method (12).

Site Groundwater Characteristics

Surface and groundwater samples collected across the site were categorized into groups based on both location and evidence for pertinent geochemical processes. The geochemical compositions for each of these groups are summarized in Table 1. “Lagoon Water” refers to surface water samples collected from three individual manure lagoons at the site. These lagoons, operated in series, receive input from the animal stalls and are tapped to fertilize animal feed crops on site; each is subject to evaporative losses, gas evolution, and some degree of leakage losses. As a result, there is much compositional variability between samples but the Lagoon water remains distinct, particularly in terms of signature elevated NH_4^+ , K^+ , Cl^- , and PO_4^{3-} concentrations. Lagoon water samples are also characterized by a relatively high pH and low oxidation-reduction potential, high CH_4 and CO_2 partial pressures, and relatively low sulfate concentrations compared to the other sample groups (Figure 3). “Near-Lagoon Groundwater” refers to those groundwater samples collected from wells in the immediate vicinity of the manure lagoons (within approximately 50 meters) from depths greater than approximately 11 meters below the ground surface. These groundwater samples are characterized by relatively low oxidation-reduction potentials, low dissolved oxygen concentrations, high CO_2 partial pressures (equivalent to those of the Lagoon water), and comparatively low sulfate concentrations. As discussed below, fractionated dissolved gas compositions provide an additional line of evidence that these groundwater samples have been impacted by the Lagoon Water. “Deep Field Groundwater” refers to groundwater samples collected across the site (i.e., under the crop fields) from depths greater than approximately 11 meters (exclusive of the Near-Lagoon water and the Downgradient Water, as described below) that are characterized by appreciable excess N_2 in comparison to NO_3^- (Table 1), likely reflecting denitrification (Singleton et al., 2006). In contrast, “Shallow Field Groundwater” refers to those samples collected from shallower depths that generally contain higher concentration of NO_3^- and less excess N_2 . Shallow and Deep Field Groundwaters differ somewhat in both oxidation-reduction potential and pH, with the Deep Field Groundwater samples being slightly more reducing and alkaline. Both Shallow and Deep Field Groundwaters are characterized by similarly low CO_2 and CH_4 partial pressures when compared to both the Lagoon Water and Near-Lagoon Groundwater. “Downgradient Groundwater” refers to groundwater samples collected from one location, 2S, southeast of the manure lagoons (Figure 1) below a depth of 11 meters where the water chemistry differs somewhat from that of Deep Field Groundwater (e.g., comparatively low pH and elevated excess N_2) and, as discussed below, dissolved gas compositions indicate a Lagoon Water impact. Finally, “Irrigation Water” refers to the median composition of groundwater samples collected from agricultural pumping wells operated onsite. These wells are screened across a wide depth interval (greater than 10 m) so that produced water is a mixture of the above-defined groups (exclusive of Lagoon Water).

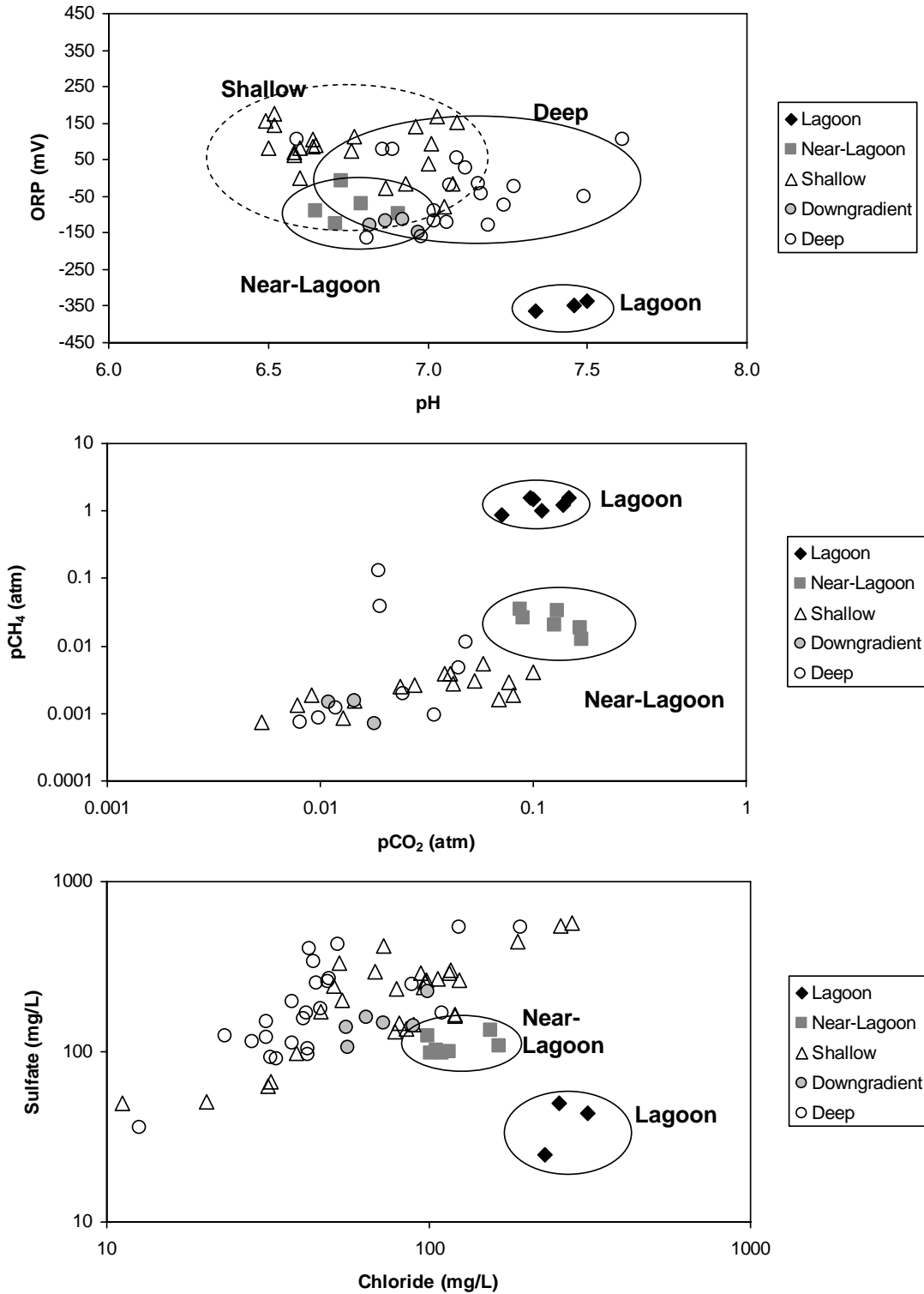


Figure 3. (a) Oxidation-reduction potential (ORP) versus pH for water samples collected across the dairy site; (b) methane versus carbon dioxide partial pressures, as measured via MIMS; and (c) sulfate versus chloride – the Lagoon and Near-Lagoon sample groups appear to be sulfate-depleted in comparison to the other groups when normalized by chloride.

Lagoon Water Chemistry

Lagoon Water Process Simulation

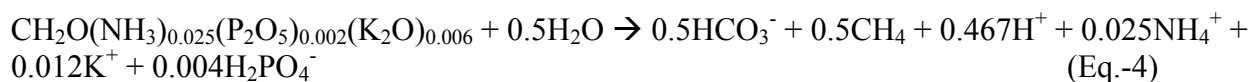
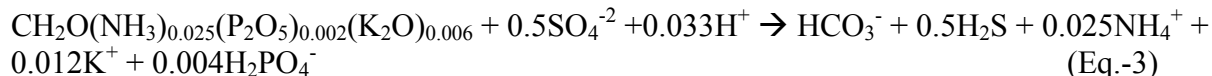
Manure lagoons clearly represent a complex, open system. Key oxidation-reduction indicators such as oxidation-reduction potential, CH₄ partial pressure, and depleted sulfate (compared to other water composition groups at the site) indicate that Lagoon Water samples from the dairy facility reflect chemically reducing conditions, which is consistent with expectation and prior studies (7). These reducing conditions are ultimately produced via the mineralization of organic matter in the pumped agriculture well water used to flush the animal stalls, a process that may require months of reaction time to reach completion (13). Nitrogen speciation is dominated by NH₄⁺ (and, presumably, organic nitrogen which was not measured), although geochemical processes in the lagoons such as nitrification, denitrification, and N₂ production from reactions between ammonium and nitrate/nitrite (14, 15) cannot be ruled out, particularly when the potential for oxidation-reduction stratification as a function of depth is considered. Moreover, because lagoon water is ultimately derived from pumped agricultural supply wells, a component of the nitrogen present in the lagoon water may reflect past cycling.

Simulation of major geochemical processes in the Lagoon Water is a useful first step in identifying potential diagnostic indicators of seepage in underlying groundwater. To model the Lagoon Water chemistry, PHREEQC was used to simulate the addition of a hypothetical manure composition to the mean irrigation water composition at the dairy site. The chemical composition of dairy manure is variable and depends on a number of factors, including feed composition, degree of mixing with urine, and storage issues that affect both decomposition and preferential loss of volatile components. Most reported manure compositions pertain mainly to nutrient content (nitrogen, phosphorous, and potassium), which is usually provided on a per weight basis. The total nutrient mass is typically listed as less than five percent for dry manure, with roughly equivalent portions of nitrogen and potassium and a much smaller phosphorous component (16, 17). For a hypothetical manure composition, we assumed that all of the nitrogen may be represented as NH₃, phosphate as P₂O₅, and potassium as K₂O that taken with an organic carbon component, CH₂O, yields a stoichiometric formula of CH₂O(NH₃)_{0.025}(P₂O₅)_{0.002}(K₂O)_{0.006} (“manure”) that is consistent with reported nutrient characteristics. This idealized composition, with a carbon-to-nitrogen ratio of approximately 34-to-1, on a per weight basis, is similar to the value of 28-to-1 listed by Cameron et al. (1).

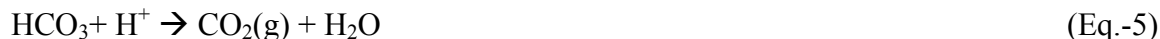
A number of reactions are anticipated as the manure composition is added to Irrigation Water. Examples include sulfate reduction, methanogenesis, solid-phase equilibration reactions involving carbonates (calcite, dolomite, siderite), ferric oxyhydroxides, iron sulfides, as well as gas (e.g., CH₄, CO₂, H₂S) evolution reactions. Multiple models can be constructed using different combinations of possible heterogeneous reactions in attempt to reproduce the lagoon water composition. However, because much of the volume of the Lagoon Water is likely not in direct contact with soil mineral assemblages, we assumed that dissolution of mineral phases into the lagoon water during the titration would be relatively unimportant. Therefore, assumed heterogeneous reactions in the titration model were limited to: (1) precipitation of Ca- and Mg-carbonates from the lagoon water upon supersaturation with idealized calcite and dolomite phases, and (2) evolution of CH₄ and CO₂ gases if the respective partial pressures exceeded 1.0

and 0.1 atmospheres. The second criterion is consistent with measured dissolved gas concentrations in Lagoon Water samples (Figure 3) and with studies of lagoon biogas emission (4).

Titration of the Irrigation Water with the postulated manure composition yields good agreement with major geochemical parameters that characterize the Lagoon Water (Figure 4). According to the model, the characteristic composition of the Lagoon Water ultimately reflects two oxidation-reduction reactions – sulfate reduction and methanogenesis – that would be expected to occur in the lagoon in the absence of appreciable dissolved oxygen:



In a system closed with respect to the atmosphere, methanogenesis would tend to reduce the lagoon water pH. However, in an open system, off-gassing of CO₂ will produce the opposite effect:



By considering the escape of CO₂ from the lagoon water, the pH of the modeled system rises from pH 6.83 to pH 7.29 which is roughly consistent with the median observed Lagoon Water pH of 7.46 (i.e., noticeably elevated compared to the Irrigation Water). This rise in pH would tend to supersaturate the Lagoon Water with carbonate minerals, leading to precipitation reactions that deplete the Lagoon Water in both Ca²⁺ and Mg²⁺ relative to the Irrigation Water starting composition. This effect is apparent in the lagoon water data (although the model appears to overestimate the loss of Ca²⁺, presumably reflecting kinetic limitations and/or compositional uncertainty of the carbonate mineral phase).

Simultaneously achieving an approximate agreement between the Lagoon Water model and field data with respect to pH, NH₄⁺, K⁺, dissolved inorganic carbon, Ca²⁺, Mg²⁺, and CH₄ and CO₂ partial pressures requires the mineralization of some 0.9 moles of the postulated manure composition per kg of water. Given the final modeled DIC concentration (representing the mineralization end-product) of approximately 0.04 mol/kg, the implication is that the vast majority of the mineralized manure (a fraction greater than 90%) could, theoretically, escape from the system as CH₄ or CO₂ gas. Speciation of sulfur in the Lagoon Water is not well constrained because no data were available for dissolved sulfide concentrations. Stripping of H₂S via gas ebullition is a possible dissolved sulfur sink, given the calculated equilibrium partial pressure of approximately 10⁻² atm (in the presumed absence of other sinks). Running the PHREEQC model with the H₂S off-gassing set to occur at a lower value – 10⁻³ atm – does indicate that the majority of the dissolved sulfur (on the order of 90%) could be stripped from the Lagoon Water but otherwise exerts little effect on the overall water chemistry (i.e., raising the calculated end-state pH to 7.33).

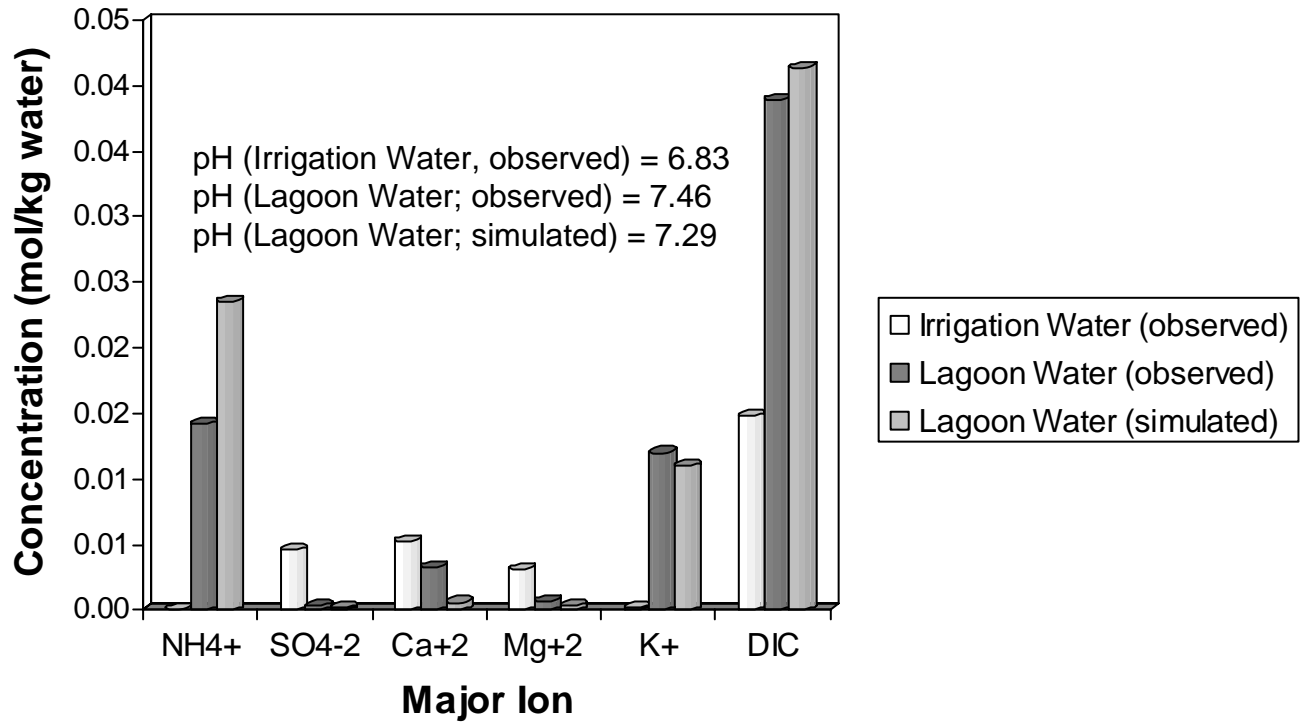


Figure 4. Comparison of key modeled and observed geochemical parameter values in median Lagoon Water (end-state) with Irrigation Water (initial condition).

Dissolved Noble Gases as Tracers

Tracking manure lagoon seepage is problematic because the lagoon water applied to field crops is chemically identical to seepage from the lagoons prior to oxidation in the soil zone. Ammonium ion is a logical tracer candidate but is only found in groundwater proximal to the lagoons because of the low mobility induced by its propensity for ion exchange. Other natural tracers of lagoon water include high concentrations of organic carbon, Cl^- , and the stable isotopic makeup of the lagoon water. Dissolved organic carbon, while measured in Lagoon Water at hundreds of parts per million (ppm), is found in comparatively low concentrations (generally on the order of 10 ppm) from samples collected from site monitoring wells. Since some solid-phase organic material has been found in sediment samples across the site, the provenance of dissolved organic material in groundwater is somewhat ambiguous. Lagoon water samples have high concentrations of Cl^- as result of salt in cow manure and urine and evaporation of lagoon water. Lagoon water samples also have elevated $\text{H}_2\text{O}-\delta^{18}\text{O}$ signatures as a result of evaporation. In dairy site groundwaters, a correlation exists between chloride content and water $\delta^{18}\text{O}$ that is consistent with mixing between local un-impacted groundwater and a high-chloride, evaporated water component characteristic of Lagoon Water (Figure 5). Such mixing is consistent with either field application of Lagoon Water or seepage of Lagoon Water directly from the lagoon. In both cases, the high-chloride and evaporated isotopic composition character of the Lagoon Water will be preserved.

To more definitively distinguish lagoon seepage from surface application, a tracer species that is unique to the lagoon environment and is mobile in groundwater is required. Biogenic production of methane and carbon dioxide in the anaerobic manure lagoons, indicated both by observation in other studies (e.g. 4) and by geochemical modeling in this study, may provide such a tracer. Specifically, significant ebullition of these gases as CH_4 and CO_2 concentrations exceed their solubility limits will induce exsolution fractionation (or “stripping”) of other gases present in the lagoon water (e.g., N_2 , Ar, Ne, He, etc.), which partition into the evolving gas phase and deplete the lagoon water of its dissolved gas load. This stripping process should lead to anomalously low and significantly fractionated dissolved gas concentrations in lagoon waters and, by extension, in lagoon seepage. Similar phenomena have been reported for groundwater coal bed methane environments (18) and ocean sediment pore waters (19). The advantage of utilizing dissolved gas data in lieu of Cl^- or $\delta^{18}\text{O}$ is that the gas-depleted signature produced in lagoons is likely to be reset when water is applied to the surface in fields, where it re-equilibrates with the atmosphere, and can thus be distinguished from direct lagoon seepage. Within the saturated zone, non-reactive dissolved gas constituents are expected to be transported conservatively.

The effects of gas exsolution in the lagoon water and re-equilibration during field application can be detected using MIMS measurements of dissolved Ar, N_2 , and O_2 which have revealed significant depletions in each of these atmospheric gases relative to air-equilibrated water (although the O_2 gas content by itself is ambiguous because of oxidation-reduction processes). Nearly all ambient groundwater samples have dissolved air concentrations in excess of equilibrium solubility concentrations (20). However, Lagoon Water with low gas contents is also characterized by fractionated gas compositions, as can be demonstrated by plotting the ratios of N_2/Ar and Ne/Ar (Figure 6) determined by noble gas mass spectrometry. Neon has a lower solubility and higher diffusivity than Ar, and is more likely to partition into the gas phase during

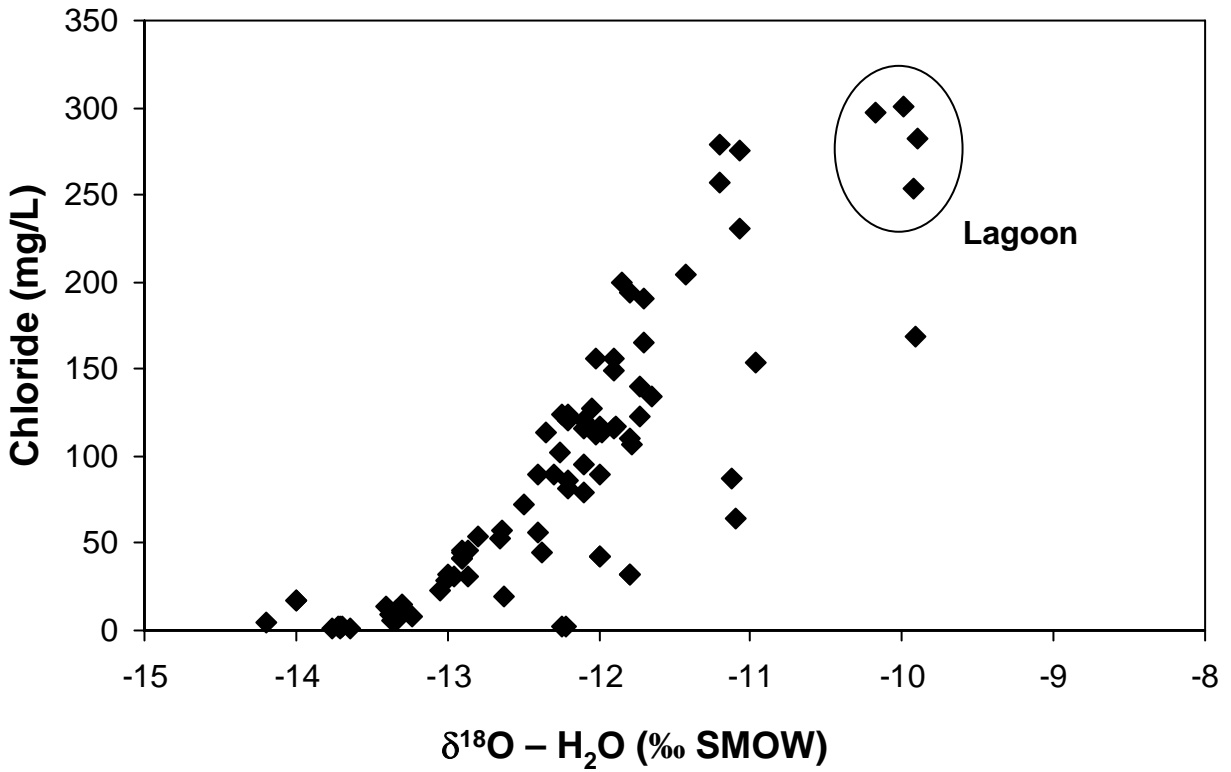


Figure 5. The correlation between chloride ion concentration and $\delta^{18}\text{O}$ in dairy site groundwaters is consistent with mixing between high-chloride, evaporated Lagoon Water and local groundwater, either through field application of Lagoon Water or through lagoon seepage.

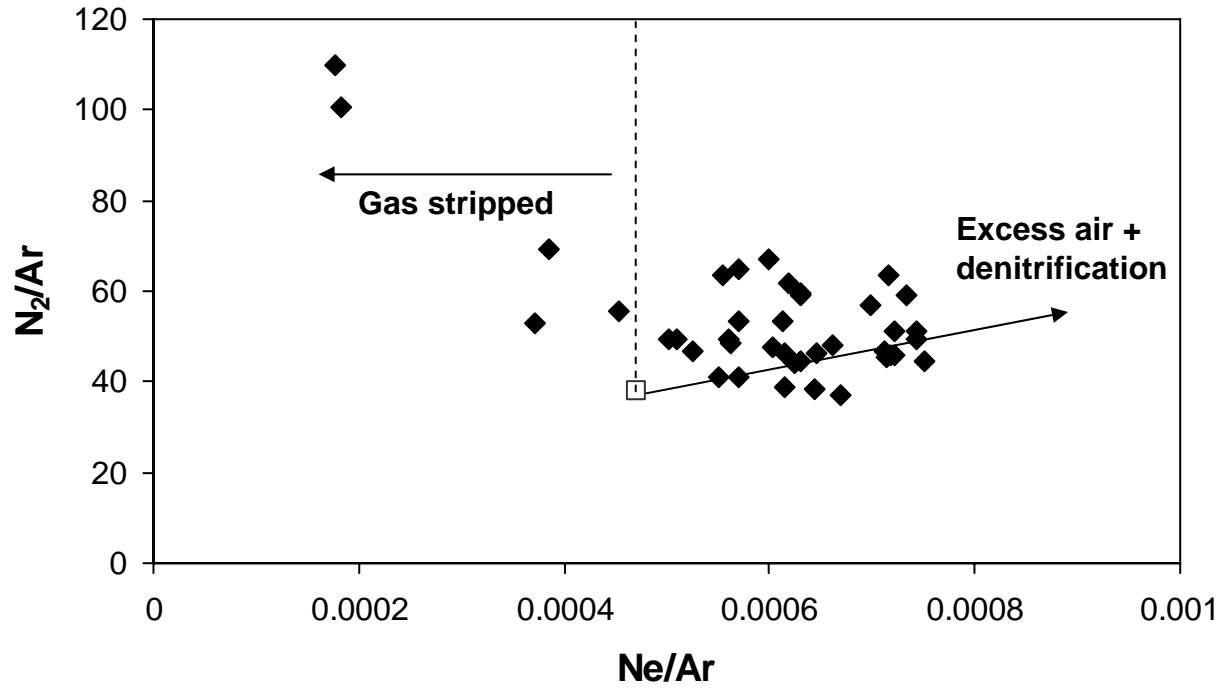


Figure 6. Evidence of gas stripping as indicated by Ar and Ne.

bubble formation. As a result, Ne/Ar ratios are highly sensitive to addition of excess air or gas stripping. Mixing of groundwater with lagoon seepage shifts the dissolved gas compositions to lower Ne/Ar ratios, whereas denitrification in the saturated zone increases the N₂/Ar ratio via production of N₂. Water in equilibrium with air would fall on an equilibrium line, with its precise position determined by the recharge temperature. Water compositions having Ne/Ar ratios lower than the equilibrium solubility value at this temperature are likely impacted by lagoon seepage. Addition of excess air during recharge will shift the dissolved gas compositions to higher N₂/Ar and Ne/Ar ratios, but this effect is confined to one of the excess air addition lines, with its starting position dependent on recharge temperature (shown as 15°C as an example on Figure 6). The water samples with the highest N₂/Ar (i.e., exhibiting the strongest evidence for denitrification) are also generally characterized by the lowest Ne/Ar ratios (i.e., exhibiting the strongest evidence for impact by lagoon seepage), suggesting a link between the two processes.

Impact of Lagoon Water Seepage on Aquifer Geochemistry

Given the geochemically distinct makeup of the Lagoon Water, identifying its footprint in the underlying groundwater requires a definitive tracer as well as a set of plausible explanations for the changes that occur in the water chemistry along the groundwater flow path between the lagoon environment and the measurement point (i.e., a monitor well). Some insight into those geochemical processes that could affect Lagoon Water seepage can be gleaned by directly modeling the transformation of Lagoon Water into Near-Lagoon water. This effort can identify, for example, the potential roles played by ion exchange and carbonate mineral equilibration reactions and which such reactions are plausible. A subsequent step, once these reactions have been identified, is to utilize the reactions together with tracer data, such as Ar concentrations, to identify mixing combinations of different waters that could explain the observed geochemistry at more distant locations using inverse geochemical modeling (Figure 7).

Proximal to Lagoon

Relationships between MIMS-measured Ar and CO₂ partial pressures for different groundwater sample groups from the dairy site are shown on Figure 8. Many of the Lagoon Water and Near-Lagoon Groundwater samples share similar characteristics in terms of relatively high CO₂ partial pressures and low (sub-atmospheric) Ar, suggesting some relationship between the two waters. With the exception of the Downgradient Groundwater samples, which are distinctively Ar-depleted but characterized by relatively low CO₂ partial pressures, the remaining groundwater samples exhibit a general positive correlation between CO₂ and Ar partial pressures, possibly reflecting the effects of entrapped air but lacking a discernable Lagoon Water signature.

Assuming that Lagoon Water does exert some effect on the Near-Lagoon Groundwater, seepage from the lagoons would be expected to bring about equilibration reactions with soil mineral assemblages, particularly ion exchange reactions, given the presence of clay liners used in the construction of the lagoons and the high concentrations of NH₄⁺ and K⁺ in the Lagoon Water (21). To explore the possible geochemical impacts of the infiltrating lagoon water composition on the underlying groundwater, the flushing of the end-state modeled Lagoon Water through an ion exchanger was simulated with PHREEQC. For this simulation, an ion exchange species characterized by a cation exchange capacity of 0.13 mol charge/kg of soil – a reasonable value

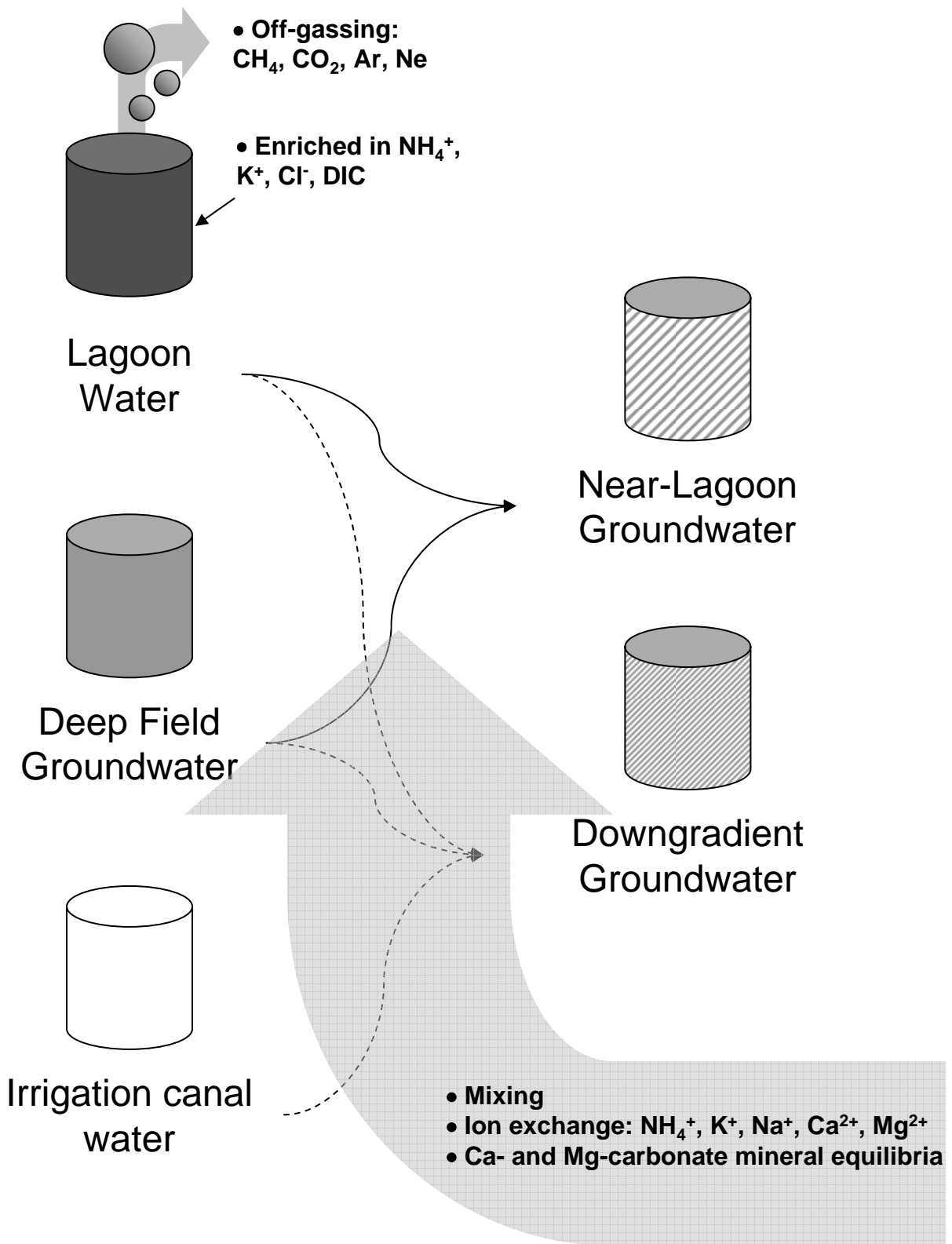


Figure 7. Conceptual model of site geochemical processes and mixing components that drives the geochemical modeling assessment of lagoon seepage.

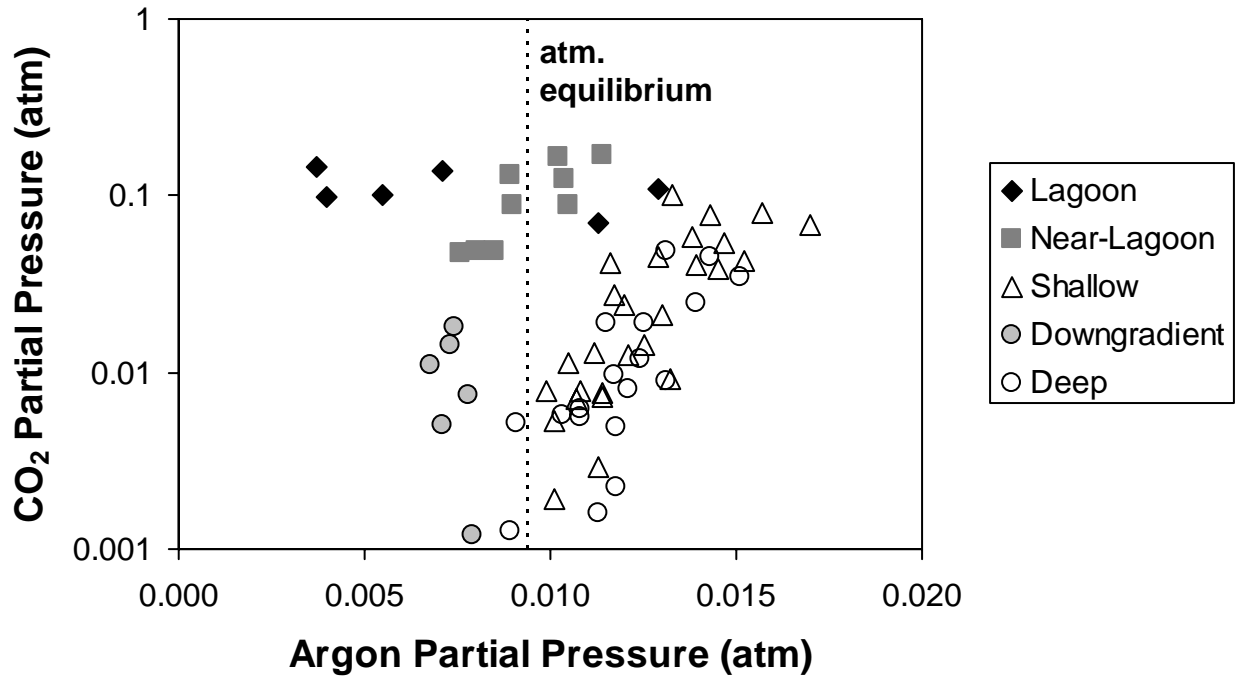


Figure 8. Relationship between dissolved argon concentrations and carbon dioxide (both expressed as partial pressures) in dairy site water samples. Samples that are undersaturated in argon relative to the atmosphere likely reflect a Lagoon Water signature; supersaturated samples likely reflect air that has been entrapped during irrigation/recharge.

DRAFT - DO NOT DISTRIBUTE OR RELEASE

for clayey soils (22) – was assumed to exist in equilibrium with the Deep Field Groundwater composition as an initial condition. Default cation exchange selectivity coefficients utilized by PHREEQC were assumed:



Equilibrium with Ca- and Mg-carbonate mineral phases was maintained during the simulated flushing. The predicted distributions of cations on the exchange sites after one pore volume and ten pore volumes are shown on Figure 9. Model results suggest that high concentrations of K^+ and NH_4^+ from the lagoon water would displace Ca^{2+} and Mg^{2+} from the exchange sites over time, leading to corresponding changes in the aqueous concentrations of these cations. This reaction would have a major (albeit latent) potential impact on groundwater quality in terms of nitrogen loading since a significant fraction of the nitrogen inventory could be sorbed on aquifer clay minerals. In turn, elevated Ca^{2+} and Mg^{2+} would lead to carbonate mineral precipitation reactions. The result of these precipitation reactions would be a decline in pH which the model matches well with respect to the observations in Near-Lagoon Groundwater (Figure 10). The alternative explanation – that the pH decline results from mineralization of organic carbon in the lagoon seepage – would imply an increase in the CO_2 partial pressure relative to the Lagoon Water, which was not observed (Table 1).

Distal

The lagoon water leaching model predicts changes in water chemistry in the Near-Lagoon Groundwater that are qualitatively consistent with observations. Simulating the effects of lagoon seepage on the Downgradient Groundwater composition (where lagoon impact is suspected owing to low Ar) is potentially more problematic because a much longer flow path is involved which creates more opportunity for mixing with water not related to the lagoon(s). To address the mixing problem directly, we utilized the inverse modeling capabilities of PHREEQC to identify mixing proportions of different water compositions, in addition to mineral equilibria, cation exchange, and gas exchange reactions that could plausibly explain the Downgradient Groundwater composition in terms of major cations, pH, Cl^- , SO_4^{2-} , nitrogen speciation, and Ar concentration. Specifically, this inverse modeling was based on the assumption that the Lagoon Water and Deep Field Groundwater compositions were available as components for mixing. In addition, water from a nearby unlined irrigation canal was assumed to also be available (water levels at this location have historically responded strongly to the presence or absence of water in the canal and water samples have generally indicated a relatively young $^3\text{H}/^3\text{He}$ age). The canal water was assumed to be characterized by low total dissolved solids (consistent with its measured chemical makeup) and an Ar concentration controlled by equilibrium solubility with

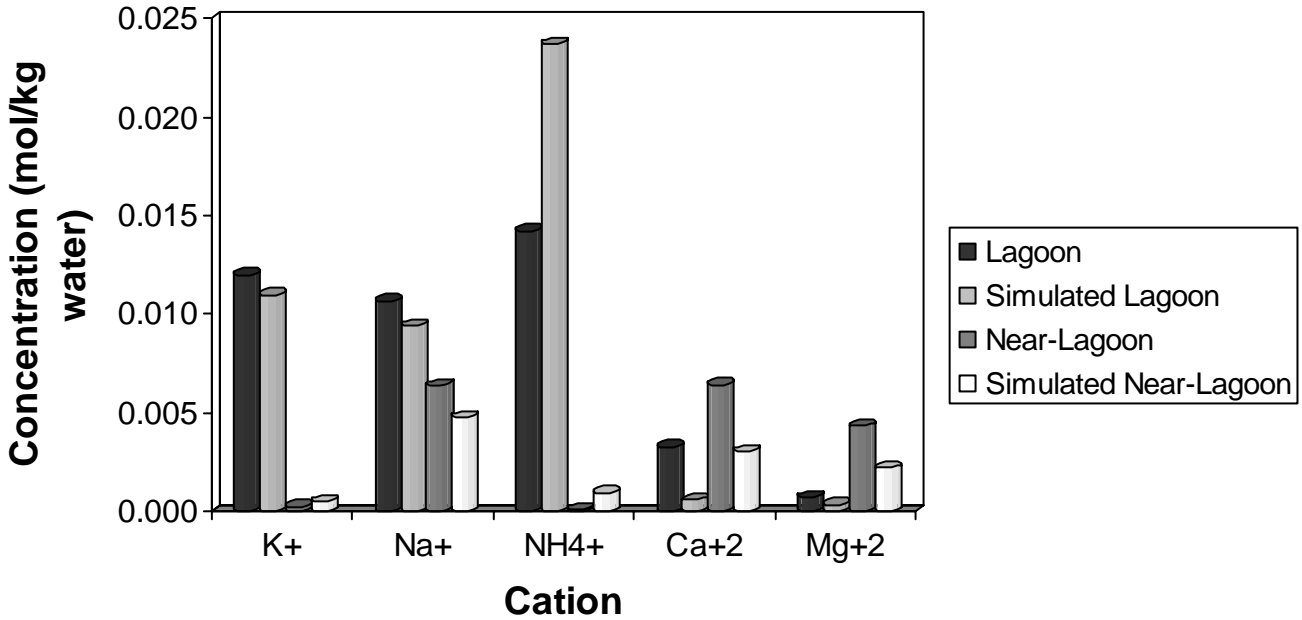
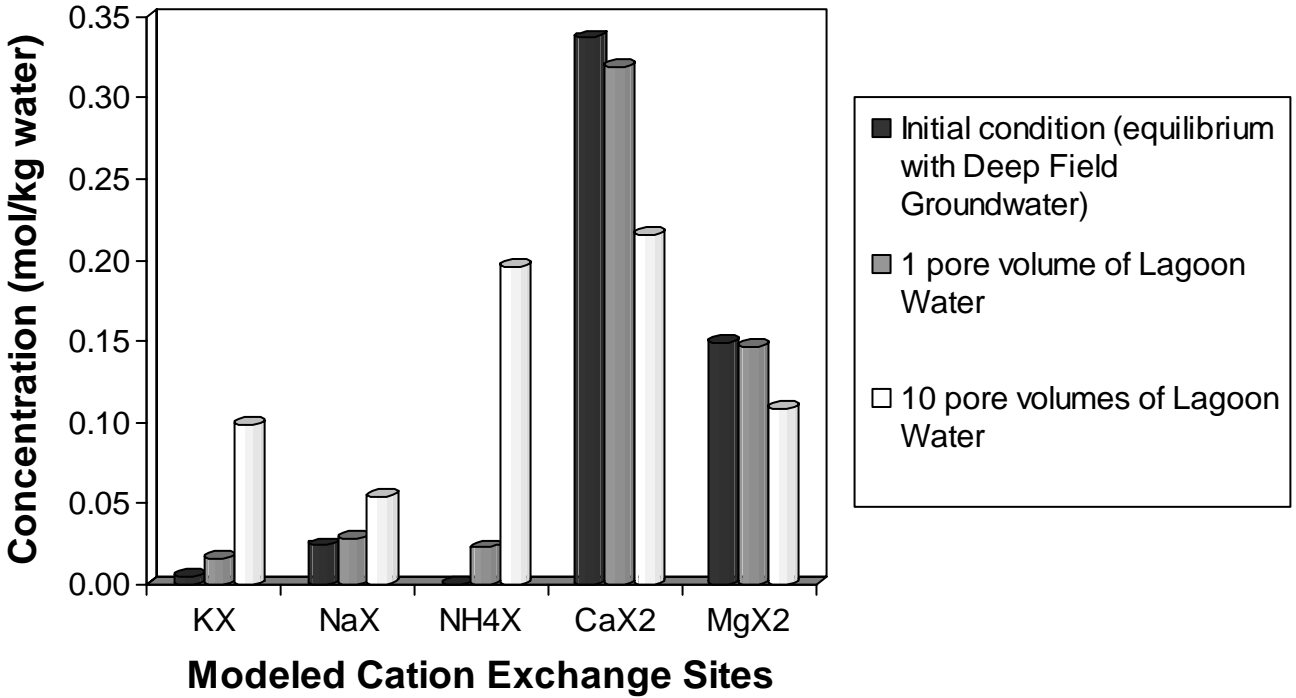


Figure 9. (a) Modeled changes in cation distributions on exchange sites in soil subjected to leaching by lagoon water; and (b) modeled changes in cation distributions after one pore volume as a result of lagoon water seepage interacting with soil minerals via cation exchange and carbonate mineral precipitation.

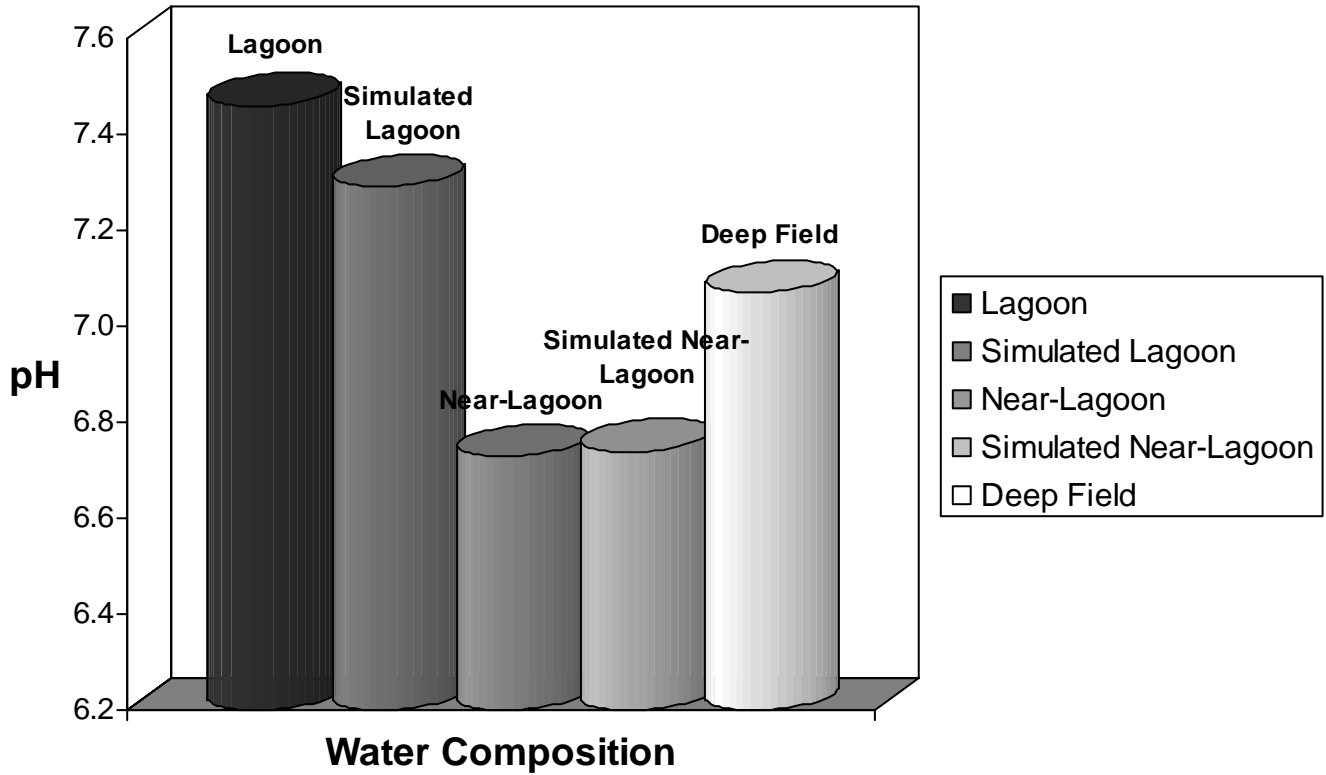


Figure 10. Modeled impact on Near-Lagoon Groundwater pH following leaching of Lagoon Water through an ion exchanger initially in equilibrium with Deep Field groundwater and subsequent carbonate mineral precipitation.

the atmosphere. Postulated mass transfer reactions available for consideration by the inverse model included cation exchange, oxygenation, and equilibration with calcite. A sample variability of 20% was assumed for all analytes, including argon. The representative end-member argon partial pressure in the Lagoon Water was estimated from the inverse modeling at 4×10^{-3} atmosphere (roughly 40% saturated with respect to 1 atmosphere) and is consistent with the lowest MIMS-measured argon partial pressures in the Lagoon Water.

Inverse geochemical modeling generally yields a number of non-unique models, so some care must be exercised in selecting candidate models that represent the most plausible scenarios. For these water compositions, inverse models were excluded that required (1) liberation of significant quantities of CO_2 along the flow path for both waters, which seems improbable given the depth below the water table, and (2) precipitation of carbonate minerals along the flow path for the Downgradient well location as these water samples have generally been thermodynamically undersaturated with respect to calcite (Figure 11). Given these constraints, reasonable inverse models that could explain the origin of the Downgradient Groundwater, and, for comparison, the Near-Lagoon Groundwater are illustrated on Figure 12, normalized to the respective Lagoon Water components for each model. For the Downgradient water, plausible mixing fractions consist of 11% Lagoon Water, 65% Deep Field Groundwater, and 25% irrigation canal water; the latter required for reconciling the median concentration of Ar with that of Cl. For the Near-Lagoon Groundwater, mixing fractions correspond to 60% Lagoon Water and 40% Deep Field Groundwater. For both examples, the normalized mass transfer reactions are consistent with the cation exchange model developed earlier in terms of displacement of Ca^{2+} and Mg^{2+} by K^+ and NH_4^+ . The principal difference between the two is the oxidation of some NH_4^+ along the flow path before it reaches the Downgradient location. The result is comparatively less displacement of Ca^{2+} along the flow path, thus reducing the potential for calcite precipitation.

Conclusions

Dissolved gas measurements in manure lagoon water and underlying shallow groundwater at an instrumented dairy site reflect the ebullition of CO_2 and CH_4 gases from the lagoons that acts to strip gases with respect to equilibrium atmospheric concentrations. Because these gases re-equilibrate with the atmosphere when the lagoon water is used for irrigation, they serve as a unique tracer for the lagoon water in the underlying aquifer and offer a clear advantage over NH_4^+ which is strongly affected by ion exchange. Geochemical modeling results are consistent with the dissolved gas measurements in two ways: (1) simulation of the lagoon water composition (mixing of irrigation water with a postulated manure composition) indicates the potential for substantial off-gassing of both CO_2 and CH_4 , which is a necessary condition for Ar and Ne depletion, and (2) measured Ar concentrations are consistent with geochemical models of the impact of lagoon seepage on underlying groundwater that incorporate mixing, ion exchange, and mineral equilibria. As such, this study has definitively shown that leakage from the manure lagoons is manifested in the shallow aquifer geochemistry at the dairy site.

The immediate environmental impact of lagoon leakage on the underlying shallow aquifer is the loading of nitrogen in the form of NH_4^+ . As NH_4^+ tends to be effectively bound by cation exchange sites, the shallow aquifer at the site is storing a significant quantity of nitrogen. The

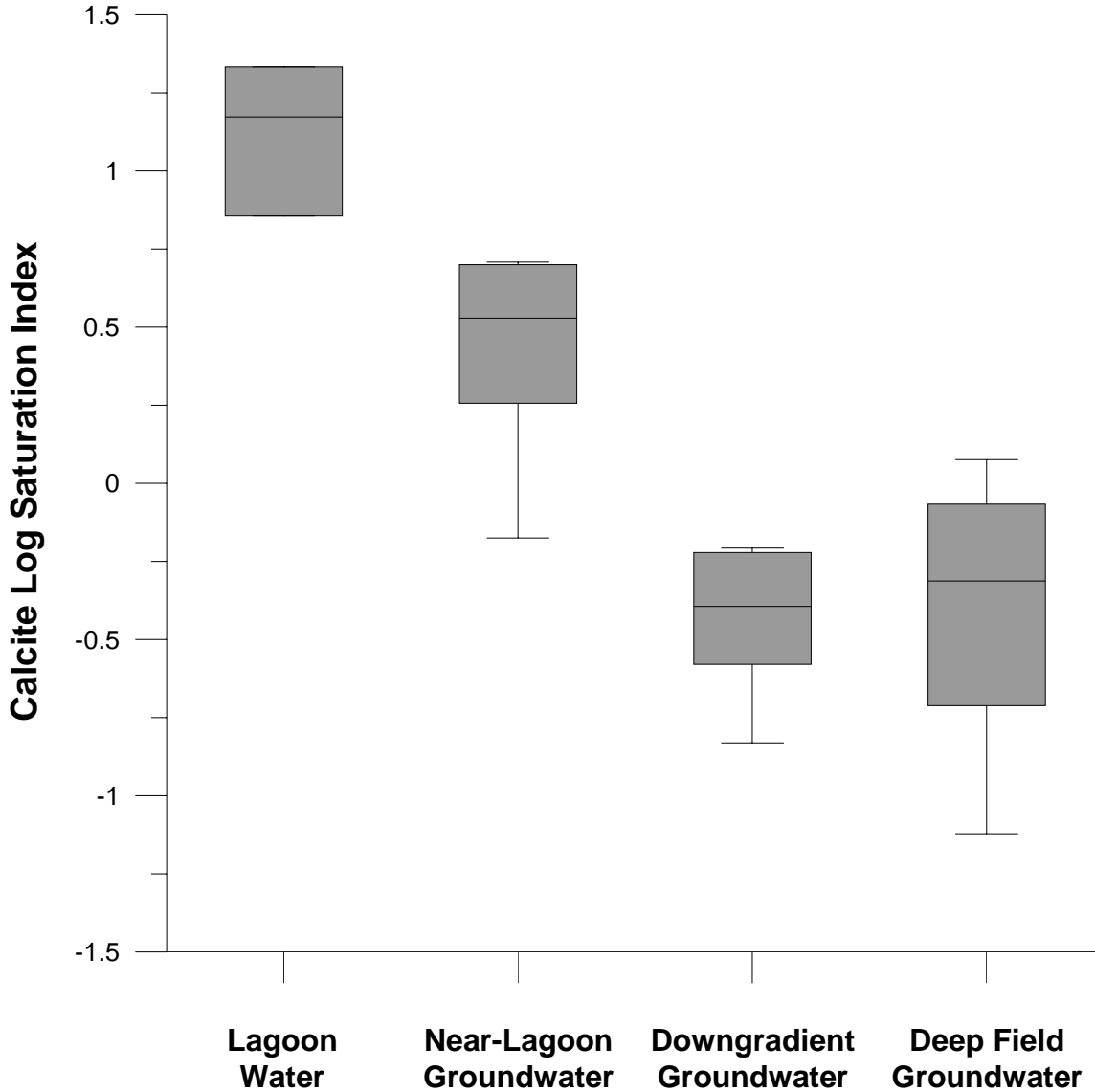


Figure 11. Box-whisker plot illustrating the distributions of calcite thermodynamic saturation indices (log scale) for the different water composition groups calculated via PHREEQC speciation of individual water samples. The box-whisker marks correspond to the minimum, maximum, median, lower quartile, and upper quartile values for each group.

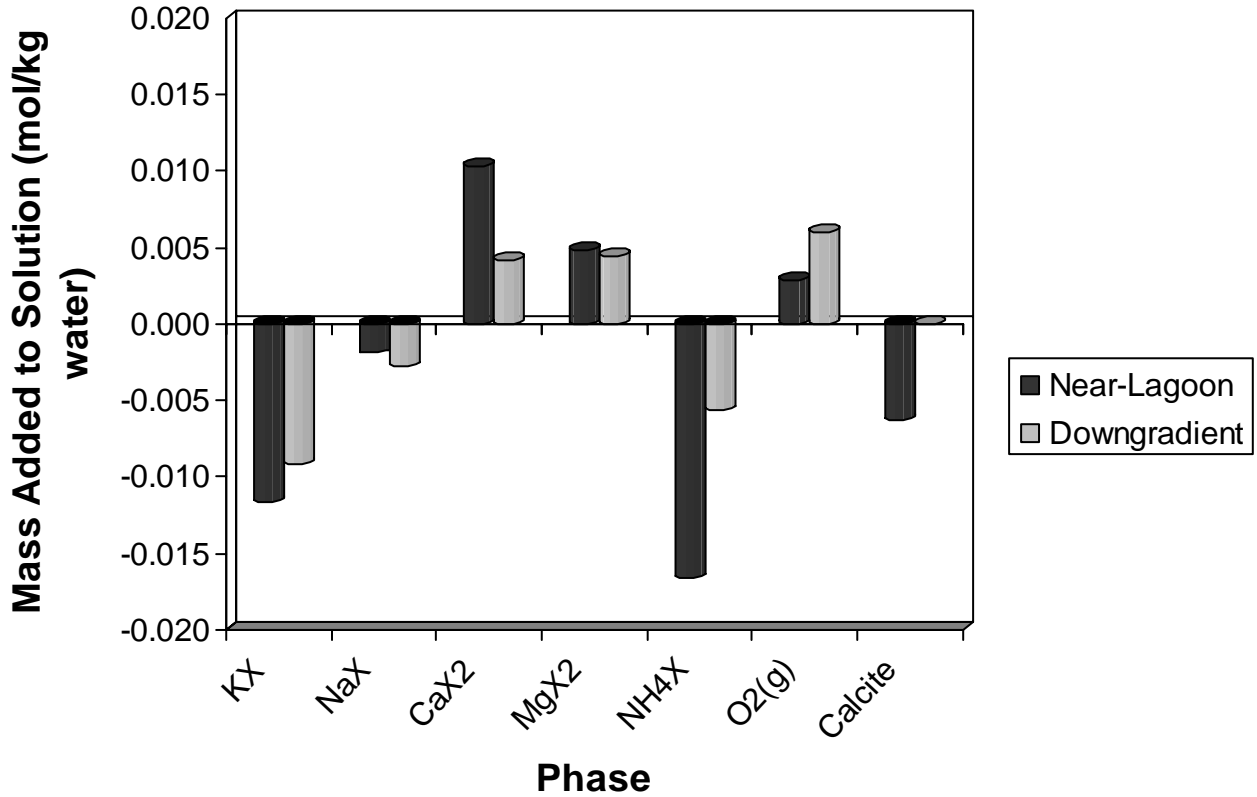


Figure 12. Mass transfer reactions that explain Near-Lagoon and Downgradient Groundwater compositions (along with mixing). Moles transferred are normalized to the modeled Lagoon Groundwater contributions (60% and 11% for the Near-Lagoon and Downgradient Groundwaters, respectively).

possibility of the conversion of the NH_4^+ to NO_3^- via nitrification, and the possible subsequent conversion of NO_3^- to N_2 via denitrification, will depend strongly on local redox conditions within the aquifer, which, in turn, appear to be influenced to some degree by the lagoon seepage itself. However, potential electron donors are also present in the subsurface in the forms of organic carbon and reduced sulfur species in the aquifer sediments. Moreover, both the oxidation of NH_4^+ and the off-gassing of N_2 will depend spatially and temporally on recharge and agricultural pumping, so that the overall nitrogen cycle operating at the site is quite complex. In this study, we have established that leakage from the manure lagoons plays a significant role in this cycle. Further research is needed to better characterize the potential long term impact of lagoon seepage and its effect on the fate of nitrogen at dairy operations.

Acknowledgements

This work was performed under the auspices of the U.S. Department of Energy by the University of California, Lawrence Livermore National Laboratory under Contract W-7405-ENG-48. . Funding for this project was provided by the California State Water Resources Control Board Groundwater Ambient Monitoring and Assessment Program and by Lawrence Livermore National Laboratory's Laboratory Directed Research and Development Program. The Groundwater Ambient Monitoring and Assessment program is sponsored by the State Water Resources Control Board and carried out in cooperation with the U.S. Geological Survey.

References

- (1) Cameron, K. C.; Di, H. J.; Reijnen, B. P. A.; Li, Z.; Russell, J. M.; Barnett, J. W., Fate of nitrogen in dairy factory effluent irrigated onto land. *New Zealand Journal of Agricultural Research*, 2002, 45, 217-216.
- (2) Karr, J. D.; Showers, W. J.; Jennings, G. D., Low-level nitrate export from confined dairy farming detected in North Carolina streams using delta N-15. *Agriculture Ecosystems & Environment* 2003, 95, 103-110.
- (3) Munoz, G. R.; Powell, J. M.; Kelling, K. A., Nitrogen budget and soil N dynamics after multiple applications of unlabeled or (15)Nitrogen-enriched dairy manure. *Soil Science Society of America Journal* 2003, 67, 817-825.
- (4) DeSutter, T. M.; Ham, J. M., Lagoon-biogas emissions and carbon balance estimates of a swine production facility. *J Environmental Quality* 2005, 34, 198-206.
- (5) Korom, S. F.; Jeppson, R. W., Nitrate contamination from dairy lagoons constructed in coarse alluvial deposits. *Journal of Environmental Quality* 1994, 23, 973-976.
- (6) Ham, J. M., Seepage losses from animal waste lagoons: A summary of a four-year investigation in Kansas. *Transactions of the Asae* 2002, 45, 983-992.
- (7) Gooddy, D. C.; Clay, J. W.; Bottrell, S. H., Redox-driven changes in porewater chemistry in the unsaturated zone of the chalk aquifer beneath unlined cattle slurry lagoons. *Applied Geochemistry* 2002, 17, 903-921.
- (8) Harter, T.; Davis, H.; Mathews, M. C.; Meyer, R. D., Shallow groundwater quality on dairy farms with irrigated forage crops. *Journal of Contaminant Hydrology* 2002, 55, 287-315.
- (9) Kana, T. M.; Darkangelo, C.; Hunt, M. D.; Oldham, J. B.; Bennett, G. E.; Cornwell, J. C., Membrane inlet mass spectrometer for rapid high precision determination of N₂, O₂, and Ar in environmental water samples. *Analytical Chemistry* 1994, 66, 4166-4170.
- (10) Parkhurst, D. L.; Appelo, C. A. J. User's Guide to PHREEQC (Version 2) - A Computer Program for Speciation, Batch Reaction One-Dimensional Transport, and Inverse Geochemical Calculations; Water-Resources Investigations Report 99-4259; U. S. Geological Survey: 2002.
- (11) Epstein, S.; Mayeda, T. K., Variation of O-18 content of waters from natural sources. *Geochim. Cosmochim. Acta* 1953, 4, 213-224.
- (12) Coleman, M. L.; Shepherd, T. J.; Durham, J. J.; Rouse, J. E.; Moore, G. R., Reduction of water with zinc for hydrogen isotope analysis. *Analytical Chemistry* 1982, 54, 993-995.
- (13) Van Kessel, J. S.; Reeves, J. B., Nitrogen mineralization potential of dairy manures and its relationship to composition. *Biology and Fertility of Soils* 2002, 36, 118-123.
- (14) Thamdrup, B.; Dalsgaard, T., Production of N₂ through anaerobic ammonium oxidation coupled to nitrate reduction in marine sediments. *Applied and Environmental Microbiology* 2002, 68, 1312-1318.
- (15) Jones, M. L.; Liehr, S. K.; Classen, J. J.; Robarge, W., Mechanisms of dinitrogen gas formation in anaerobic lagoons. *Advances in Environmental Research* 2000, 4, 133-139.
- (16) Van Averbeke, J. S.; Yoganathan, S. Using Kraal manure as a fertiliser; Agricultural Development and Rural Research Institute, Republic of South Africa Department of Agriculture: Pretoria, South Africa, 2003.
- (17) Christensen, P.; Peacock, B. Manure as a Fertilizer; NG7-97; University of California Cooperative Extension: Tulare, CA, 1998.

DRAFT - DO NOT DISTRIBUTE OR RELEASE

- (18) Zhou, Z.; Ballentine, C. J.; Kipfer, R.; Schoell, M.; Thibodeaux, S., Noble gas tracing of groundwater/coalbed methane interaction in the San Juan Basin, USA. *Geochimica Et Cosmochimica Acta* 2005, 69, 5413-5428.
- (19) Brennwald, M. S.; Kipfer, R.; Imboden, D. M., Release of gas bubbles from lake sediment traced by noble gas isotopes in the sediment pore water. *Earth and Planetary Science Letters* 2005, 235, 31.
- (20) Aeschbach-Hertig, W.; Peeters, F.; Beyerle, U.; Kipfer, R., Interpretation of dissolved atmospheric noble gases in natural waters. *Water Resources Research* 1999, 35, 2779-2792.
- (21) Liua, F.; Mitchell, C. C.; Odom, J. W.; Hill, D. T.; Rochester, E. W., Effects of swine lagoon effluent application on chemical properties of loamy sand. *Bioresources Technology* 1998, 63, 65-73.
- (22) Sposito, G., *The Chemistry of Soils*. Oxford University Press: New York, 1989.

DRAFT - DO NOT DISTRIBUTE OR RELEASE

Table 1. Summary of compositional parameters measured for water samples collected at the dairy site.
The top number in each entry is the median value (number of samples shown in parentheses); the range of values – 25th to 75th percentile – is indicated on the next line. Units for ion concentrations are mg/L.

Parameter	Lagoon Water	Near-Lagoon Groundwater	Shallow Field Groundwater	Downgradient Groundwater	Deep Field Groundwater	Irrigation Water
pH	7.46 (3); 7.40 – 7.48	6.73 (5); 6.71 – 6.79	6.76 (23); 6.59 – 7.01	6.90 (4); 6.86 – 6.93	7.07 (23); 6.94 – 7.17	6.83 (3); 6.78 – 6.92
Redox potential (mV)	-350 (3); -358 – -343	-91 (5); -96 – -70	+85 (22); +46 – +134	-123 (4); -134 – -116	-33 (18); -112 – 49	-
Ar (cm ³ STP/g)	2.1 x 10 ⁻⁴ (6); 1.5 x 10 ⁻⁴ – 3.5 x 10 ⁻⁴	3.1 x 10 ⁻⁴ (9); 2.9 x 10 ⁻⁴ – 3.6 x 10 ⁻⁴	4.1 x 10 ⁻⁴ (27); 3.8 x 10 ⁻⁴ – 4.7 x 10 ⁻⁴	2.5 x 10 ⁻⁴ (6); 2.4 x 10 ⁻⁴ – 2.6 x 10 ⁻⁴	4.1 x 10 ⁻⁴ (23); 3.9 x 10 ⁻⁴ – 4.5 x 10 ⁻⁴	3.4 x 10 ⁻⁴ (6); 3.0 x 10 ⁻⁴ – 4.0 x 10 ⁻⁴
pCO ₂ (atm)	0.105 (6); 0.098 – 0.132	0.089 (9); 0.048 – 0.131	0.021 (27); 0.008 – 0.044	0.009 (6); 0.006 – 0.014	0.008 (18); 0.005 – 0.019	0.036 (2); 0.035 – 0.036
pCH ₄ (atm)	1.376 (6); 1.072 – 1.527	0.024 (6); 0.019 – 0.031	0.003 (16); 0.002 – 0.003	0.001 (3); 0.001 – 0.002	0.002 (9); 0.001 – 0.011	-
Na ⁺	245 (4); 197 – 292	147 (7); 139 – 165	113 (25); 91 – 155	61 (6); 53 – 68	65 (20); 41 – 95	217 (9); 203 – 237
K ⁺	468 (4); 436 – 520	9 (7); 7 – 13	4 (25); 4 – 6	5 (6); 3 – 7	5 (20); 3 – 8	6 (9); 5 – 8
Ca ²⁺	131 (4); 109 – 154	257 (7); 178 – 303	125 (25); 82 – 143	76 (6); 68 – 89	69 (20); 55 – 80	210 (9); 164 – 233
Mg ²⁺	17 (4); 16 – 42	105 (7); 91 – 116	53 (25); 33 – 60	32 (6); 31 – 34	30 (20); 23 – 36	76 (9); 73 – 84
Cl ⁻	242 (4); 213 – 269	111 (7); 104 – 136	86 (29); 53 – 116	68 (6); 58 – 85	42 (24); 33 – 49	156 (9); 128 – 169
SO ₄ ²⁻	34 (4); 21 – 45	103 (7); 100 – 117	238 (29); 144 – 291	145 (6); 139 – 155	169 (24); 114 – 260	441 (9); 398 – 523
NO ₃ ⁻	22 (4); 7 – 40	5 (8); 2 – 15	152 (30); 108 – 199	1 (6); 1 – 4	2 (24); 0 – 64	72 (9); 68 – 107
NH ₄ ⁺	256 (4); 233 – 289	1.7 (7); 0.6 – 2.0	0.3 (29); 0.0 – 0.5	1.4 (6); 0.9 – 1.8	1.2 (24); 0.5 – 1.4	1.9 (9); 1.8 – 2.9
N ₂ (as equivalent NO ₃ ⁻)	24 (6); 21 – 52	53 (9); 49 – 55	21 (27); 12 – 29	64 (6); 53 – 82	44 (23); 37 – 54	-

DRAFT - DO NOT DISTRIBUTE OR RELEASE

Parameter	Lagoon Water	Near-Lagoon Groundwater	Shallow Field Groundwater	Downgradient Groundwater	Deep Field Groundwater	Irrigation Water
Br ⁻	0.56 (4); 0.50 – 0.60	0.78 (4); 0.55 – 0.95	0.07 (16); 0.01 – 0.51	0.17 (3); 0.09 – 0.21	0.08 (14); 0.02 – 0.55	0.13 (7); 0.13 – 0.19
F ⁻	0.33 (4); 0.26 – 0.77	0.58 (7); 0.17 – 0.72	0.30 (29); 0.11 – 0.50	0.14 (6); 0.06 – 0.20	0.28 (24); 0.07 – 0.47	0.23 (9); 0.20 – 0.27
Li ⁺	0.013 (4); 0.009 – 0.014	0.004 (7); 0.003 – 0.006	0.007 (25); 0.004 – 0.010	0.006 (6); 0.004 – 0.007	0.003 (20); 0.003 – 0.005	0.007 (9); 0.003 – 0.007
NO ₂ ⁻	0.82 (4); 0.51 – 1.21	0.32 (7); 0.01 – 0.70	0.15 (29); 0.01 – 0.84	0.01 (6); 0.01 – 0.21	0.12 (22); 0.01 – 0.51	0.53 (9); 0.32 – 0.57
PO ₄ ³⁻	3.45 (4); 2.78 – 16	0.02 (7); 0.02 – 0.02	0.02 (29); 0.02 – 0.02	0.02 (6); 0.02 – 0.02	0.02 (22); 0.02 – 0.35	0.02 (8); 0.02 – 0.08